(2)

COLLEGE OF ENGINEERING

THE EFFECT OF VORTEX GENERATORS ON CROSSFLOW SEPARATION ON A SUBMARINE IN A TURNING MANEUVER

by

Todd G. Metzel, and Dr. Roger L. Simpson
Department of Aerospace and Ocean Engineering
Virginia Polytechnic Institute and
State University

Report VPI-AOE-186

February 1992

VIRGINIA POLYTECHNIC INSTITUTE AND STATE UNIVERSITY

BLACKSBURG, VIRGINIA

UNCLASSIFIED
SECURITY CLASSIFICATION OF THIS PAGE

REPORT DOCUMENTATION PAGE

Form Approved
OMB No. 0704-0188

1a. REPORT SECURITY CLASSIFICATION UNCLASSIFIED	1b. RESTRICTIVE MARKINGS
2a. SECURITY CLASSIFICATION AUTHORITY	3. DISTRIBUTION / AVAILABILITY OF REPORT Approved for public release, distribution unlimited
2b. DECLASSIFICATION / DOWNGRADING SCHEDULE	
4. PERFORMING ORGANIZATION REPORT NUMBER(S) VPI - AOE - 186	5. MONITORING ORGANIZATION REPORT NUMBER(S)
6a. NAME OF PERFORMING ORGANIZATION Aerospace and Ocean Engineering Department 6b. OFFICE SYMBOL (If applicable)	7a. NAME OF MONITORING ORGANIZATION Office of Naval Research Fluid Dynamics Program
6c. ADDRESS (City, State, and ZIP Code) Virginia Polytechnic Institute and State University Blacksburg, VA 24061	7b. ADDRESS (City, State, and ZIP Code) 800 N. Quincy St. Arlington, VA 22217
8a. NAME OF FUNDING / SPONSORING ORGANIZATION Defense Advanced Research Projects Agency 8b. OFFICE SYMBOL (If applicable)	9. PROCUREMENT INSTRUMENT IDENTIFICATION NUMBER N00014-91-J-1732
8c. ADDRESS (City, State, and ZIP Code) Submarine Technology Program 1400 Wilson Blv. Arlington, VA 22209	10. SOURCE OF FUNDING NUMBERS PROGRAM ELEMENT NO. / PROJECT NO. / TASK NO. / WORK UNIT ACCESSION NO

11. TITLE (Include Security Classification)
The Effect of Vortex Generators on Crossflow Separation on a Submarine in a Turning Maneuver

12. PERSONAL AUTHOR(S)
Todd G. Wetzel, and R. L. Simpson

13a. TYPE OF REPORT	13b. TIME COVERED	14. DATE OF REPORT (Year, Month, Day)	15. PAGE COUNT
Technical	FROM 5/15/91 TO 2/28/92	2/28/92	130

16. SUPPLEMENTARY NOTATION

17. COSATI CODES		
FIELD	GROUP	SUB-GROUP
13	10	01
20	04	

18. SUBJECT TERMS (Continue on reverse if necessary and identify by block number)
Boundary Layer Control
Three Dimensional Separation
Turbulence

19. ABSTRACT (Continue on reverse if necessary and identify by block number)

The effect of vortex generators on the crossflow separation of a 688 class submarine in a turning maneuver was studied. The vortex generators are located on the top and bottom centerline of the submarine. The intent of the vortex generators is to improve turning performance by changing the inherent hydrodynamic forces incurred from crossflow separation in such a maneuver. The number, size, axial location, and local angle of attack of the vortex generators are studied.

Oil flow visualization was used as the primary diagnostic in determining the effectiveness of various vortex generator configurations. Force and moment measurements were taken to relate the fluid dynamics to changes in force and moment distribution.

The vortex generators were found to be very effective in delaying crossflow separation. Separation was delayed by as much as 35 on the bottom

20. DISTRIBUTION / AVAILABILITY OF ABSTRACT	21. ABSTRACT SECURITY CLASSIFICATION
☒ UNCLASSIFIED/UNLIMITED ☐ SAME AS RPT. ☐ DTIC USERS	None
22a. NAME OF RESPONSIBLE INDIVIDUAL	22b. TELEPHONE (Include Area Code) / 22c. OFFICE SYMBOL

DD Form 1473, JUN 86 *Previous editions are obsolete.*

SECURITY CLASSIFICATION OF THIS PAGE
UNCLASSIFIED

of the submarine model. With the addition of vortex generators, the normal force was reduced up to 33%, the axial force was increased up to 233%, and the yaw moment was increased up to 150%. Also, the vertical force increased up to 150%, the pitching moment increased up to 40%, and the roll moment was unaffected.

THE EFFECT OF VORTEX GENERATORS ON CROSSFLOW SEPARATION ON A SUBMARINE IN A TURNING MANEUVER

by

Todd G. Wetzel, and Dr. Roger L. Simpson
Department of Aerospace and Ocean Engineering
Virginia Polytechnic Institute and
State University

Report VPI-AOE-186

February 1992

Sponsored by the Defense Advanced Research Projects Agency
under contract #N00014-91-J-1732.

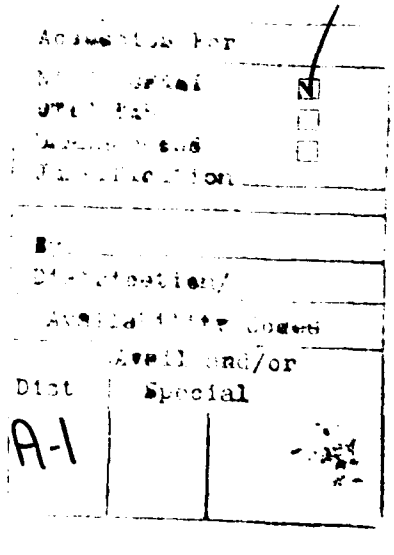

TABLE OF CONTENTS

ABSTRACT

The effect of vortex generators on the crossflow separation of a 688 class submarine in a turning maneuver was studied. The vortex generators are located on the top and bottom centerline of the submarine. The intent of the vortex generators is to improve turning performance by changing the inherent hydrodynamic forces incurred from crossflow separation in such a maneuver. The number, size, axial location, and local angle of attack of the vortex generators are studied.

Oil flow visualization was used as the primary diagnostic in determining the effectiveness of various vortex generator configurations. Force and moment measurements were taken to relate the fluid dynamics to changes in the force and moment distribution.

The vortex generators were found to be very effective in delaying crossflow separation. Separation was delayed by as much as 35° on the bottom of the submarine model. With the addition of vortex generators, the normal force was reduced up to 33%, the axial force was increased up to 233%, and the yaw moment was increased up to 150%. Also, the vertical force increased up to 150%, the pitching moment increased up to 40%, and the roll moment was unaffected.

NOMENCLATURE

b	submarine semi-span (radius)
c	submarine chord (length)
C_{Dt}	drag force coefficient, tunnel axes, D_t/qS
C_{Lb}	roll moment coefficient, body axes, L_b/qSc
C_{Lt}	lift force coefficient, tunnel axes, L_t/qS
C_{Mb}	pitching moment coefficient, body axes, M_b/qSc
C_{Mt}	pitching moment coefficient, tunnel axes, M_t/qSc
C_{Nb}	yaw moment coefficient, body axes, N_b/qSc
C_{Nt}	yaw moment coefficient, tunnel axes, N_t/qSc
C_{Rt}	roll moment coefficient, tunnel axes, R_t/qSc
C_{Xb}	axial force coefficient, body axes, X_b/qS
C_{Yb}	normal or side force coefficient, body axes, Y_b/qS
C_{Yt}	side force coefficient, tunnel axes, Y_t/qS
C_{Zb}	vertical force coefficient, body axes, Z_t/qS
$d(-C_{xb})/dn$	the derivative of the negative of the axial force (drag) with respect to the number of vortex generators, or the average contribution to the drag per vortex generator
D_t	drag force, tunnel axes
h	referencing moment arm for ϕ_x' definition
L_t	lift force, tunnel axes
L_b	roll moment, body axes
M_t	pitching moment, tunnel axes
M_b	pitching moment, body axes

n	number of vortex generators
N_t	yaw moment, tunnel axes
N_t	yaw moment, body axes
q	dynamic pressure, $\frac{1}{2}\rho U_\infty^2$
R_1	primary reattachment
R_2	secondary reattachment
R_t	roll moment, tunnel axes
S	frontal area
S_1	primary separation
S_2	secondary separation
S_3	tertiary separation
U_∞	free stream velocity
U_n	component of free stream velocity normal to submarine
x	longitudinal distance along submarine from nose
x_{bal}	x location of balance
x_{cg}	estimated x location of center of gravity
X_b	axial force, body axes
Y_b	normal or side force, body axes
Y_t	side force, tunnel axes
Z_b	vertical force, body axes
α	angle of attack of vortex generators to local flow velocity
β	sideslip angle
ρ	fluid density
ϕ	angular location around cross section measured from windward side

ϕ' mean separation line

ϕ_x' mean separation line weighted by a separation moment arm

I. INTRODUCTION

Turning maneuvers of submarines result in crossflow separation that substantially opposes the maneuver. Theoretically, flow control devices could be used to decrease this separation. Pearcey (1961) and Bragg and Gregorek (1987) have shown that strategically placed vortex generators can be used to control flow separation on wings at stall. It is therefore presumed that vortex generators can be used to control the crossflow separation on submarines in turning maneuvers.

The design concept pursued here (Figure 1) calls for deployable vanes for vortex generators that are free to move in both the amount of penetration into the flow and in the angle of attack to the local flow. The deployability and variable orientation are important for two reasons. The vortex generators should be deployable because the added drag of deployed vortex generators would most likely greatly detract from cruise performance. The variable orientation will allow the vortex generator configuration to adapt to the particular flow situation encountered. The vortex generators are placed along the top and bottom centerlines of the submarine from bow to stern in order to energize the crossflow of the boundary layer and move the crossflow separation further around the leeside of the submarine.

After identifying some key concerns in the design of a vortex generator system, results are presented from tests relating these conceptual guidelines to actual fluid dynamics and forces and moments.

II. PREVIOUS VORTEX GENERATOR RESEARCH

Axisymmetric bodies, like submarines, produce large amounts of vortical separation when yawed to the free-stream flow. Such is the case for a submarine in a turning maneuver. These vortical flows, though necessary in order to produce the required hydrodynamic forces and moments for the dynamics of the maneuver, affect many aspects of the submarine, most of them undesirably (Bushnell and Donaldson, 1990). Bushnell and Donaldson note that vortical flow affects acoustic and non-acoustic stealth, propulsor efficiency and body drag, control effectiveness, and maneuverability. The focus of this paper is on submarine maneuverability. However, it must be kept in mind that any modifications to the submarine vortical flow structure will concomitantly affect these other submarine performance parameters.

Specifically, with the submarine in a turning maneuver, the separation is dominated by the crossflow component of the flow velocity. Figure 2 shows typical flow structures in such a crossflow separation. The crossflow usually separates just past the wide point of the submarine cross section.

Bushnell and Donaldson also note that in the past it has been assumed that these vortical flows are largely insensitive to Reynolds number effects. However, Bushnell and Donaldson identify several aeronautical experiments that

document Reynolds number effects for various vortical flows. Ahn and Simpson (1992) have studied the vortical flow on a prolate spheroid at angle of attack, which is similar to the submarine at yaw. In such a case, the primary separation location is largely dependent on the state of the boundary layer, that is, whether it is laminar, transitory, or turbulent (Ahn and Simpson, 1992). Of course, laminar boundary layers occur at low Reynolds numbers, while turbulent boundary layers are associated with high Reynolds numbers. For high Reynolds number flows or flows with boundary layer transition fixed such that the boundary layer is turbulent at separation, Ahn shows that the separation line dependency on Reynolds number is greatly reduced. The separation line no longer moves circumferentially, but gradually extends upstream on the body with an increase in Reynolds number.

Ahn also studied the effects of angle of attack on the primary separation line. At higher angles of attack, the separation line moves farther towards the leeside and farther upstream on the body (Ahn and Simpson, 1992).

Because of the adverse effect of vortical flow on submarine performance, specifically submarine maneuverability, it is desirable to attempt to reduce the magnitude of the vortical separation due to the submarine body at yaw. One method commonly used to reduce two-dimensional separation in aeronautics is the vortex generator. Pearcey (1961) offers a very complete survey of

vortex generator theory for two-dimensional flow. According to Pearcey, as viscous friction and adverse pressure gradients slow the boundary layer, separation becomes imminent. In general, the role of the vortex created by a vortex generator is to provide a mechanism whereby higher energy fluid outside the boundary layer can swirl with the near surface low velocity fluid in order to re-energize the boundary layer and delay or prevent this separation. This idea can be extended to the more complex, three-dimensional vortical separation experienced by a yawed submarine.

Bushnell and Donaldson identify several potential problems for this type of configuration. The vortex generation usually causes a drag penalty. Also, as discussed above, vortical separation is dependent on the submarine motion (angle of attack or sideslip and Reynolds number), so the location and amount of separation is constantly changing on a submarine at sea. Vortex generator effectiveness is dependent on proximity to separation, so this separation variability makes placing vortex generators complicated. Also, selectively altering the vortical structure complicates the force and moment variations on the submarine and the control effectiveness of the stern planes and rudder, which makes control systems more difficult to design and submarine dynamics performance more difficult to compute. With these problems in mind, Bushnell and Donaldson recommend that a successful vortex generator system would need to be "active, dispersed, rapidly

deployable, and triggered by distributed sensors." This configurational concept is compatible with double hulled submarine design. (Bushnell and Donaldson, 1990). This configuration is assumed in this paper.

II.A Types and Configurations.

There are many types of vortex generators. The kind used in this study is a vane half delta wing type vortex generator, which is the most simple to implement and consists of small plates mounted normal to the local body surface. Vanes are most attractive because they are very easy to retrofit to existing craft. Other types of vortex generators include ramps, wedges, notches, fences, and riblets (Pearcey, 1961).

Different configurations of the vanes will offer different vortical structure and therefore various advantages and disadvantages. Co-rotating vanes were selected for this experimentation. As indicated by the name, co-rotating vortex generators produce several vortices that rotate in the same direction. Co-rotating systems offer relative insensitivity to spacing and local flow direction, and the vortical structure is relatively constant in the streamwise direction (Pearcey, 1961). These facts make the co-rotating vortex generators easiest to implement successfully. Also, the flow separation off the submarine is vortical in nature, so a unidirectional vortex is most suitable to counteract that separation. Other vortex

systems include counter-rotating and biplane vortex generators.

II.B Design and Implementation.

There are several considerations in the design of a vortex generator system. According to Pearcey, the most important consideration in designing a vortex generator system is not the boundary layer profile just upstream of the vortex generator but rather the range and severity of separation that needs to be controlled. With co-rotating vortex generators, it is important to space the vanes apart by at least a certain minimum distance. If they are too close together the resulting vortices will damp each other out. Pearcey suggests that the separation (D) to height (h) ratio be kept above D/h = 3. Pearcey also notes that once above that minimum, vortex generator effectiveness only drops off very slowly. Therefore, values of D/h often fall around 5 or 6.

Pearcey also stresses the importance of vortex generator uniformity. Non-uniform vortex generators create non-uniform vortices, which can result in "displacement of the vortices normal to the surface and relative to each other." (Pearcey,1961)

Another consideration Pearcey points out is that the vortices do not travel purely in the streamwise direction, but rather deviate through a curved path that never deviates more than about 15° from the streamwise flow. This can

alter control surface effectiveness aft of the vortex generators.

Often a given amount of separation can be controlled by one row of vortex generators if those generators are made large enough. However, one consequence of vortex generators is increased drag in any normally unseparated flows, i.e. in the case of straight ahead cruise of the submarine. Larger vortex generators carry a larger drag penalty. Therefore, multiple rows of smaller vortex generators may be more effective than one row of large ones. Unfortunately, multiple rows are difficult to place. According to Pearcey, the generators of the second row must be placed so that the vortices from the first row pass either in between the new vortex generators or over top of them. Otherwise, the new vortices will damp out the original ones and the system as a whole will be less effective than just the single row. The downstream deflection of co-rotating vortices makes multiple row placement even more difficult.

The shape of vortex generators plays a role in the effectiveness of the system. The vanes are almost always low aspect ratio plates. While rectangular vanes are often used for simplicity, more streamlined shapes can help alleviate drag penalties while retaining the original vortical effectiveness. Pearcey points out that the general goal in optimizing vane shape design is to increase the lift-to-drag ratio of the vane. This will generate the largest vortex for the least amount of drag. Airfoil shapes

and in fact camber may make vortex generators more efficient, but usually the scale involved in the tests is too small to account for such differences.

II.C Effects on Aerodynamics.

Vortex generators can make substantial improvements in the aerodynamic characteristics of objects. Bragg and Gregorek (1987) describe the effect of several different vortex generator systems on a laminar flow canard that in certain situations was experiencing premature stall. At the design lift coefficient, vortex generators returned almost all of the lost lift due to early separation, and delta wing vortex generators were found to have the least drag penalty.

III. EXPERIMENTAL APPARATUS

III.A The Wind Tunnel.

All tests were performed in the VPI&SU Stability Wind Tunnel. This continuous, closed jet, single return, subsonic wind tunnel has a 25 ft. long, 6 x 6 ft. square interchangeable test section. The tunnel has a flow speed range of 0-220 ft/s and a maximum unit Reynolds number of 1.33×10^6 per foot. The tunnel is powered by a 600 hp D.C. motor which turns a 14 ft diameter prop. The flow is directed through honeycomb screens and a 9:1 contraction with a very low turbulence intensity of around 0.03%. The tunnel allows force and moment measurements to be taken from either a strut or sting mounted strain gauge balance. The sting was selected for its lower interference with the flow and its higher range of force and moment measurement.

III.B The Model Submarine.

The model is a 1/48 scale nominal Los Angeles class (688) submarine (Figure 3). By the term nominal it is meant that the basic proportions of the true submarine are preserved on the model, but the exact shape of a 688 was not modeled. The co-ordinates for the exact shape of the model are included in Appendix 1. The model is nominally 90.25" long and has a nominal 8.25" maximum diameter.

The model is cast fiberglass purchased from the Scale Shipyard (1990). An aluminum skeleton was added to stiffen the model for the tests, provide mounting points for the balance, and force the model to be as axisymmetric as

possible (Figure 4). After the main construction was completed, a 15 mil black gelcoat was applied to the model surface to give a smoother, cleaner surface finish and to protect the model from the chemicals in the oil flow solution. The body surface was then marked with a white grid spaced every 4" in the longitudinal direction and every 45° in the circumferential direction. Finally, the entire model was painted with a special clear coat that resists the oil flow mixture chemicals.

The rear 5 in. of the model was removed to allow the sting to enter the model. The clearance between the model and the sting was 3/8". Because the propeller was not modeled and because the major crossflow separation flow phenomena occur closer to the bow, none of the rear control surfaces were modeled. The towed array housing, diving planes and sail were all modeled.

The sting is not long enough to reach the model center of gravity, so lead ballast was added to the rear of the model in order to move the center of gravity closer to the balance center. When the model was in the tunnel, all mounting holes were filled in with wax and/or plaster.

Posts 21 mils high were placed around the nose and along the length of the model at +/-45° from the windward side of the model to act as trip strips (Figure 5). The posts were made by first laying up 3 layers of 3M brand 7 mil black electrical tape onto a metallic data tape backing. This tape was then run through a computer paper tape

punching machine which punched out a continuous string of evenly spaced holes (10 holes per inch) of the same diameter (0.05 inches). The tape was pealed off its backing and applied to the model. Then, a polyester filler (Akemi #7) was forced into the holes and allowed to cure. Finally, the tape was removed and the 21 mil posts remained (Smith, 1989).

To simulate a turning maneuver, the model was placed in a sideslip. The model was mounted in the tunnel on it's side in order to utilize the adjustable angle of attack feature of the strut-mounted sting and to reduce gravitational effects on the oil flows (Figure 6). The towed array was placed on the windward side, so a left turn was modeled. Sideslip angles of up to 15° were simulated.

III.C Vortex Generators

The vortex generators were made out of sheet aluminum. The leading and trailing edges were rounded with a radius half the thickness of the sheet aluminum. The vortex generators were glued on the model with 5-minute epoxy so they could be easily removed and replaced (Figure 7). A jig that held a generator in the proper position and orientation was used to mount the delta wings in order to guarantee uniformity. The jig (Figure 8) simply consisted of a block of wood with the submarine radius cut into it and a thin flat area cut as the mounting plane. Then, slots were cut into the block at the desired vortex generator angles in order to hold the vortex generators. The vortex generators

were mounted 15° to the local flow based on wall skin-friction lines (Figure 9). Two sizes were used in the experimentation. Almost all of the tests used 1" long, 1/2" high, and 1/16" thick vortex generators. However, oil flows 16, 17, 23 and 24 used some vortex generators that were 1/2" long, 1/4" high, and 1/32" thick.

IV. INSTRUMENTATION AND EXPERIMENTAL TECHNIQUES

IV.A Oil Flow.

The main diagnostic for these tests was surface oil flow visualization. The oil flow visualization technique has been used extensively at VPI for flow visualization by Seungki Ahn, Dr. Semih Olcmen, and Dr. William Devenport. The oil flow mixture, attributable to E.P. Sutton of Cambridge University, consisted of titanium dioxide (TiO_2) as a pigment, kerosene for the solvent, and oleic acid to prevent coagulation or lumping of the TiO_2. The mixture is made by adding 40 ml of sifted, unpacked TiO_2 to a 100 ml graduated cylinder. Kerosene is added up to the 100 ml mark, and 5 ml of Oleic acid is added in on top of that. Several variations of this mixture were tried during the first couple runs, and the quality of the runs was found to be relatively insensitive to small changes from this recipe. The mixtures are then thoroughly stirred and transferred to a pail. A sponge brush is used to apply a coat of the mixture to the model. It is important to make brush strokes normal to the expected flow direction so that brush marks are not later misinterpreted as skin friction lines.

After the tunnel is turned on and the oil mixture is almost entirely dry, the tunnel is turned off. The oil flows are recorded by photographing the model in sections and from different peripheral orientations.

Lines of separation are indicated by converging surface skin friction line patterns. The peripheral angle separation location ø is measured according to the convention in Figure 10. The separation location ø indicated by this method is probably premature for two reasons. The oil flow mixture is drawn down (towards the windward side) due to gravitational effects, and the oil flow mixture itself initiates separation earlier then would occur on a clean surface (Simpson et. al., 1992). Simpson et. al. have shown that these effects can add errors of up to -5° for a similar flow at 30° angle of attack to the free-stream flow. No attempts were made to correct any of the data. After carefully recording the flow separation location, the dried mixture is then cleaned off with kerosene.

Lines of separation were recorded with color-coded marks so a "hard copy" of each of the runs could be preserved. A cardboard mask was made with a 1/2" by 1/8" hole in it. It was placed at some point along the separation line, and acetone was used to clean off all of the oil flow mixture in that hole. Then, an acrylic paint marker was used to make a short line in that cleaned area that indicated position and direction of the separation line. Finally, the mask was applied again and the mark was sprayed with clear coat paint in order to protect the mark from future applications of the oil flow mixture. Marks

were made between longitudinal grid marks along the length of the separation line.

It can be very difficult to determine exactly where longitudinally separation begins. Separation lines are located at converging skin friction lines in the oil flow pattern. Simpson has proposed, as a general rule of thumb, that the point where the angle of incidence of converging skin friction lines is smallest but positive be interpreted as the start of separation. For most of the runs, this location was still difficult to pick out with any degree of certainty, so no numerical studies are presented. Downstream of this location the skin friction lines on each side of the separation line intersect the separation line at a sharp finite angle.

The "hard copy" separation lines are characterized by two values. The mean separation line is defined by integrating the separation line to find the area of separation. This area of separation is then nondimensionalized by the length of the separation and the average radius r' in the separation region in order to find the mean separation line, ϕ', which is the angle for the equivalent separation line on a cylinder of radius r':

$$r' = \frac{1}{(x_f - x_i)} \int_{x_i}^{x_f} r(x)\, dx,$$

$$\phi' = \pi - \frac{1}{(x_f - x_i)\, r'} \int_{x_i}^{x_f} (\pi - \phi(x))\, r(x)\, dx,$$

where x_i and x_f bound the separation zone, $\phi(x)$ is the separation line location at x, and r(x) is the radius at station x. Hypothetically, one would think that the aerodynamic forces acting on the submarine due to separation should be somehow directly related to the amount of separation and therefore ϕ'. Using similar logic, it would seem that in order to relate the separation to a moment, the differential separation area should be multiplied by some moment arm, thus:

$$\phi'_x = \pi - \frac{1}{(x_f-x_i)^2\, r'} \int_{x_i}^{x_f} (\pi-\phi(x))\; r(x)\; (x-h)\; dx,$$

where h is some referencing moment arm. Simpson's rule was used to carry out the numerical integrations.

IV.B Forces and Moments.

A six-component strain gauge balance made by the Transducer Systems Division of Modern Machine and Tool, Inc., of Newport News, Virginia, was used for all the force and moment measurements. All data were collected with a Hewlett-Packard Model 3052 data acquisition unit. Each reading was the average of 50 values. The computer program produced the six force and moment coefficients in tunnel axes, with the following reference values:

Area:	S = 0.371 ft^2	(Model Frontal Area)
Chord:	c = 7.500 ft	(Model Length)
Span:	b = 0.344 ft	(Model semi-span)

The six tunnel-axes force and moment coefficients were then converted to body axes, with the main interest in the normal

force, the axial force, and the yaw moment, following the conventions in Figure 10. Also, the yaw moment was transferred from the balance location to the estimated center of gravity location, the quarter chord of the sail. The force and moment transfer relations through a sideslip angle β are:

$$C_{Xb} = C_{Lt} \sin \beta - C_{Dt} \cos \beta$$

$$C_{Yb} = -C_{Lt} \cos \beta - C_{Dt} \sin \beta$$

$$C_{Zb} = -C_{Yt}$$

$$C_{Nt}' = C_{Nt} + C_{Yt} (x_{cg} - x_{sail})$$

$$C_{Mt}' = C_{Mt} - C_{Yb} (x_{cg} - x_{sail})$$

$$C_{Rt}' = C_{Rt}$$

$$C_{Lb} = N_t' \sin \beta - C_{Rt}' \cos \beta$$

$$C_{Mb} = -C_{Nt}' \cos \beta - C_{Rt}' \sin \beta$$

$$C_{Nb} = -C_{Mt}'$$

Runs were made for wind tunnel speeds of 100 to 200 ft/s (Reynolds numbers of 4.60 million to 6.77 million) to establish Reynolds number independence, and at sideslip angles of 0 to 15°. All of the vortex generator oil flows were run at Re = 6.77×10^6 and 15° of sideslip.

V. EXPERIMENTAL RESULTS

V.A Oil Flows.

V.A.1 Submarine without Vortex Generators

After determining experimentally the best oil flow mixture, runs were made without vortex generators (naked submarine) at Reynolds numbers of Re = 4.60×10^6 to Re = 6.77×10^6 for sideslip angles of 0°, 5°, 10°, and 15°. The naked submarine runs were oil flows 1 through 14 as listed in Appendix II, and photos documenting these runs are listed as Figures 47 to 106. Most of this discussion will focus on cases with 15° of sideslip at Re = 6.77×10^6. The oil flows indicate several important phenomena.

Separation lines were easy to identify. The separation lines are identified by converging skin friction lines. The beginning of separation is defined as that point where the angle between the converging skin friction lines is smallest but positive.

Figure 13 shows the bottom of the submarine from x = 52" to x = 68" from the nose. This run, oil flow 3 as listed in Appendix II, was made at 15° sideslip and Re = 6.78×10^6. Primary separation (indicated as S_1) occurred at 97° on the sail side and 115° on the bottom side of the submarine. Secondary lines of separation (indicated as S_2) were also found in some of the cases. The towed array was

found to have a substantial effect on the flow especially with respect to separation.

Figures 47 to 66 document oil flow 11 for which Re = 6.85×10^6 and $\beta = 5°$. Although separation data were not recorded for this run, the photos indicate that on the sail side separation occurred at roughly $\phi = -135°$ and seemed to begin somewhere around x = 48" (Figure 51). On the bottom side, separation occurs at roughly $\phi = 150°$ and begins somewhere in the neighborhood of x = 44" (Figure 61).

Figures 67 to 86 show oil flow 7 for which Re = 6.77×10^6 and $\beta = 10°$. Separation line data from this run result in $\phi' = 130°$ on the sail side and $\phi' = 119°$ on the bottom side of the submarine. As expected, separation occurred earlier in this 10° sideslip case than in the 5° sideslip case of oil flow 11. On the sail side, it seems that separation begins somewhere near the trailing edge of the sail (Figure 73), while separation begins at around x = 40" on the bottom side (Figure 82).

Figures 87 to 106 document oil flow 2, with Re = 6.78×10^6 and $\beta = 15°$. All of the vortex generator runs were compared to this configuration. Although separation data were not recorded for this particular run, separation was recorded for oil flow 9, which was identical to oil flow 2 in Reynolds number, sideslip, and configuration. Therefore, it is assumed that the separation line data from oil flow 9 is applicable to oil flow 2. Once again, it was predicted that separation would occur earlier in this run as compared

to oil flows 7 and 11 due to the steep angle of sideslip. Separation occurred considerably earlier in this case, with $\phi' = 100°$ on the sail side and $\phi' = 109°$ on the bottom side. Also, this flow had a secondary separation line at roughly $\phi = 150°$ on the sail side and $\phi = 145°$ on the bottom side. Separation began upstream of the sail at about x = 20" (Figure 94), while on the bottom side of the submarine separation also began at about x = 20" (Figure 104).

Also, as shown in Figures 127 to 129, the sail plays a very important role in the flow development on the submarine. At 0° sideslip (Figure 127), the flow is completely attached on the hull surface. A wake does form off the trailing edge of the diving planes.

At 10° sideslip (Figure 128), the flow seems to separate off the trailing edge of the sail and in fact initiates the main vortex sheet that separates off the submarine on that side of the body. The wake on the trailing edge of the sail is bigger, and the flow separates on the inboard section of the diving planes.

At 15° sideslip, (Figure 129), a large vortex sheds off the sail. This is accompanied by some very complex flow patterns, which include a smaller vortex now on the sail itself, more separation on the inboard surface of the diving planes, and a stagnation point/saddle point combination on the submarine behind the sail. Because of the sail, appreciable dissimilarities between the sail side and the bottom of the submarine should be expected.

The towed-array housing also affects the flow. Figure 11 is from oil flow 1, which was run at Re = 6.78×10^6 and ß = 15°. This figure shows that perhaps a small amount of separation occurs off the semi-circular leading edge of the housing. Also, the streamlines on the towed array housing are much steeper than those just windward of the housing. Also, careful inspection reveals slight separation on the leeward side of the towed array housing for its entire length. Figure 12 shows the trailing edge of the towed array housing from the same flow. In this photo, the primary separation line is seen to converge onto the trailing edge of the towed array.

V.A.2 Submarine With Vortex Generators

After these initial runs, vortex generators were added progressively from the stern toward the bow. The goal of each run was to delay the line of separation as much as possible to higher angles ø on the leeside. The vortex generators did indeed delay separation. Figure 14 shows the separation line for the same portion of the submarine as shown in Figure 13. The run in Figure 14, oil flow 20, was also done at 15° of sideslip and Re = 6.43×10^6, but this run included the larger vortex generators placed along the submarine. It is quite clear that the separation line has moved toward the leeside as compared to Figure 13.

In fact, with the eventual addition of 43 vortex generators on the entire submarine (20 on the sail side, 23 on the bottom), the separation line was delayed 33° on the

sail side and 37° on the bottom of the submarine. In addition, the secondary separation line was completely eliminated. Consequently, a tremendous change in the force and moment distribution was observed, as discussed below. The test run configurations and separation data are summarized in Appendix II.

Figures 15 through 24 show plots of the separation line for each of the cases where the separation line was recorded on the model. Refer to Appendix II for a description of each run. Examination of these separation lines shows the improvement made with the addition of the vortex generators. Figure 18 (oil flow 9) shows the separation lines for the naked submarine at Re = 6.78×10^6 and 15° of sideslip. As could be predicted, separation occurs just past ϕ = 90°, where the pressure gradient becomes adverse. Separation is a little earlier on the sail side due to the sail and the towed array housing. The mean separation lines for this configuration are ϕ' = 99.9° on the sail side and ϕ = 108.8° on the bottom.

This contrasts with oil flow 20, Figure 24, which represents the most successful configuration tested. For this flow, the separation line is delayed even beyond 135° in some places. The only place where the separation line hasn't moved is just behind the sail on the sail side. The mean separation lines for this vortex generator configuration are ϕ' = 128.5° on the sail side and ϕ' = 146.8° on the bottom.

The separation line plots seem to indicate a Reynolds number dependency. Both oil flows 9 and 10, plotted in Figures 18 and 19, were run at 15° of sideslip. However, oil flow 9 was run at Re = 6.78×10^6, while oil flow 10 was run at Re = 4.54×10^6. The plots seem to indicate that separation occurred earlier at the lower Reynolds number. This phenomenon also occurs at $\beta = 10°$, as evidenced by oil flows 6, 7 and 8 (Figures 15-17). The mean separation lines for these flows are given in Table 1.

Several observations were made during these runs. First, it is important to introduce vorticity relatively far upstream. In the initial vortex generator configuration (oil flow 15), the first half delta wing was placed at 27% of the length downstream of the nose. This configuration delayed separation by almost 25°. Later configurations added vortex generators all the way from 4.4% of the length from the nose, with a consequent additional delay in separation of 12°.

The behavior of each individual vortex generator is such that it seems to have a zone of influence. If, for example, a vortex generator is removed, the separation quickly dips toward the windward side of the submarine just downstream of that location. Downstream at the next vortex generator, the separation line does not jump back up to the position achieved before the missing vortex generator, but instead slowly climbs and in fact never really reaches the original separation line. The most exaggerated display of

this effect occurs at the sail. More indications of this zone of influence can be seen by examining the surface flow pattern between the row of vortex generators and the separation line. The separation line is seen to oscillate a little in coordination with the placement of the vortex generators. Also, the dark stripe off each vortex generator (see Figure 14), which is an indication of the vortical wake produced by each vortex generator, shows where downstream the produced vorticity affects the separation line. By examining this figure, this zone of influence seems to be a band four inches wide (the distance between vortex generators) that extends downstream at about a 30° angle off horizontal from the vortex generators to the separation line.

The oil flows clearly delineate the difficulties in reducing separation on the sail side of the submarine as opposed to the bottom of the submarine. First of all, the flow separates off the towed array housing, and then reattaches to the submarine surface closely behind the towed array (see Figure 11). Also, as shown in Figures 129 and 130, at 15° sideslip, the flow separates off the sail. Consequently, a large vortex forms off the sail, and the hull flow separation line aft of the sail is forced down to the trailing edge of the sail. This greatly limits the amount of separation reduction possible on this side of the submarine. Also, the vortex generators ahead of the sail modify these complex flow structures. While the location of

these structures really is not changed, the size and rotational orientation of the main vortex off the sail is affected. It is hard to predict what effect this has on the submarine performance.

During the study, attempts were made to reduce the separation off the sail by putting small vortex generators on the sail itself. For oil flow 23, two small vortex generators were placed on the sail just behind the trip posts (about 0.5" from the sail leading edge), at 0.5" and 1.5" from the hull surface (see Figure 25). For oil flow 24, these two vortex generators were moved just ahead of the trip posts (Figure 26). Neither of these attempts proved effective. One potential reason for this is that the sail's maximum thickness is so far forward that the resultant negative pressure gradient is extremely strong and may therefore require a very strong vortex generator system. Also, the scale of the flow structures involved in this region coupled with the relative violence of the flow around the sail makes diagnosis much more difficult.

Several runs point to the effect of local vortex generator angle of attack, α, on the flow separation. For oil flow 19, two vortex generators were added at x = 8" at peripheral locations $\phi = \pm 135°$ (Figure 27). They were placed at 15° to the local flow, but since the flow is only about 15° off horizontal, this means they were only 30° off horizontal. For oil flow 20 these two vortex generators were inclined a little steeper so that they were 55° off

horizontal (Figure 28). By examining Figures 27 and 28, it is clear that the steeper vortex generators in oil flow 20 produced the stronger vortices and pushed the separation line slightly farther towards the leeside. So as expected, the steeper vortex generators produce stronger vortices which are more effective at delaying separation. However, it was found that these particular vortex generators had a minimal effect on the overall flow. On the sail side, $\phi' = 129°$ for oil flow 19 and $\phi' = 128°$ for oil flow 20. On the bottom side, $\phi' = 145°$ for oil flow 19 and $\phi' = 147°$ for oil flow 20.

It was noted that these vortex generators at x = 8" were in an unfavorable pressure gradient. Therefore, for oil flow 21 (Figure 29), the top two vortex generators were moved to x = 4". In addition, these vortex generators were moved to $\phi = \pm 150°$. Then, for oil flow 22 (Figure 30), two more vortex generators were added at x = 4", $\phi = \pm 90°$. Neither of these changes delayed separation any farther than the configuration in oil flow 20.

For oil flow 23, two of the leading vortex generators were rotated so their local angle of attack was negative instead of positive in order to examine the effect of the sign of the local vortex generator angle of attack and resulting vorticity rotation direction on the flow (see Figure 31). These two vortex generators allowed the flow to separate earlier than in the previous run and were therefore detrimental to the configuration.

For oil flows 16 and 17, the smaller vortex generators were used on the sail side. For oil flow 16, the vortex generators were placed just ahead on the towed array. This configuration was relatively ineffective, as the separation line was delayed by only about 5°. Then for oil flow 17, the vortex generators were moved up to ø = 90°, which is where the vortex generators had been placed on the bottom side of the sub. These vortex generators were more effective and delayed separation by almost 13° (see figure 32). For oil flow 18, the small vortex generators were replaced with the larger ones so that the same vortex generators were being used on both sides of the sub. The larger vortex generators were effective in delaying the separation line an additional 15° (see figure 33).

V.B Forces and Moments.

The large reduction of the region of flow separation produces a complete alteration of the force and moment distribution of the submarine. Specifically, the normal force decreased and the axial force and yaw moment increased. Also, the vertical force and pitching moment increased, while the roll moment changed minimally. The test run configurations and force and moment data are summarized in Appendix II.

V.B.1 Effects of Angle of Sideslip and Reynolds Numbers

Figures 34 through 39 show the variation of the force and moment coefficients with respect to sideslip ß for both the naked submarine and the submarine with vortex generators

in the same configuration as oil flow 22. There are several important things to learn from these graphs. The first important piece of information stems from the fact that the data are plotted for different Reynolds numbers. The relative invariance of the data at given sideslip angles proves that there was no significant Reynolds number dependency for the forces and moments, which proves that the trip strips were effective. This is in direct contrast to the oil flows which did indicate a Reynolds number dependency.

The most interesting thing to note is the drastic change in the force and moment distribution of the submarine due to the vortex generators. At 15°, the designed sideslip for the configuration tested, the normal force is reduced by 66%, the yaw moment is increased by 350%, and the axial force is increased by 233%. In addition, the vertical force is increased by 150%, the pitching moment is increased by 40%, and the roll moment stays constant. This drastic change in the forces and moments on the submarine would change the submarine's turning performance.

The third thing to notice is the dashed line on the normal force, axial force, and yaw moment graphs. This line represents a low order approximation to the true force and moment curves for a truly variable vortex generator configuration. The data plotted at the lower angles of sideslip were recorded with the vortex generator configuration designed for $\beta = 15°$. It is assumed that

vortex generators on the submarine will not be deployed at all when cruising straight ahead, so the zero sideslip values for the naked submarine case is connected with the 15° sideslip values for the vortex generator configurations to approximate this predicted curve.

V.B.2 Effect of Number of Vortex Generators

A series of tests (runs 31.23, 32 through 51, and 52.24-52.28) was run to determine the variation of the forces and moments with the number of vortex generators. This series began with the submarine in its "best case" vortex generator configuration, which is defined as the same vortex generator configuration as oil flow 22. For each run, a pair (one on the top, one on the bottom) of vortex generators was removed and forces and moments were calculated. This process was repeated until there were no vortex generators left on the submarine (the naked case). So really, this series of tests measured the effect of starting location of the vortex generators on the forces and moments. It is important to note that there were two rows at the sail where only one vortex generator was removed per run (runs 39 and 40). This is because on the sail side, no vortex generators could be placed in the vicinity of the sail.

The results of this series are presented in Figures 40-42. The normal and axial force vary relatively smoothly with respect to the number of vortex generators. In fact, the axial force plot looks very linear with respect to the

number of vortex generators. If a linear regression is attempted on the data, the data are found to be very linear, with the correlation coefficient R = 0.9983. Through this linear regression, the average contribution of one vortex generator to the overall axial force (drag) acting on the sub, $d(-C_{xb})/dn$, was found to be $d(-C_{xb})/dn = 0.0095$.

The other four graphs show significant changes in force and moment behavior when using more than 25 vortex generators. Use of 25 or less vortex generators corresponds to having them only downstream of the sail region of the submarine. The yaw moment (Figure 42) is seen to peak out at around 25 vortex generators. The vertical force (Figure 43) falls steeply as the initial vortex generators are removed up until the sail region, and then remains constant. The roll moment (Figure 44) stays fairly constant. The pitching moment plot (Figure 45) shows a minimum pitching moment at about 15 vortex generators, with higher values at the extremes.

Therefore, the sail plays a very integral role in the forces and moments of the submarine and subsequently in the placement of the vortex generators. The explanation for these variations can be found by examining the Figures 129 and 130. These two photos show the difference between the separation locations for the submarine at 15° sideslip and $Re = 6.75 \times 10^6$ for both the naked submarine and the submarine with the vortex generators from oil flow 22. The vortex generators only slightly alter the separation line behind

generators only slightly alter the separation line behind the sail. In both cases the separation line begins at the sail trailing edge and then steadily moves leeward farther downstream. In the case with the vortex generators, the separation line moves leeward a little more quickly than in the naked submarine case. A more substantial portion of the separation improvement comes upstream of the sail, where the vortex generators move the separation line leeward by as much as 35°. Thus, removing the vortex generators forward of the sail more drastically alters the amount of separation and the forces and moments acting on the submarine. The fact that the sail is only on one side of the submarine then explains why the vertical force, and pitching moment, are affected by these phenomena.

These variances also indicate that an optimum configuration may not necessarily be the one that reduces separation the most. It would be interesting to run a similar series of tests, but remove the vortex generators from the tail forward. It is conjectured that the normal and axial force plots would not change much, but that the other four curves would be altered significantly.

VI. CONCLUSIONS

Turning performance of a submarine is limited by the crossflow separation off the leeward side. Vortex generators offer a possible means of lessening that crossflow separation and improving turning performance.

It has been shown that vortex generators placed along the submarine centerline from bow to stern do indeed significantly reduce crossflow separation on a submarine in a turning maneuver. Oil flow visualization was used to locate flow separation. With the addition of vortex generators, separation was delayed by as much as 35°.

The oil flows indicated several important phenomena. One of these is the importance of introducing vorticity as far upstream as possible in order to delay separation as much as possible. It was found that in general the first vortex generators seem to initiate the vorticity while the subsequent vortex generators merely propagate the vorticity. Also, the oil flows pointed out the huge impact the sail has on the crossflow of the submarine.

The vortex generators tremendously alter the force and moment distribution. Due to the vortex generators, the normal force was reduced by up to 33%, the axial force was increased by up to 233%, and the yaw moment was increased up to 150%. In addition, the vertical force went up as much as

150%, the pitching moment increased up to 40%, and the roll moment was unaffected.

By varying the number of vortex generators on the submarine, it was found that the vortex generators have a critical effect on the forces and moment of the submarine. This leads to the identification of three important configurations: no vortex generators, vortex generators from stern to sail, and vortex generators from stern to bow. Figure 46 shows pictorially the forces and moments for each of these three configurations. The three force and moment components directly related to a turning maneuver are the normal force, the axial force, and the yaw moment. The normal force decreases while the axial force increases evenly over the progression through the three cases. The yaw moment, however, increases with the addition of the vortex generators up to the sail, but additional vortex generators upstream of the sail do not change the yaw moment significantly.

Equally interesting to note is the vortex generator effect on the other three forces and moments that are not related to the turning maneuver. These forces describe out-of-plane motions that would be experienced and would need to accounted for in any control system. The vertical force is relatively unaffected by the addition of vortex generators up to the sail, but deployment of vortex generators ahead of the sail cause a sudden increase in the downforce. Therefore, the vortex generators in this full configuration

would cause the submarine to dive. The pitching moment shrinks a little with the addition of the vortex generators up to the sail, but then drastically increases with the deployment of vortex generators ahead of the sail. The sign of this moment would cause a nose-down motion. Once again, the roll moment stays relatively constant for all three configurations.

As a concept, the vortex generators are definitely a viable means for flow control. Further reductions in separation could most likely be achieved by more carefully optimizing size, shape, distribution, and orientation of the vortex generator system. In fact, other vortex generators and flow control devices would be worth studying.

VII. REFERENCES

Ahn, S. and Simpson, R.L., Cross-Flow Separation on a Prolate Spheroid at Angles of Attack, AIAA Paper no. 92-0428, 1992.

Bushnell, D.M., and Donaldson, C.D., Control of Submersible Vortex Flows, NASA Technical Memorandum no. 102693, June, 1990.

Bragg, M.B. and Gregorek, G.M., "Experimental Study of Airfoil Performance with Vortex Generators," Journal of Aircraft, Vol 24., May 1987, pp. 305-309.

Pearcey, H.H., "Shock-Induced Separation and its Prevention by Design and Boundary Layer Control," Boundary Layer and Flow Control, Its Principal and Applications, Vol. 2, edited by G.V. Lachman, Pergamon Press, Oxford, England, 1961, pp. 1166-1344.

Simpson, R.L., Walker, D.A., and Shinpaugh, K.A., Description of a 1000 Sensor Constant Current Anemometer System for Locating Three-Dimensional Turbulent Boundary Layer Separations, Report VPI-AOE-185, 1992.

Smith, D.G., Private Communication, Aerodynamics Laboratory, Boeing Commercial Airplanes, October, 1989.

Table 1. Separation location dependence on Reynolds number.

Side	β, °	ϕ' Re = 6.77x106	ϕ' Re = 4.60x106
Sail Side	15	99.8	99.5
Bottom	15	108.8	101.6
Sail Side	10	130.1	113.5
Bottom	10	119.5	108.9

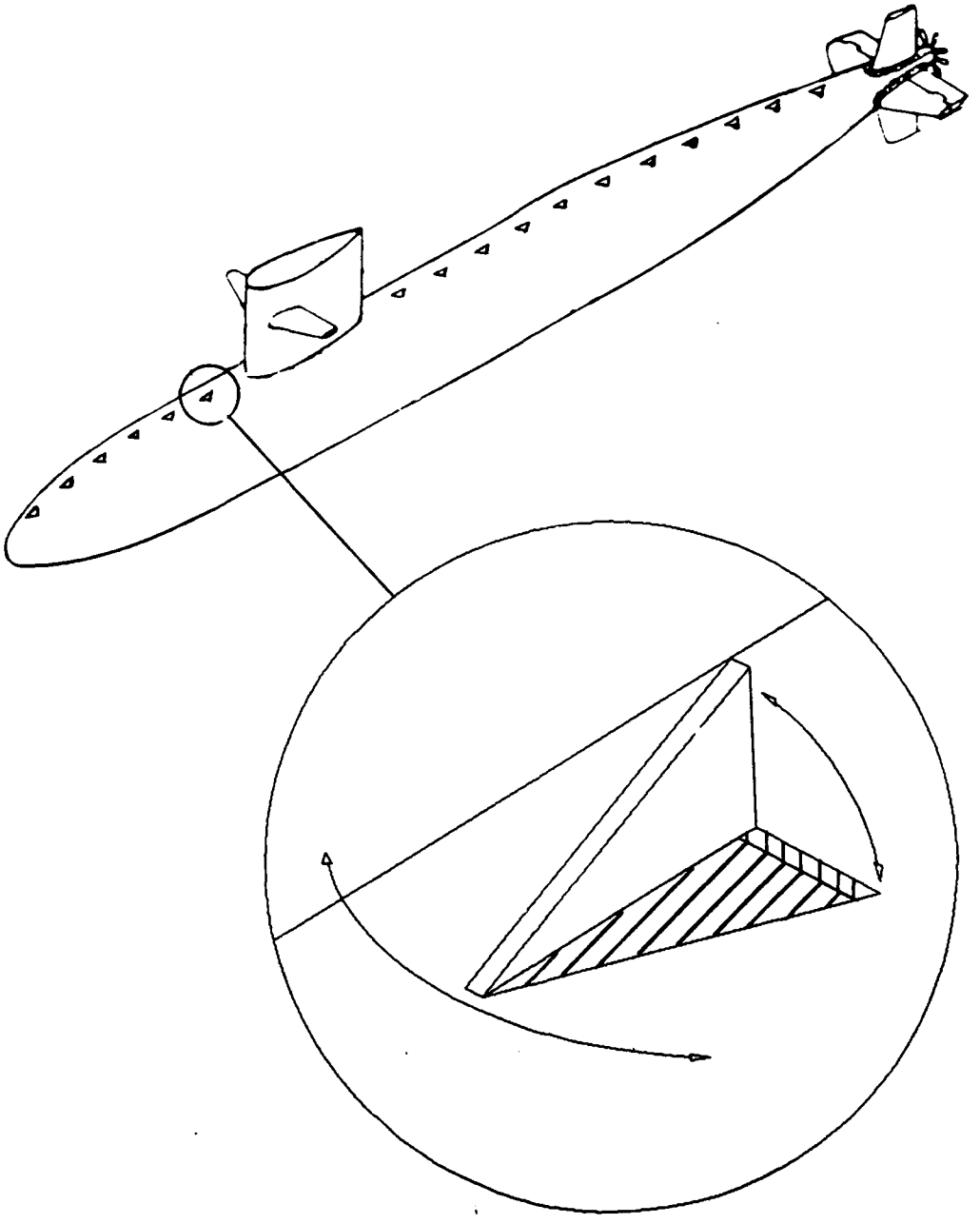

Figure 1. Vortex generator configuration. The half delta wing vortex generators line the top and bottom of the submarine in a single row from bow to stern. The vortex generators are only deployed for turning maneuvers, and have variable angle of attack.

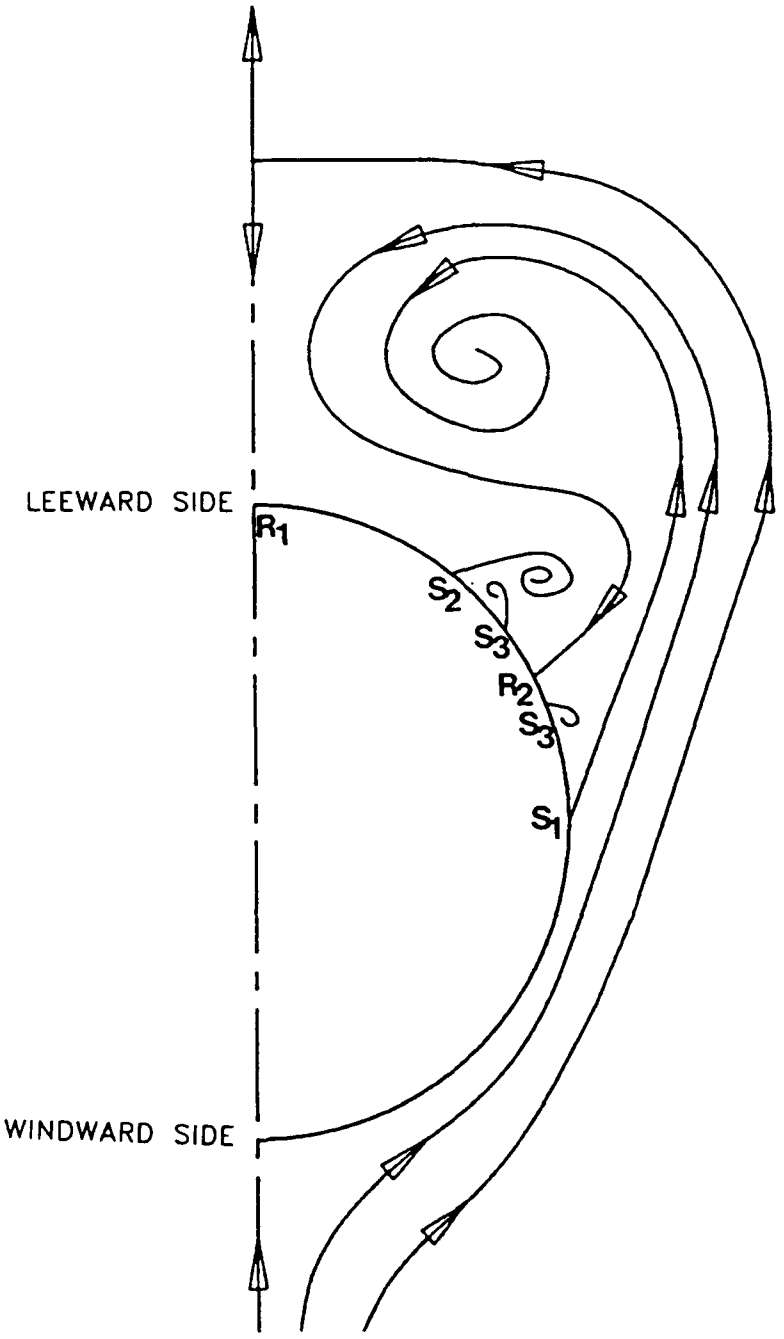

Figure 2. Crossflow separation. This half cross-section of the submarine shows the important flow phenomena. S_1 denotes primary separation; S_2 denotes secondary separation; S_3 denotes tertiary separation; R_1 denotes primary reattachment; and R_2 denotes secondary reattachment. The addition of vortex generators delays separation (S_1 and S_2) farther around the leeward side of the submarine. Primary separation (S_1) is the flow phenomenon discussed in this report. (S. Ahn, 1991, Ph.D Dissertation, VPI&SU).

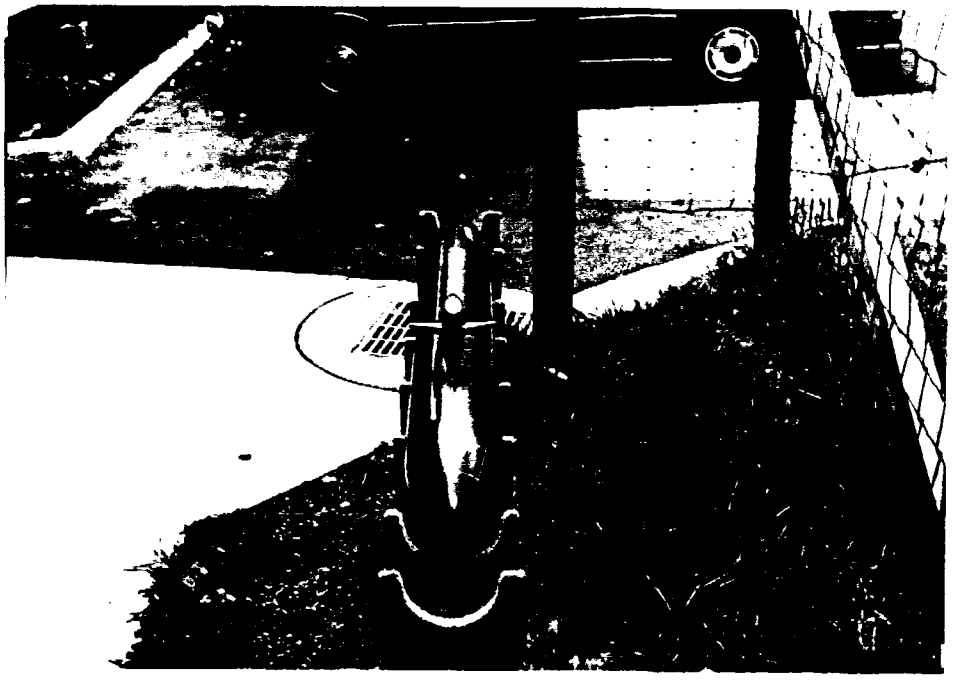

Figure 3. The model.

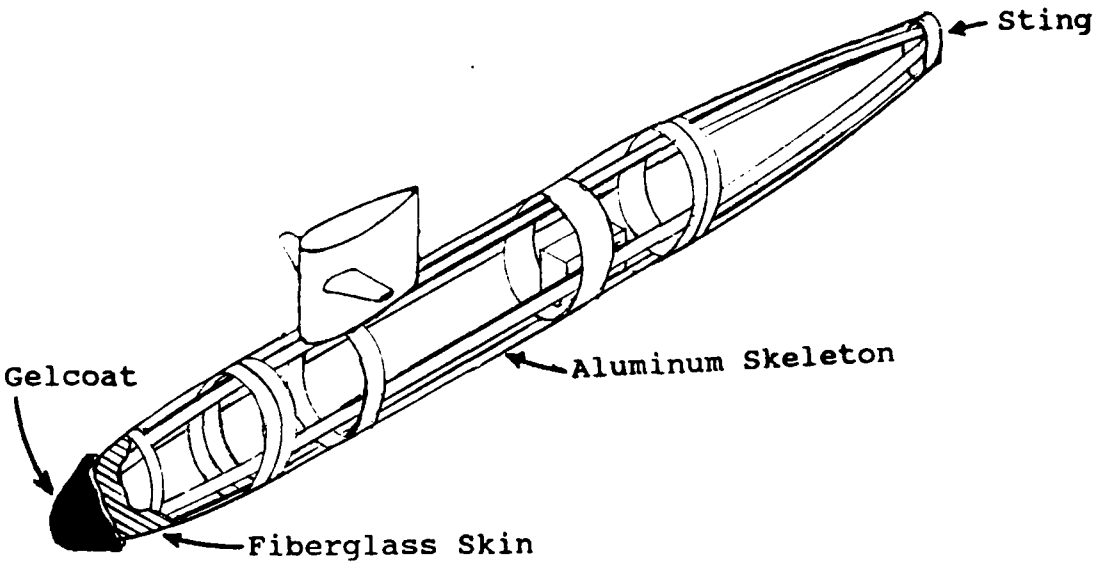

Figure 4. Model construction. The model originated as a fiberglass skin purchased from the Model Shipyard. An aluminum skeleton was added on the inside, and a gelcoat was applied to the outside.

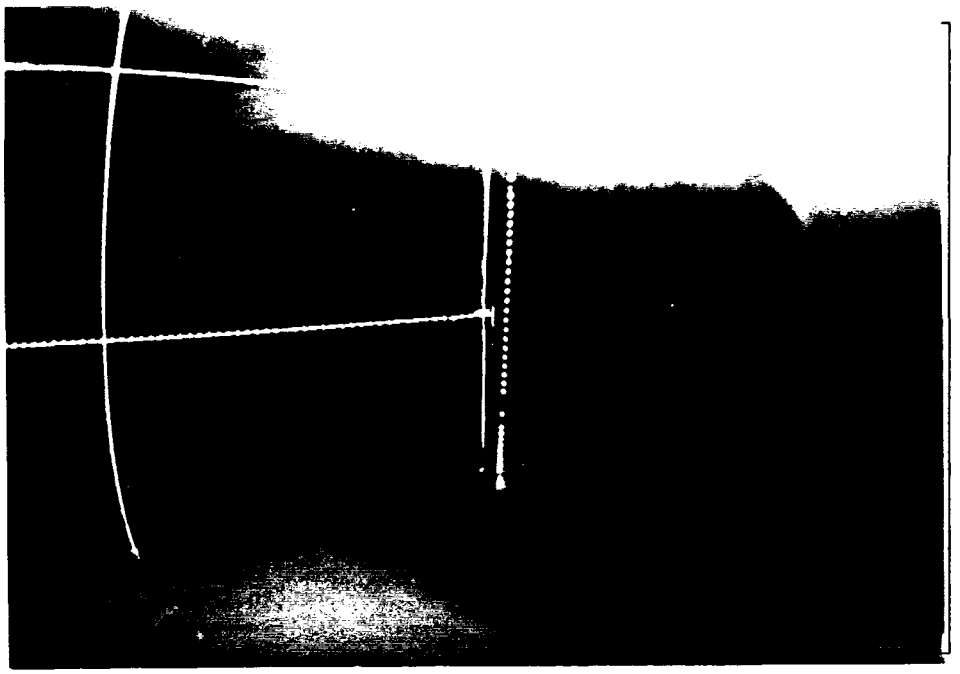

Figure 5. Trip strips. The 23 mil posts were placed circumferentially around the nose and longitudinally along $\phi = \pm 45°$ lines.

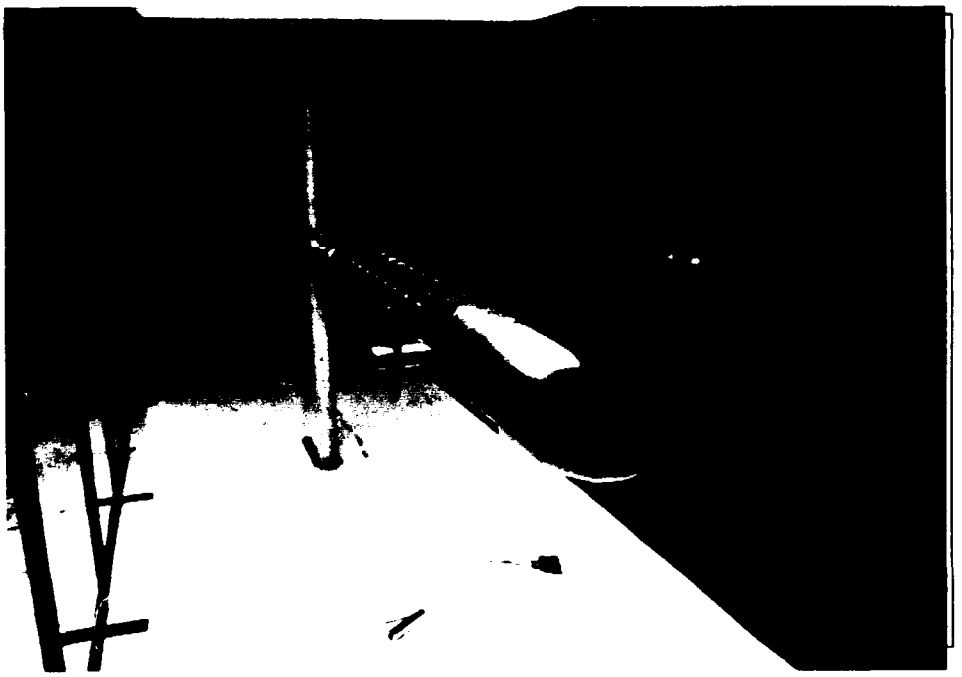

Figure 6. Model in the wind tunnel.

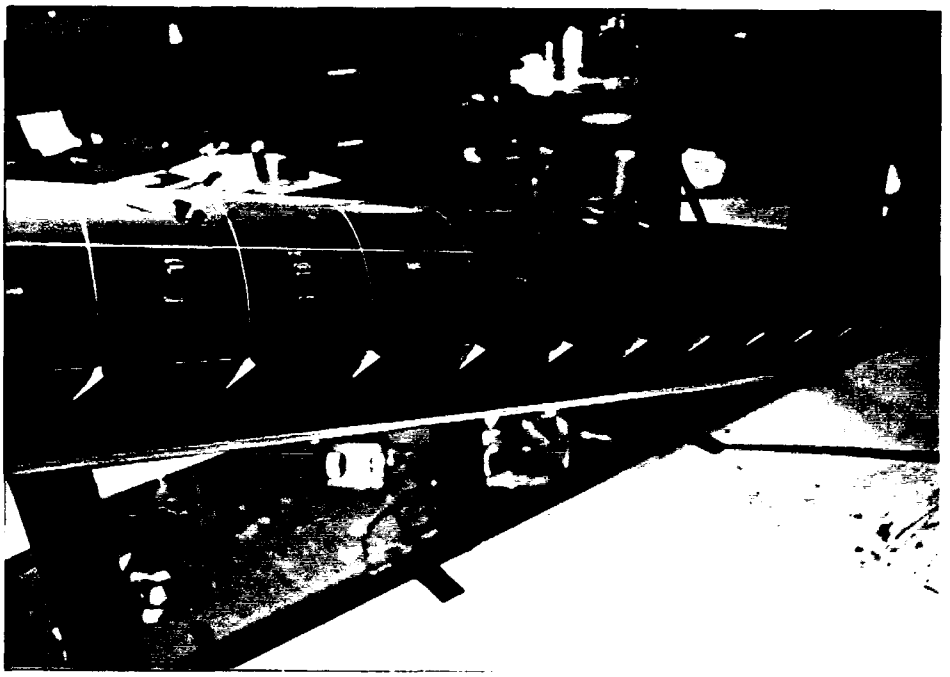

Figure 7. Vortex generators mounted on the submarine.

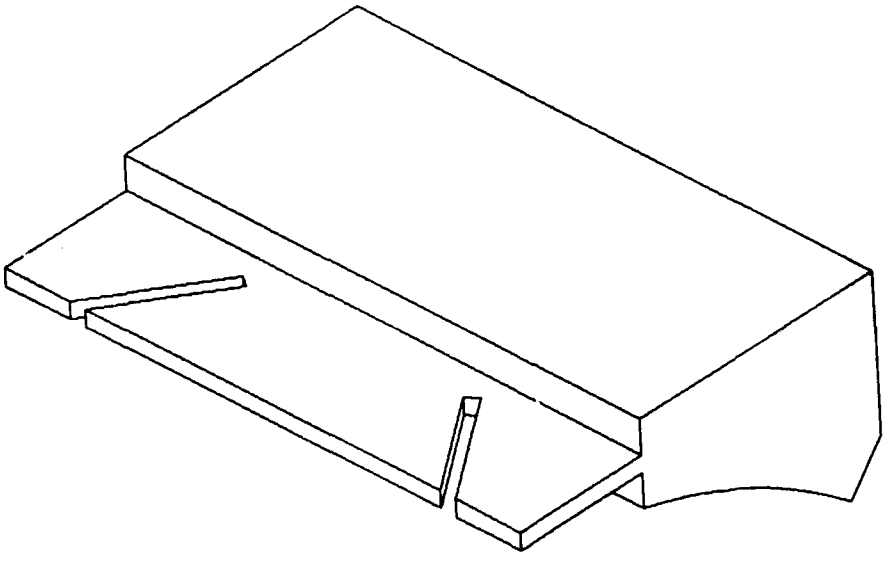

Figure 8. Jig used to mount vortex generators.

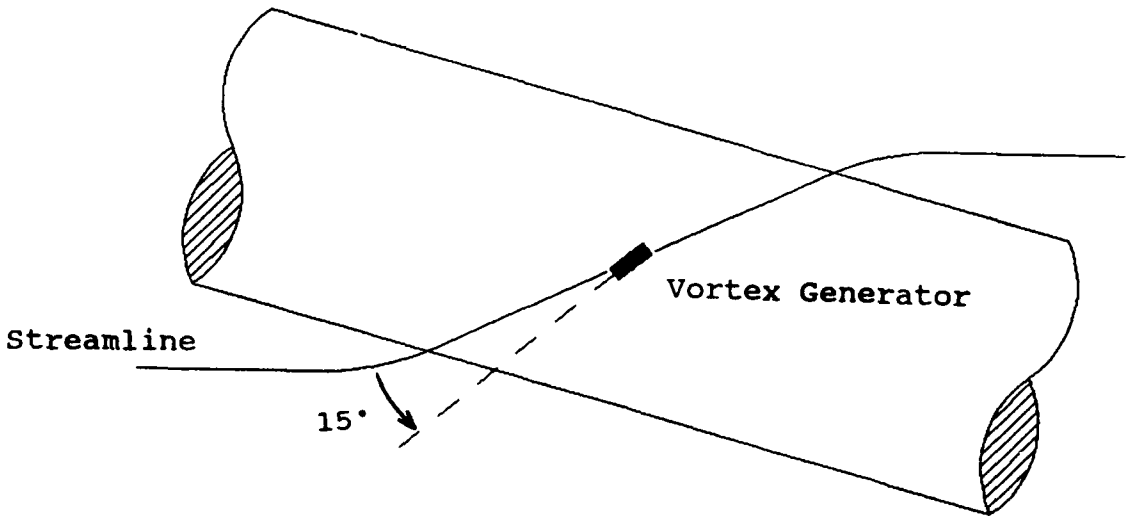

Figure 9. Orientation of vortex generators to local flow.

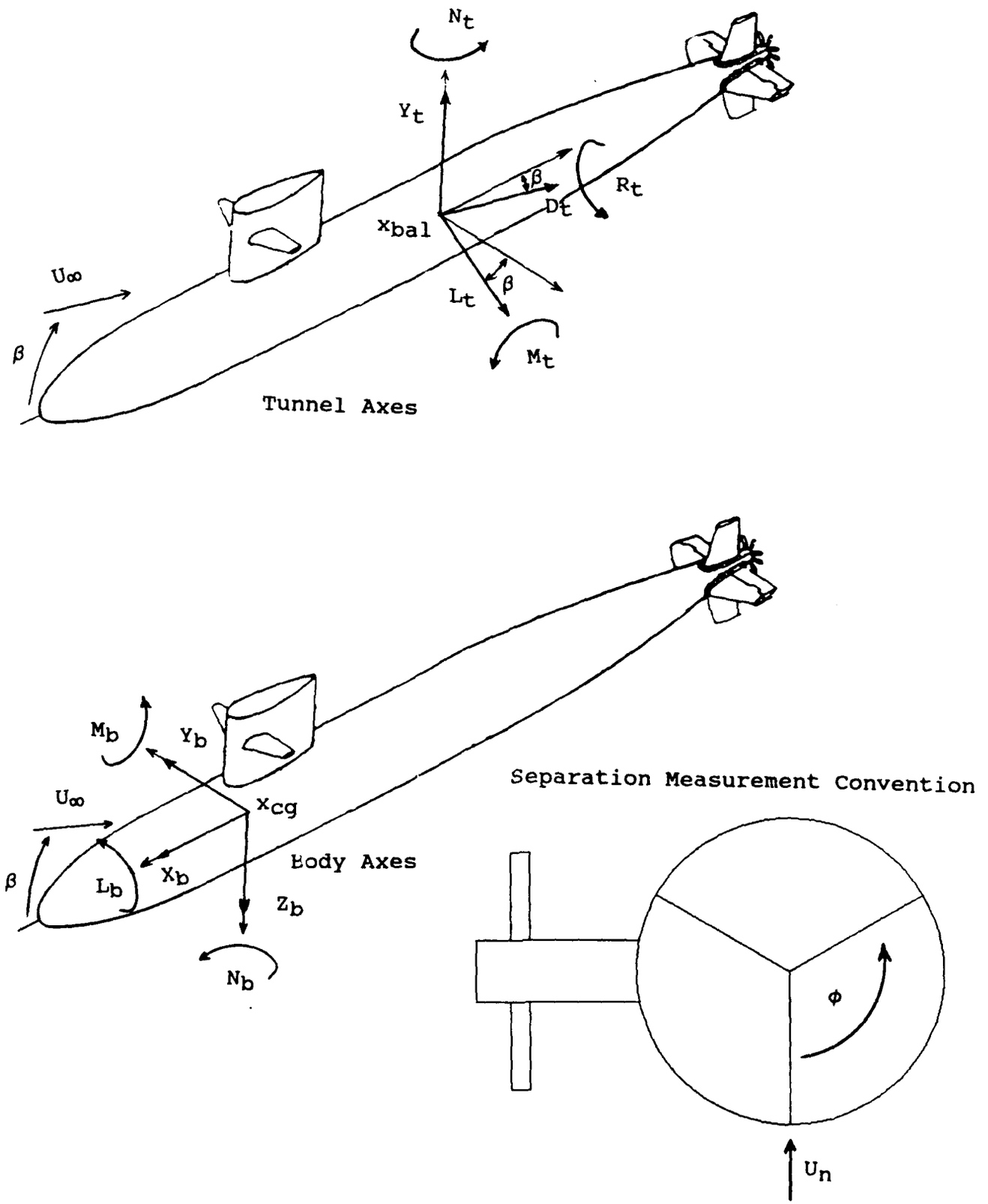

Figure 10. Force and moment conventions.

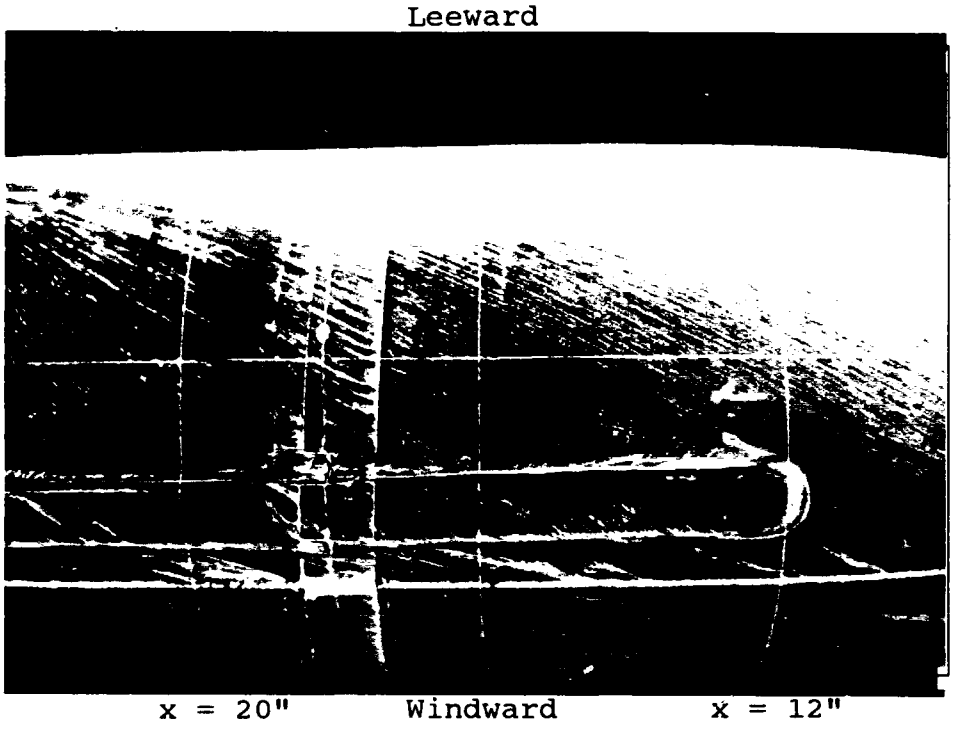

Figure 11. Oil flow 1, naked submarine, Re = 6.78×10^6, β = 15°. Leading edge of towed array housing.

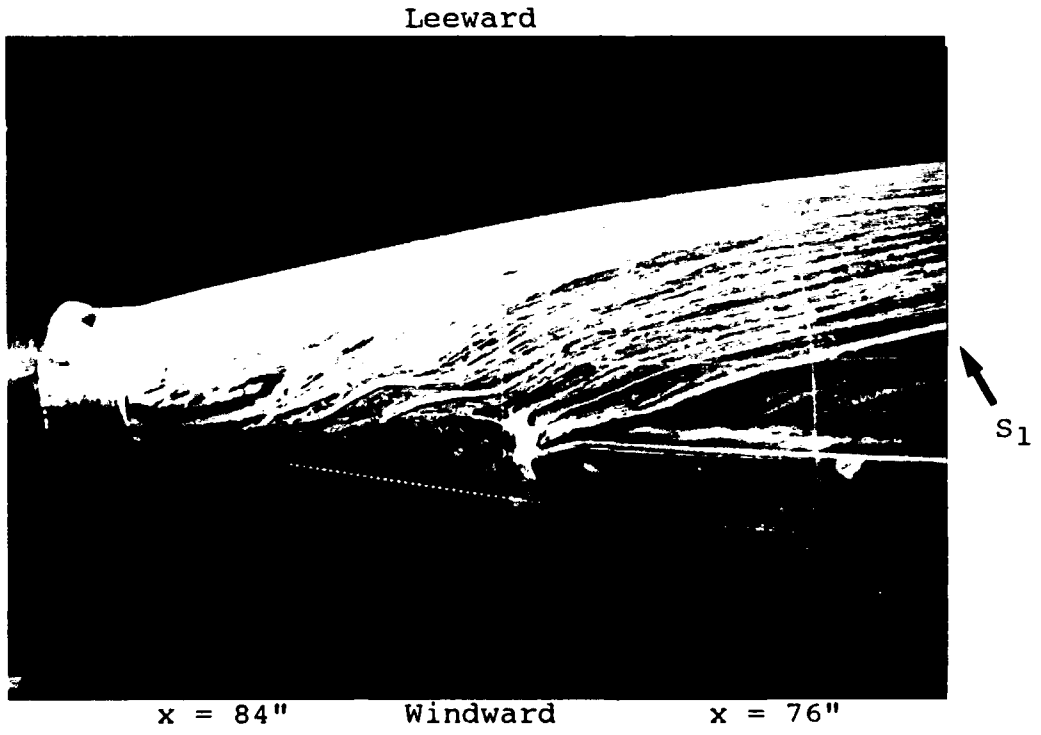

Figure 12. Oil flow 1, naked submarine, Re = 6.78×10^6, β = 15°. Trailing edge of towed array housing.

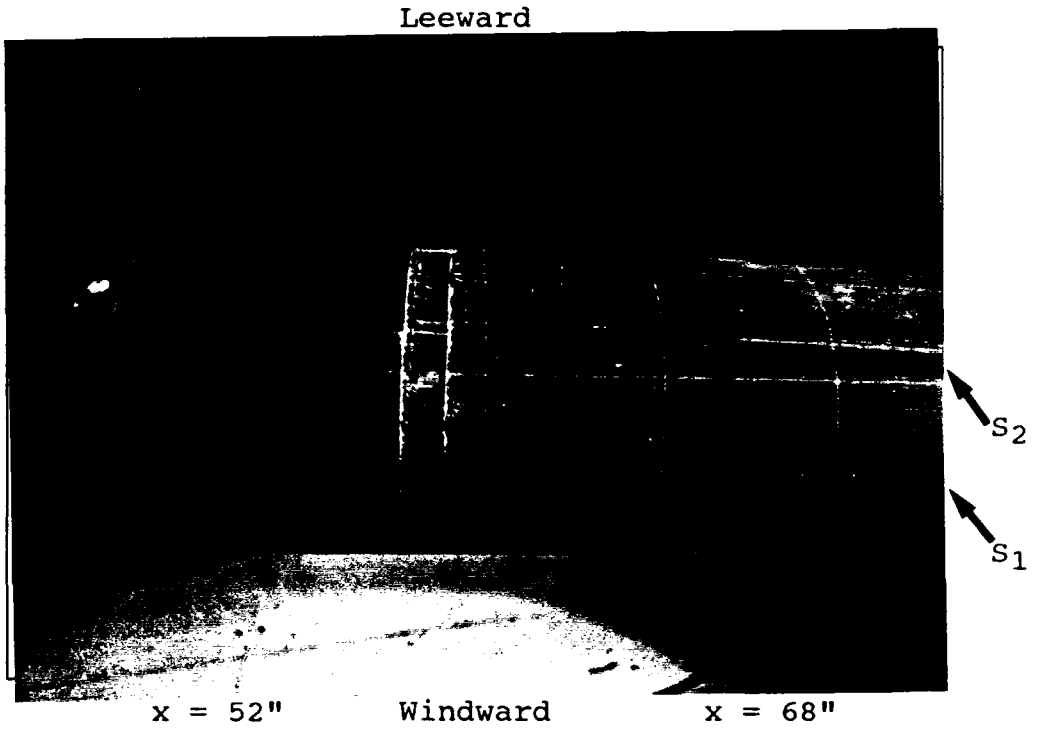

Figure 13. Oil flow 3 for naked submarine, Re = 6.78×10^6, β = 15°.

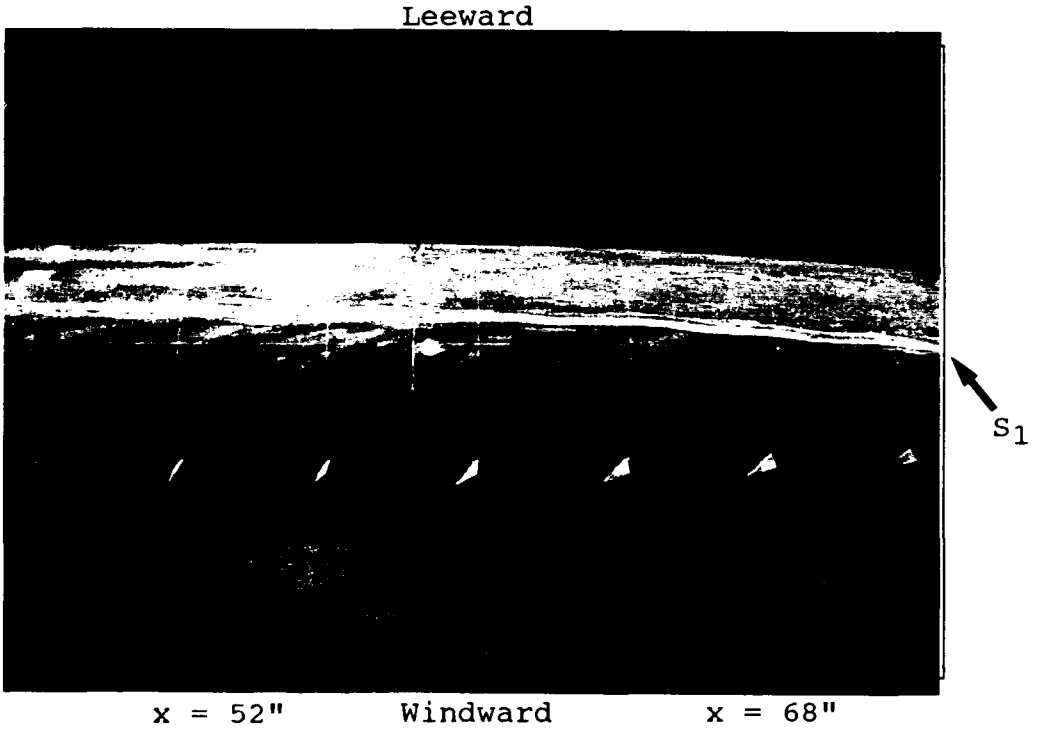

Figure 14. Oil flow 20 with vortex generators, Re = 6.43×10^6, β = 15°.

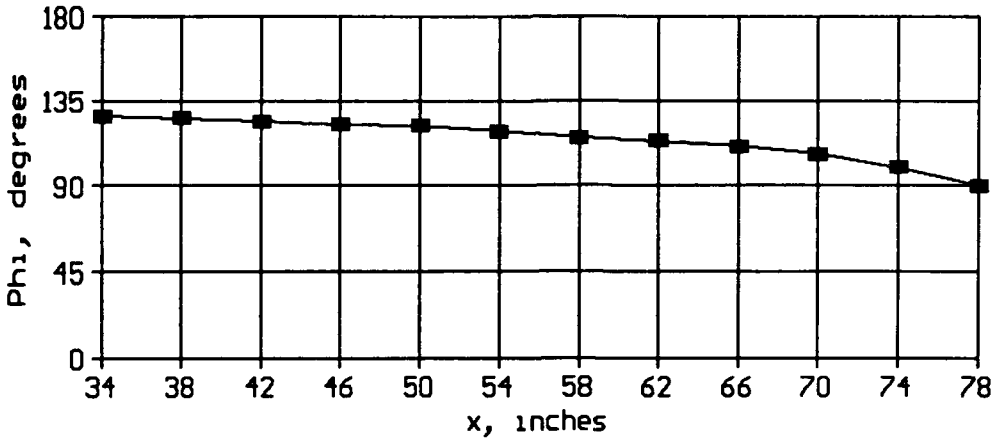

Figure 15. Separation line location from oil flow 6. Bottom side, naked submarine. Re = 6.77×10^6. β = 10°.

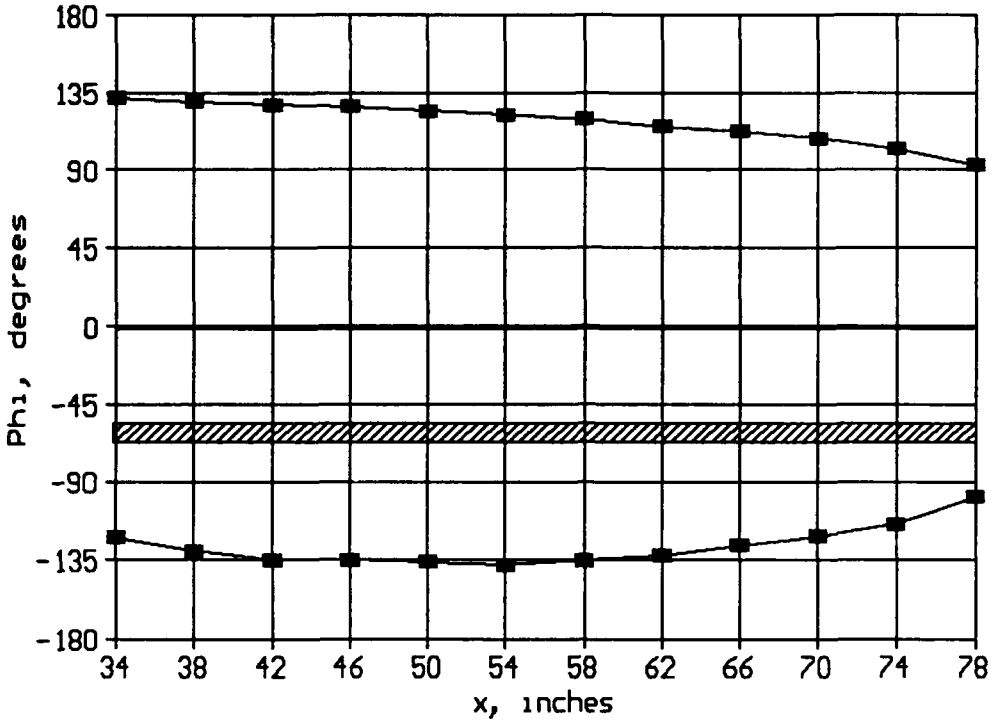

Figure 16. Separation line location from oil flow 7. Naked submarine. The shaded bar represents the towed array. Re = 6.77×10^6. $\beta = 10°$.

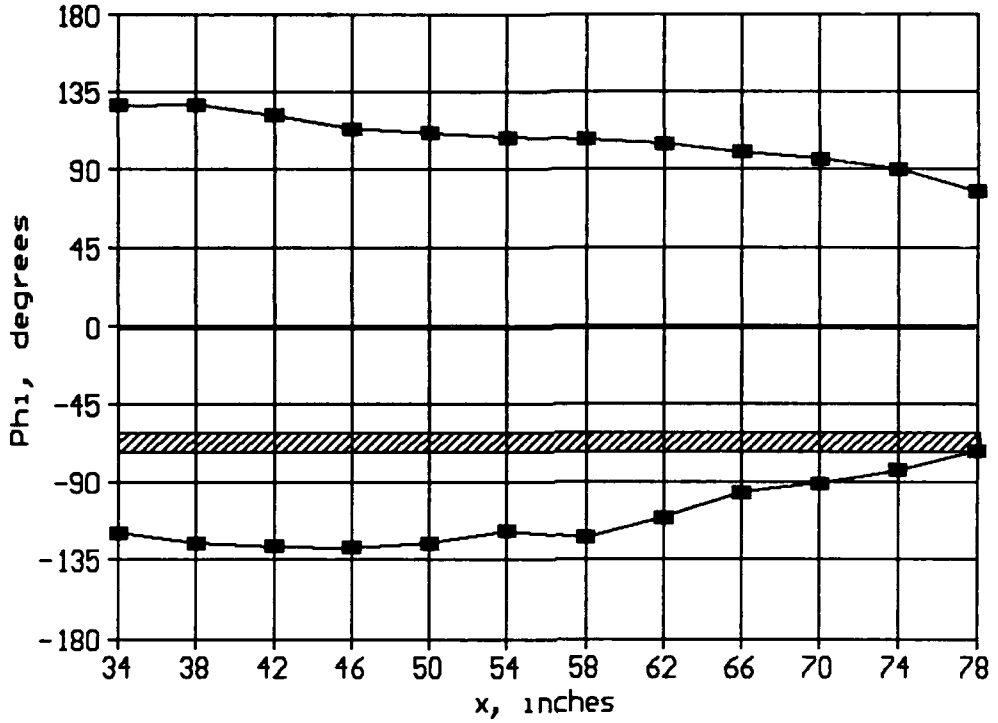

Figure 17. Separation line location from oil flow 8. Naked submarine. The shaded bar represents the towed array. Re = 4.53×10^6. β = 10°.

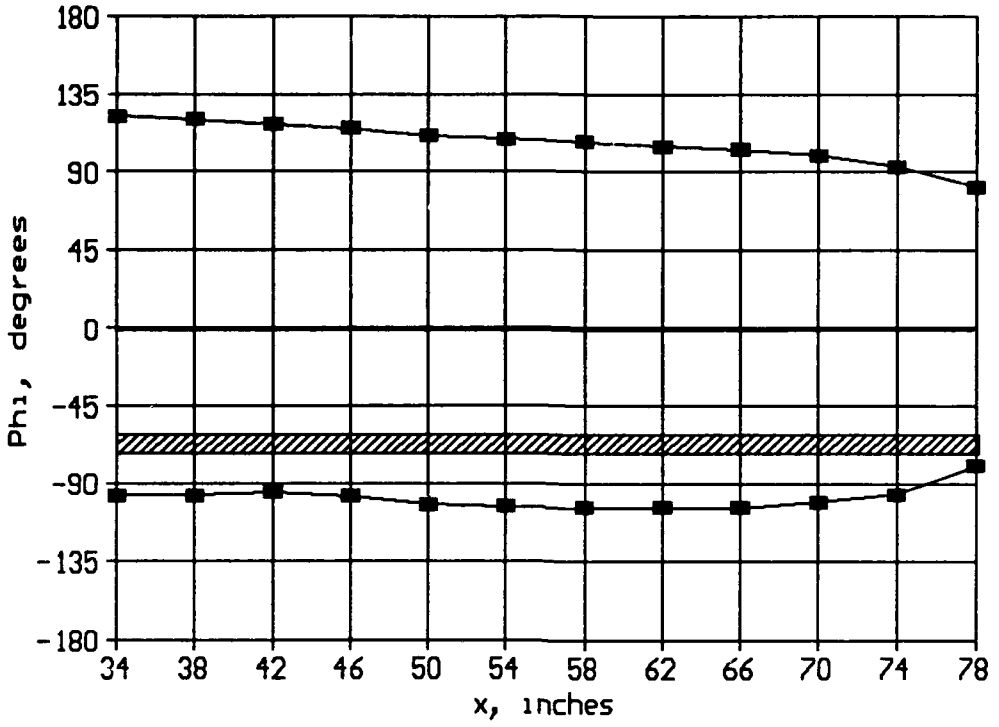

Figure 18. Separation line location from oil flow 9. Naked submarine. The shaded bar represents the towed array. Re = 6.78×10^6. β = 15°.

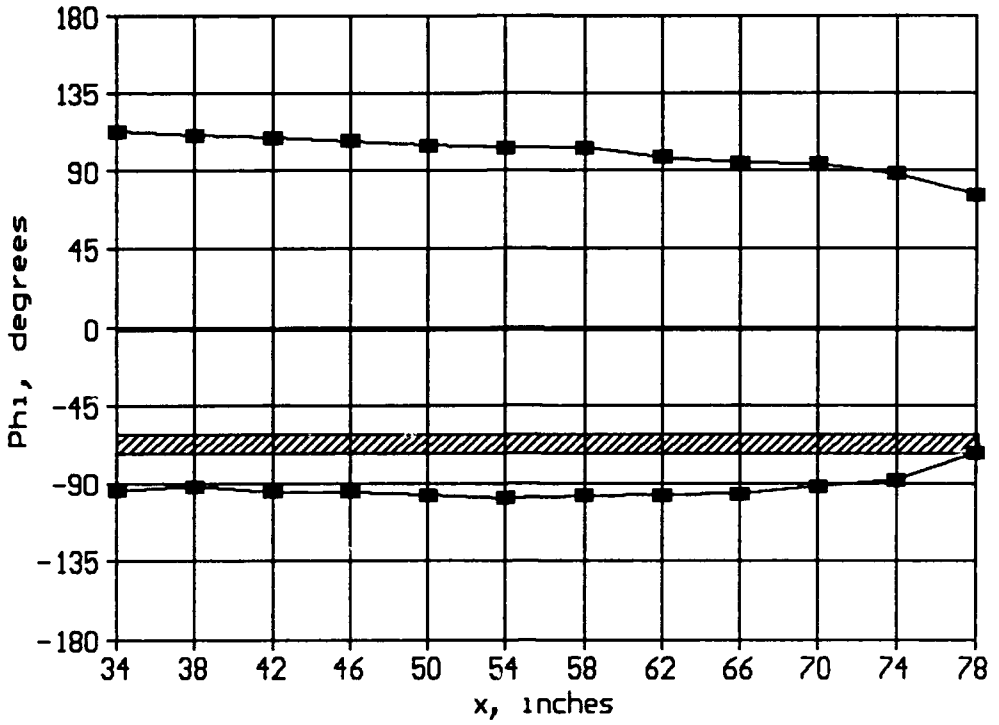

Figure 19. Separation line location from oil flow 10. Naked submarine. The shaded bar represents the towed array. Re = 4.540×10^6. β = 10°.

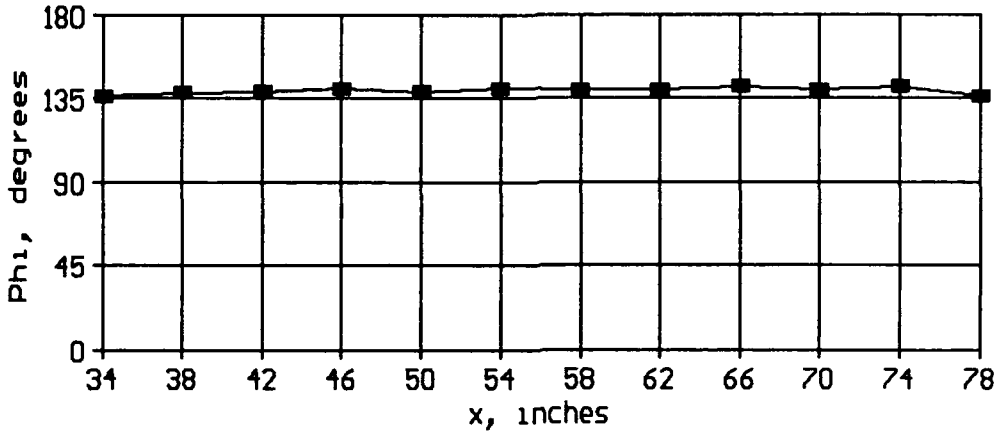

Figure 20. Separation line location from oil flow 15. Bottom side, with large vortex generators on bottom only, beginning at x = 24" and extending to x = 72". Re = 6.87×10^6. $\beta = 15°$.

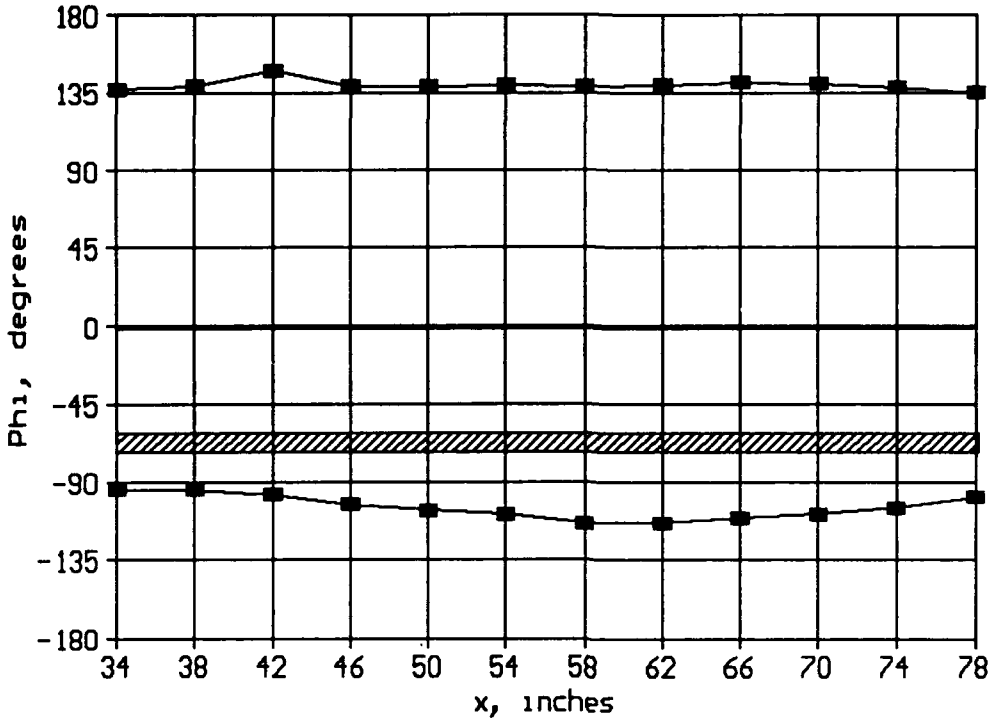

Figure 21. Separation line location from oil flow 16. On the sail side, small vortex generators at ϕ = -60° extend from x = 12" to x = 76". On the bottom side, large vortex generators extend from x = 24" to x = 72". The shaded bar represents the towed array. Re = 6.79×10^6. β = 15°.

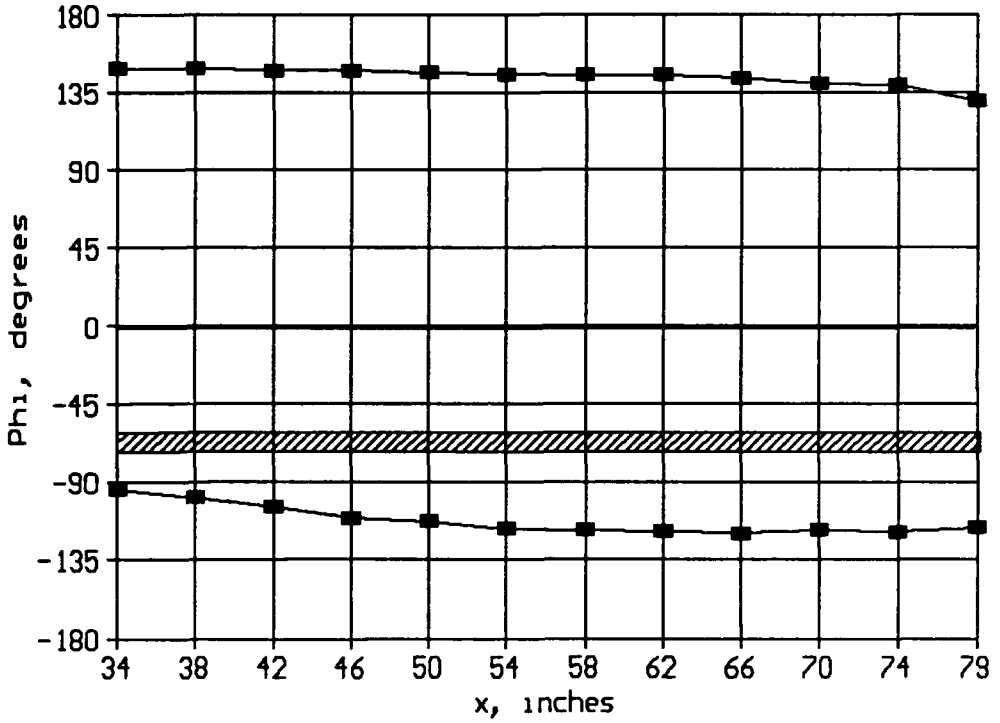

Figure 22. Separation line location from oil flow 17. On the sail side, small vortex generators relocated to ϕ = 90° extend from x = 12" to x = 76". On the bottom side, large vortex generators extend from x = 12" to x = 76". The shaded bar represents the towed array. Re = 6.81×10^6. β = 15°.

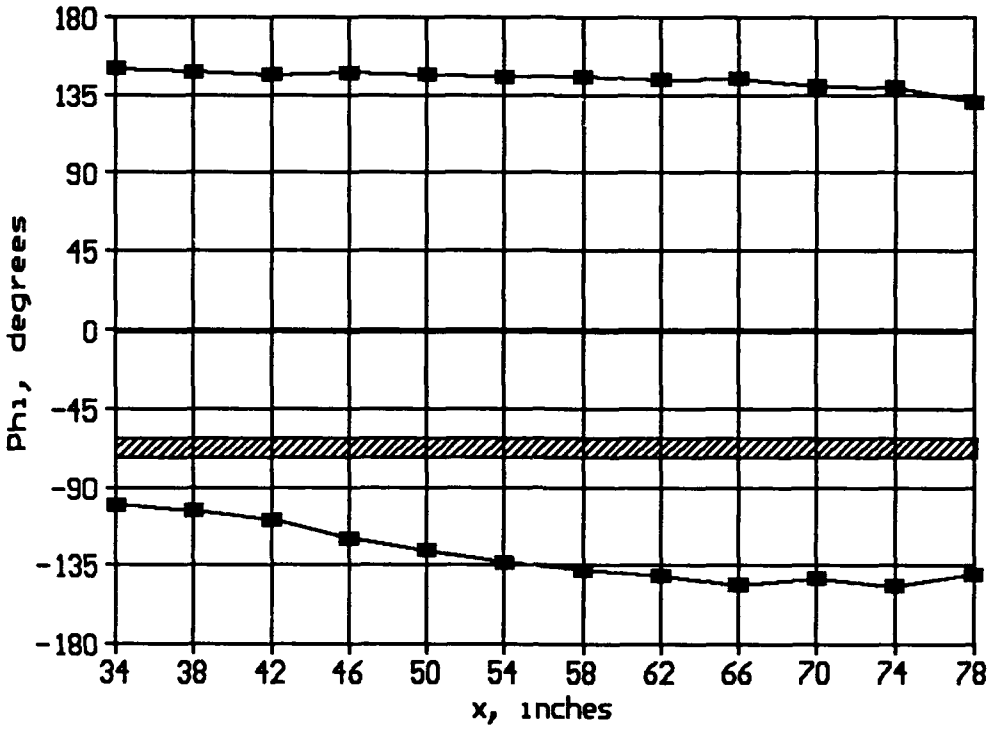

Figure 23. Separation line location from oil flow 19. On both sides, large vortex generators extend from x = 8" to x = 80", with two additional vortex generators at x = 8", ϕ = ±135°, and inclined 30° off horizontal. The shaded bar represents the towed array. Re = 6.48×10^6. β = 15°.

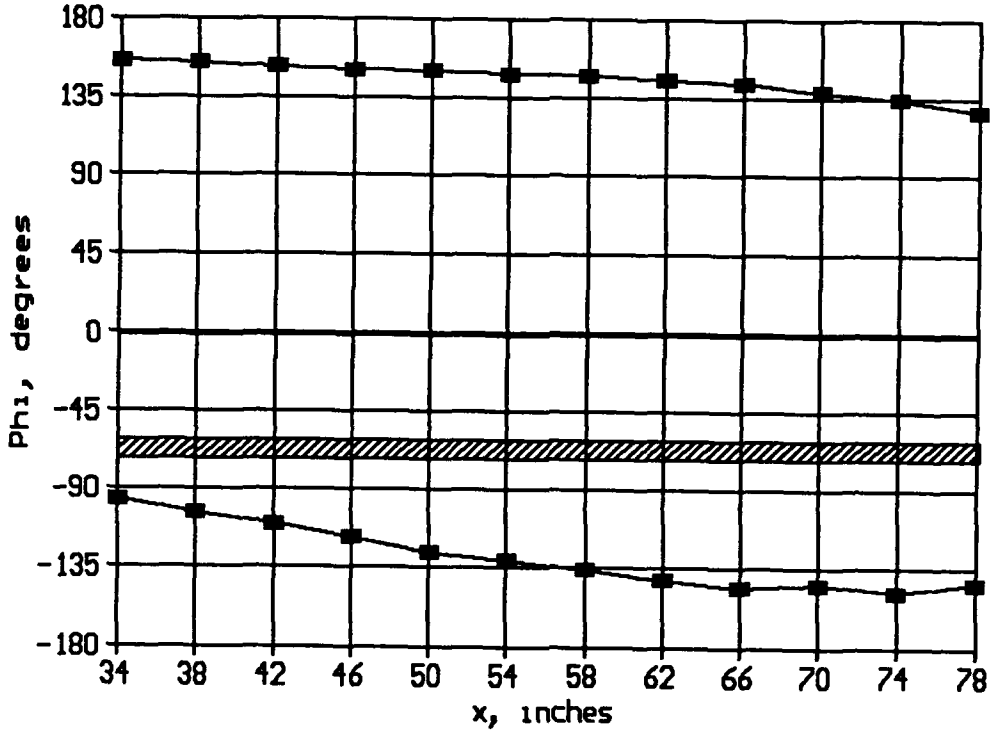

Figure 24. Separation line location from oil flow 20. On both sides, large vortex generators extend from x = 8" to x = 80", with two additional vortex generators at x = 8", ϕ = ±135°, and inclined 55° off horizontal. The shaded bar represents the towed array. Re = 6.43×10^6. β = 15°.

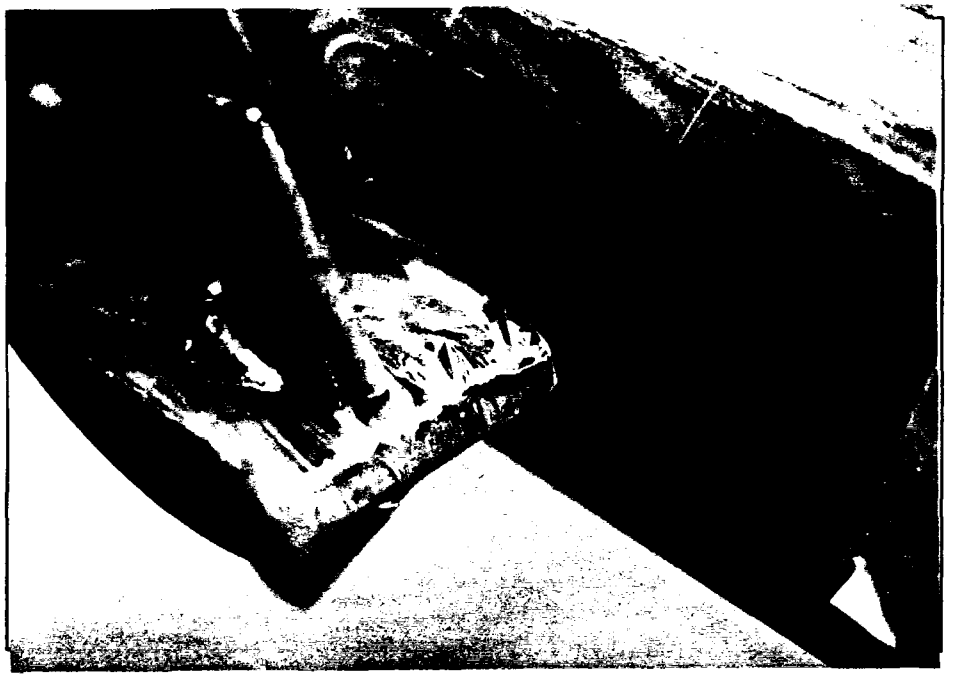

Figure 25. Oil flow 23, Re = 6.65×10^6, β = 15°. Note small vortex generators on sail.

Bottom

Figure 26. Oil flow 24, Re = 6.77×10^6, β = 15°. Note small vortex generators on leading edge of sail.

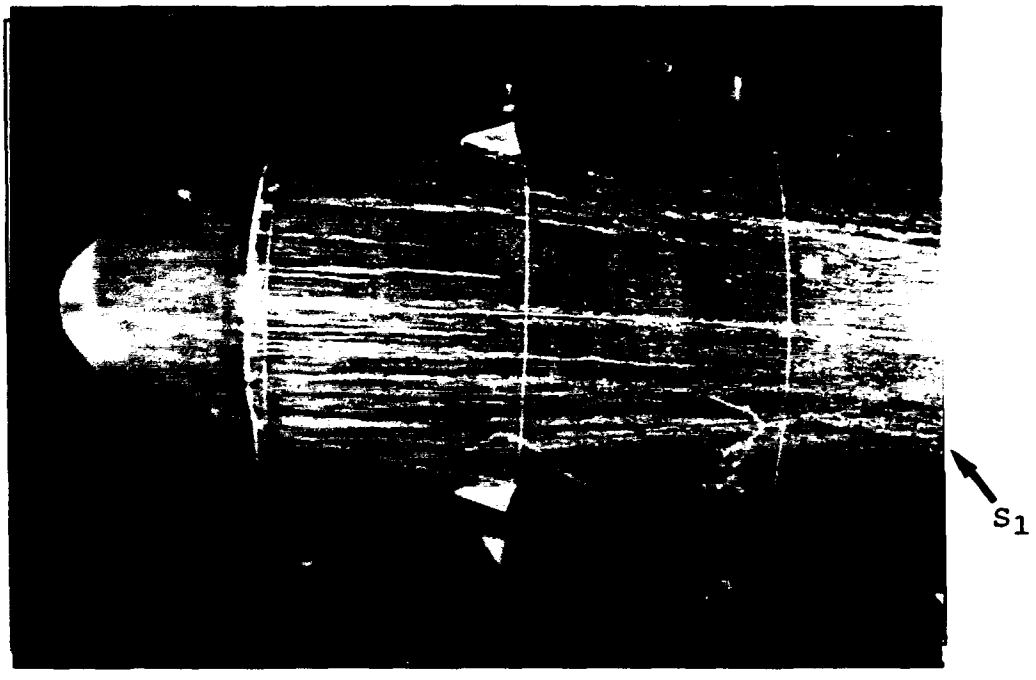

Figure 27. Oil flow 19, top view. Re = 6.48×10^6, β = 15°.

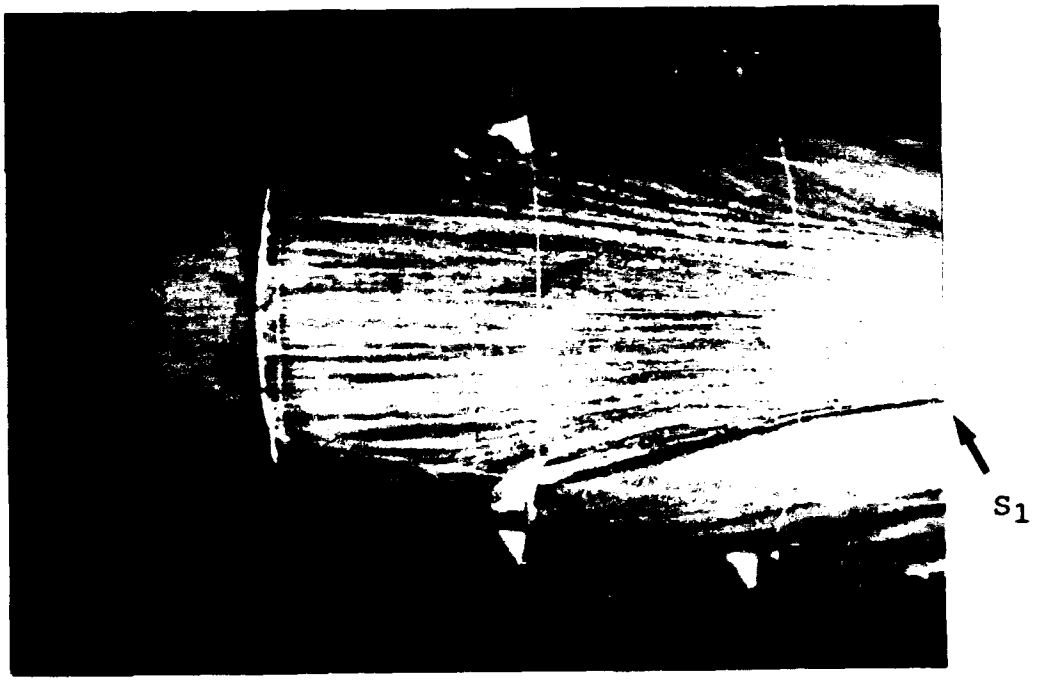

Figure 28. Oil flow 20, top view. Re = 6.43×10^6, β = 15°.

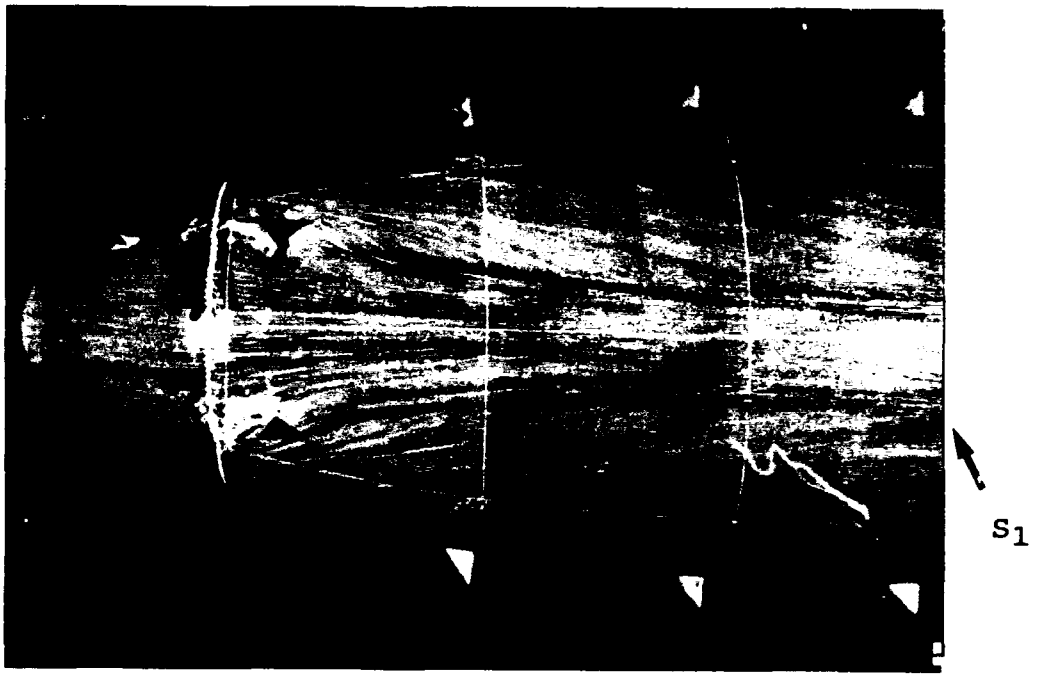

Figure 29. Oil flow 21, top view. Re = 6.65×10^6, β = 15°.

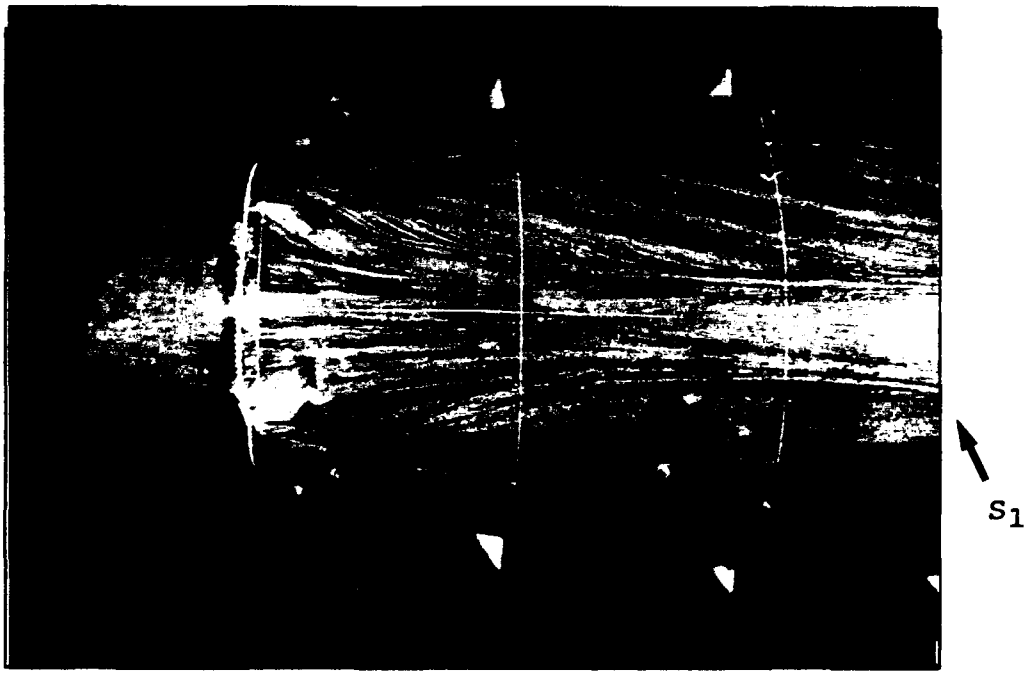

Figure 30. Oil flow 22, top view. Re = 6.43×10^6, β = 15°.

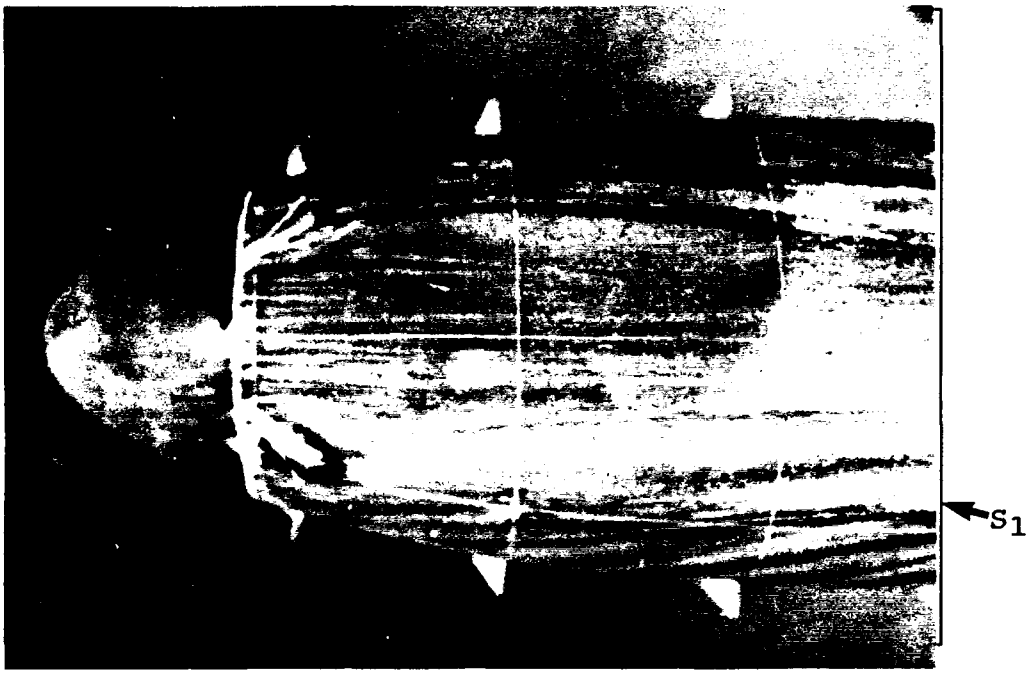

Figure 31. Oil flow 23, top view. Re = 6.48×10^6, β = 15°.

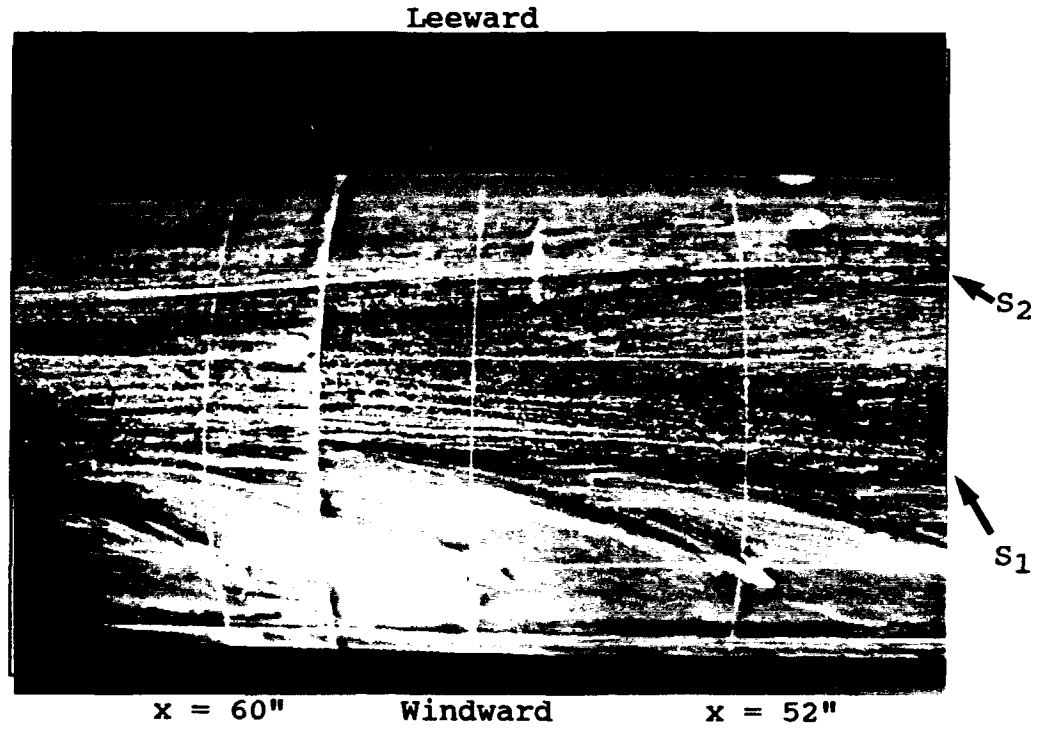

Figure 32. Oil flow 17. Separation line sample for 0.5" high vortex generators. Re = 6.78×10^6, $\beta = 15°$.

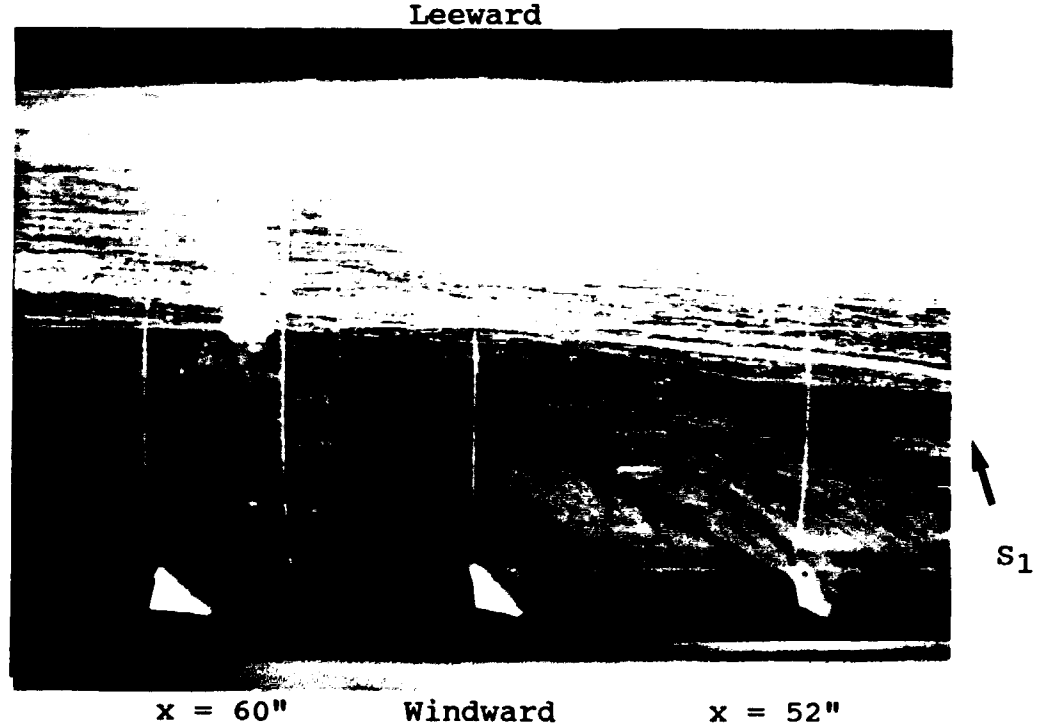

Figure 33. Oil flow 18. Separation line sample for 1" high vortex generators. Re = 6.43×10^6, $\beta = 15°$.

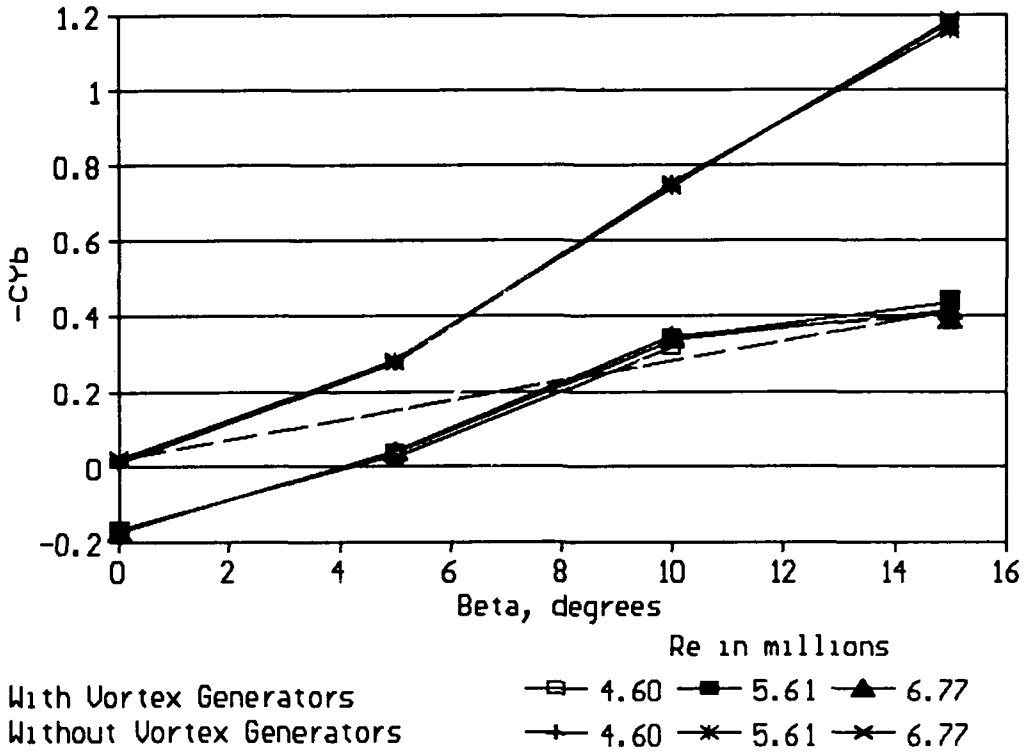

Figure 34. Normal side force coefficient versus ß for different Re. The naked submarine data come from runs 52.00 through 52.33, which includes oil flows 1 through 14. The data for the submarine with vortex generators come from runs 31.00 through 31.23, which utilized the same vortex generators configuration as oil flow 22. The dashed line is the approximated curve for a variable vortex generator configuration. Connecting lines shown for visual aid only.

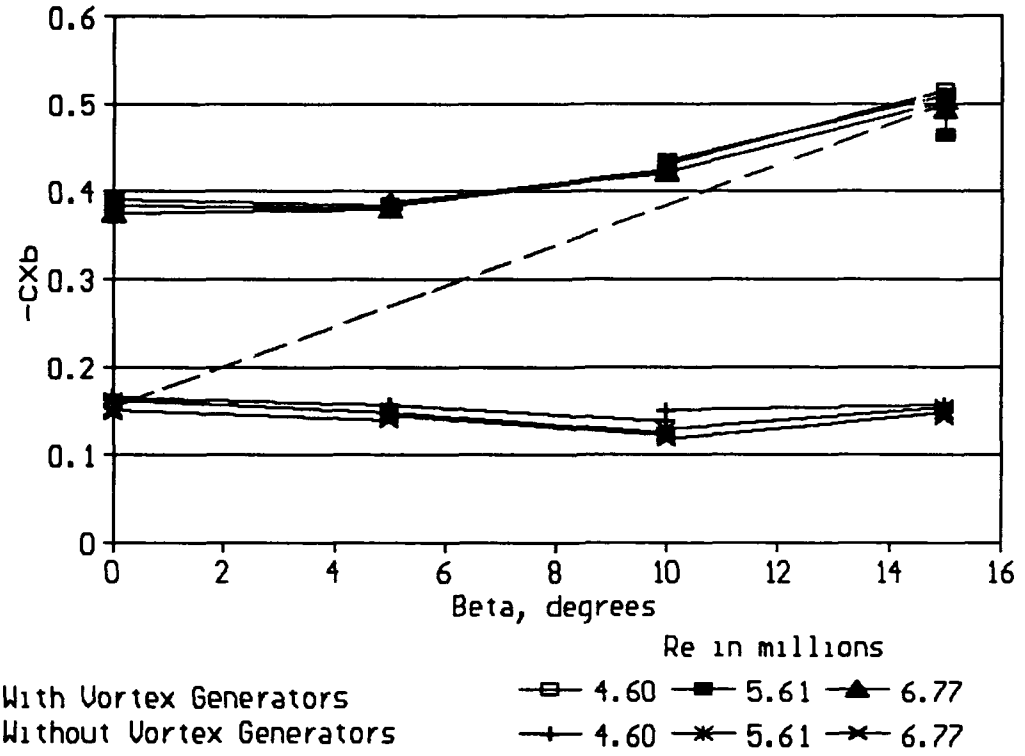

Figure 35. Axial force coefficient versus ß. The naked submarine data come from runs 52.00 through 52.33, which includes oil flows 1 through 14. The data for the submarine with vortex generators come from runs 31.00 through 31.23, which utilized the same vortex generators configuration as oil flow 22. The dashed line is the approximated curve for a variable vortex generator configuration. Connecting lines shown for visual aid only.

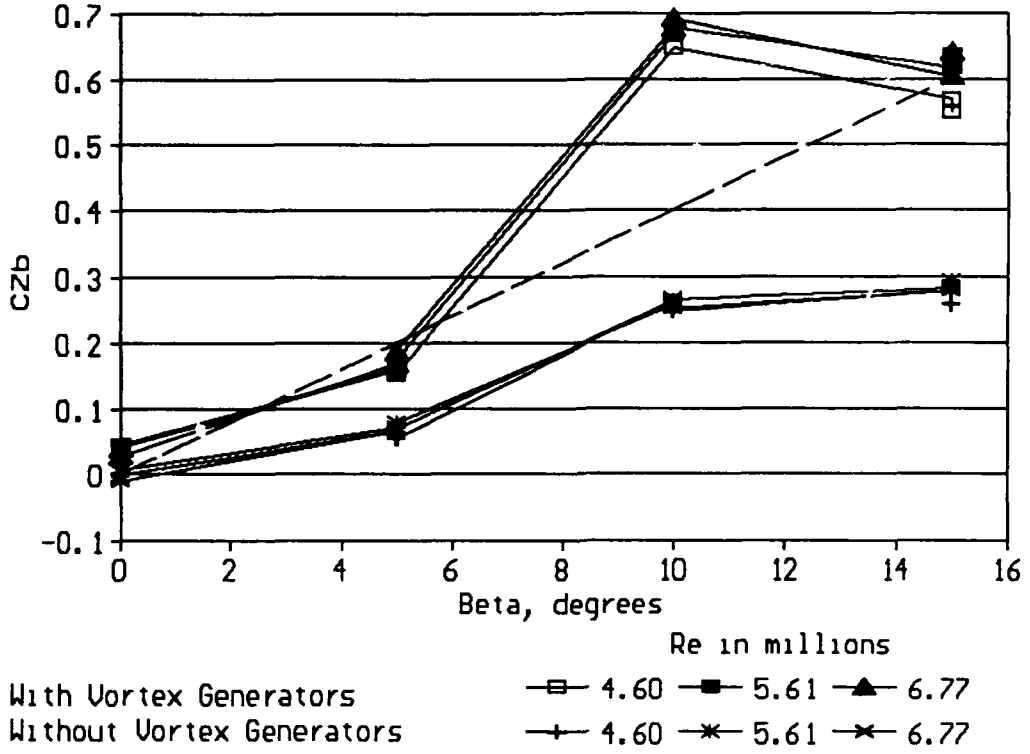

Figure 36. Vertical force coefficient versus ß. The naked submarine data come from runs 52.00 through 52.33, which includes oil flows 1 through 14. The data for the submarine with vortex generators come from runs 31.00 through 31.23, which utilized the same vortex generators configuration as oil flow 22. Connecting lines shown for visual aid only.

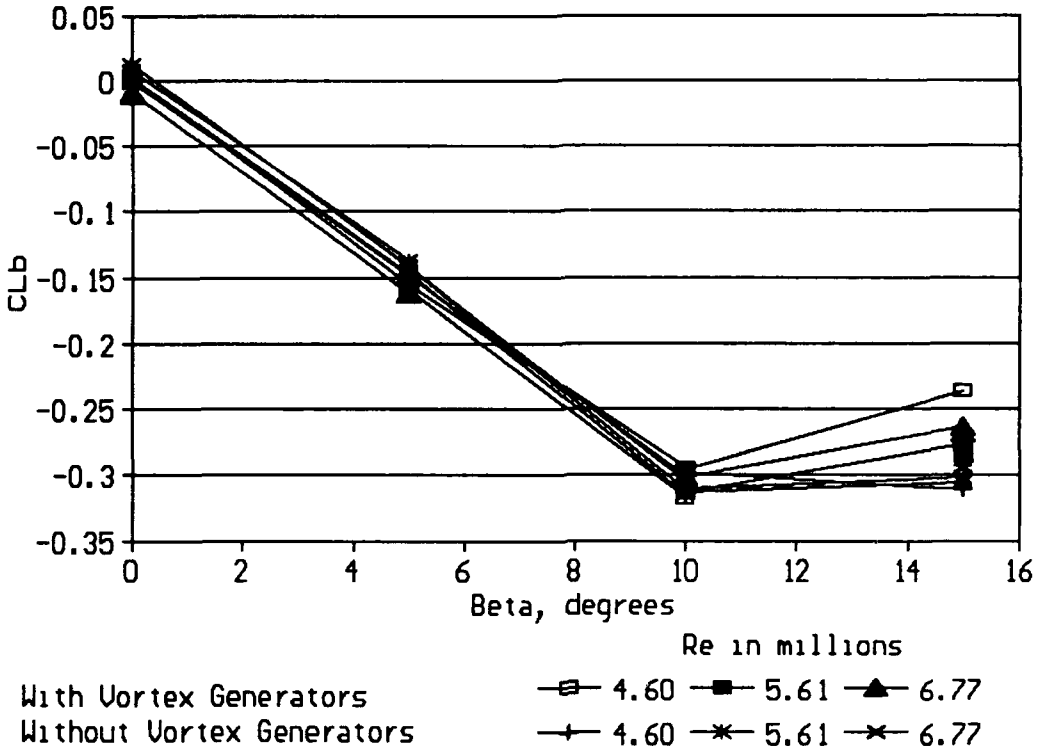

Figure 37. Roll moment coefficient versus ß. The naked submarine data come from runs 52.00 through 52.33, which includes oil flows 1 through 14. The data for the submarine with vortex generators come from runs 31.00 through 31.23, which utilized the same vortex generators configuration as oil flow 22. Connecting Lines shown for visual aid only.

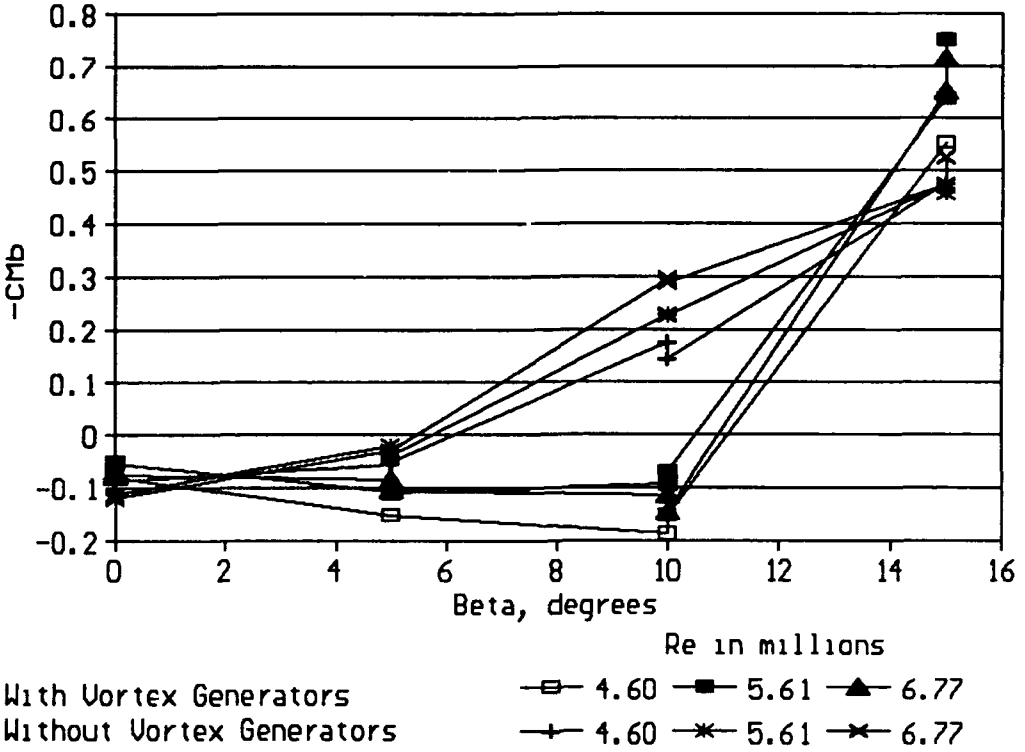

Figure 38. Pitching moment coefficient versus ß. The naked submarine data come from runs 52.00 through 52.33, which includes oil flows 1 through 14. The data for the submarine with vortex generators come from runs 31.00 through 31.23, which utilized the same vortex generators configuration as oil flow 22. Connecting lines for visual aid only.

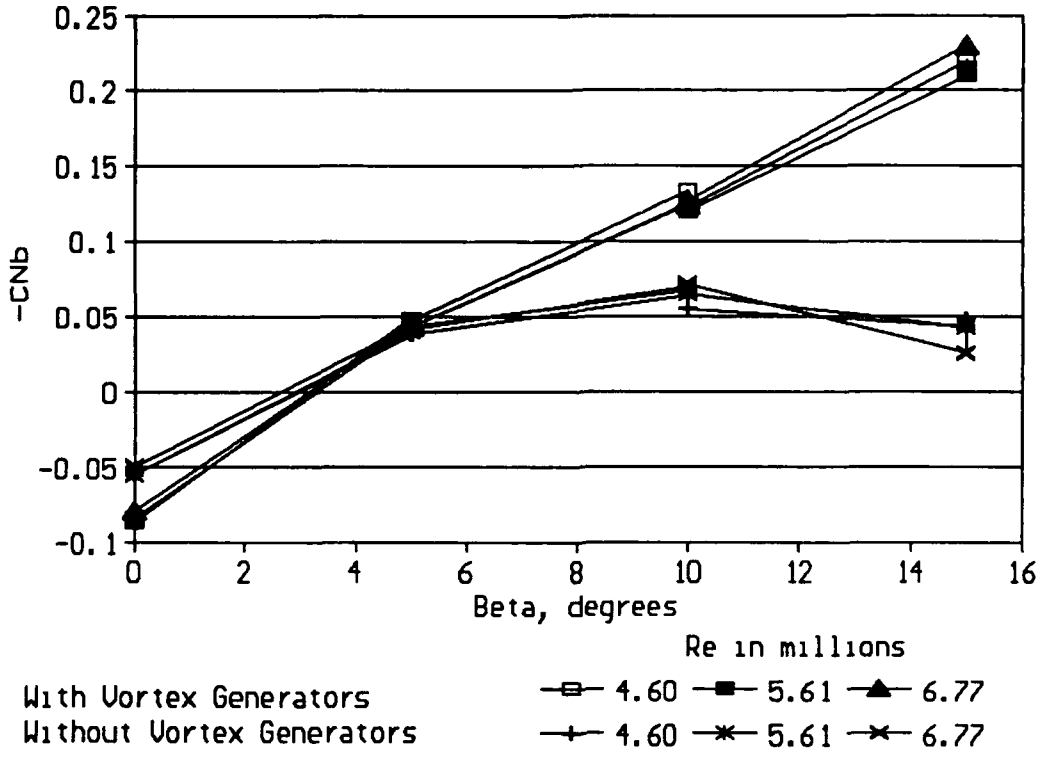

Figure 39. Yaw moment coefficient versus ß. The naked submarine data come from runs 52.00 through 52.33, which includes oil flows 1 through 14. The data for the submarine with vortex generators come from runs 31.00 through 31.23, which utilized the same vortex generators configuration as oil flow 22. The dashed line is the approximated curve for a variable vortex generator configuration. Connecting lines shown for visual aid only.

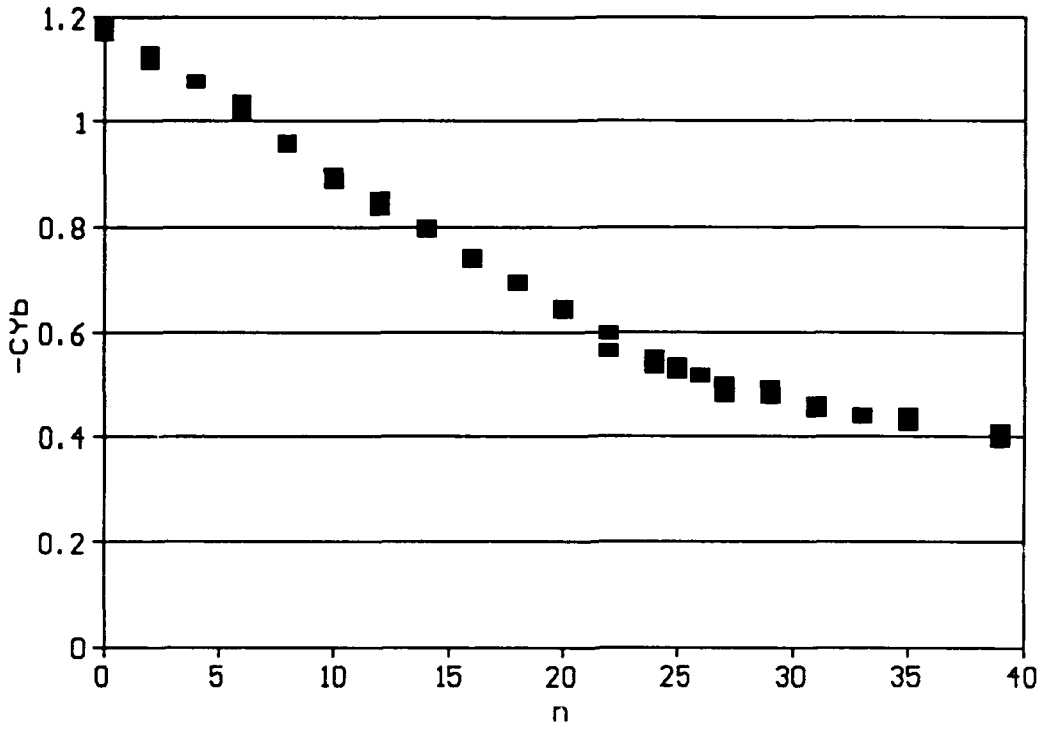

Figure 40. Normal force coefficient versus number of vortex generators. Data from runs 31 through 52. Re = 6.77x10, ß = 15°.

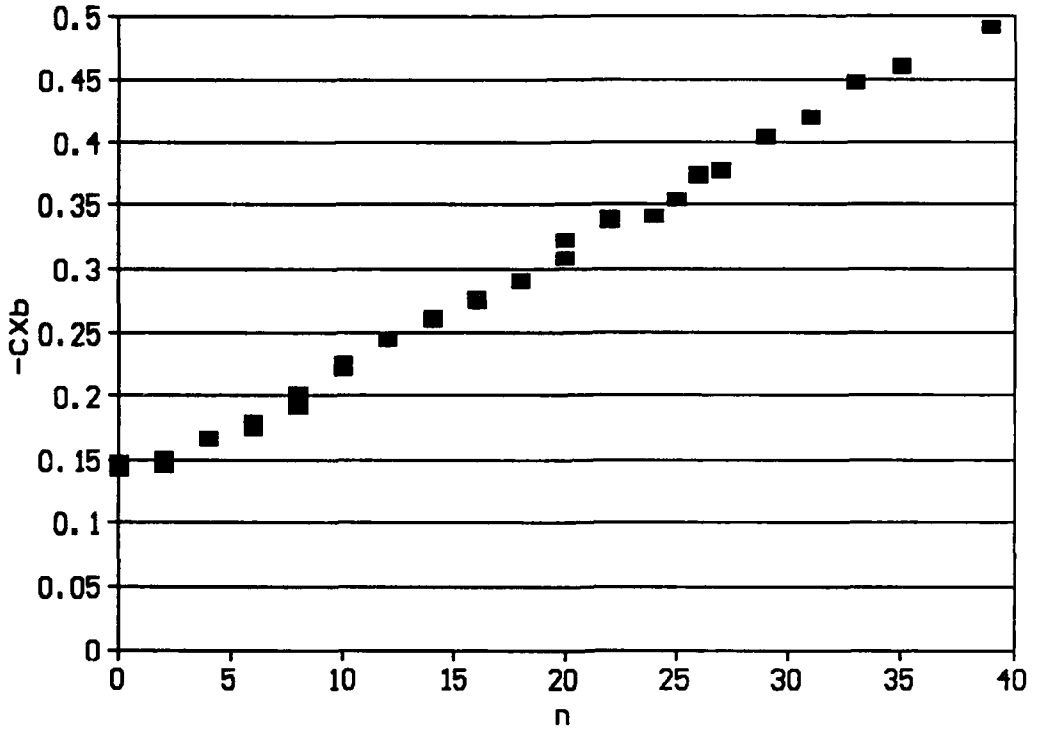

Figure 41. Axial force coefficient versus number of vortex generators. Data from runs 31 through 52. Re = 6.77x10, ß = 15°.

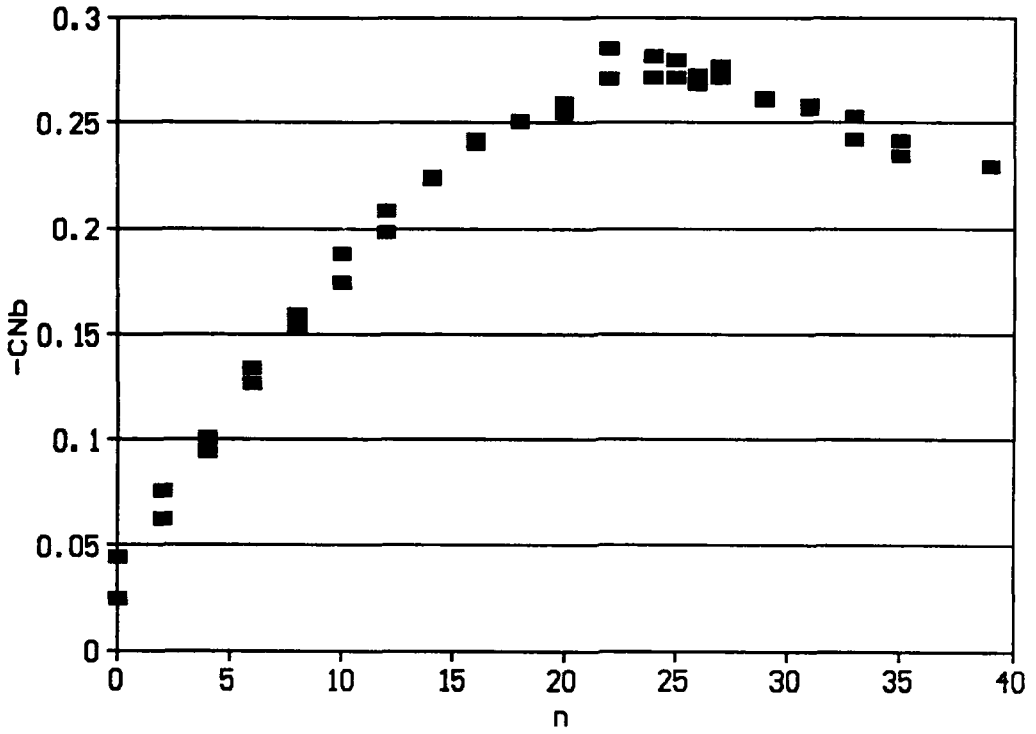

Figure 42. Yaw moment coefficient versus number of vortex generators. Data from runs 31 through 52. Re = 6.77x10, ß = 15°.

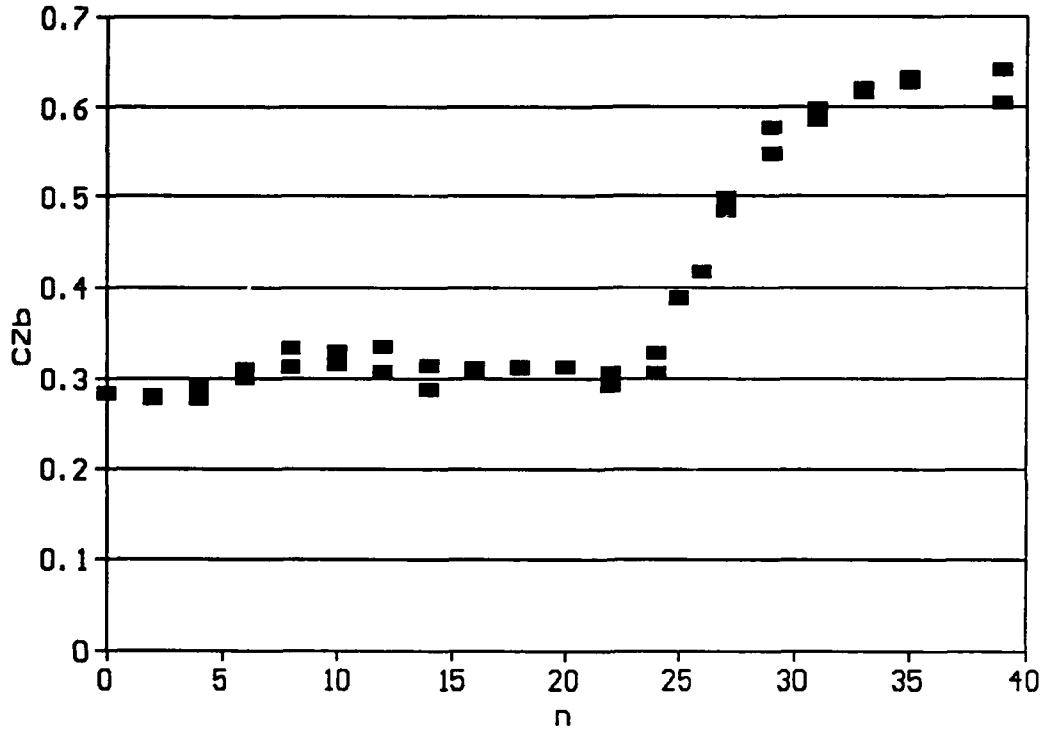

Figure 43. Vertical force coefficient versus number of vortex generators. Data from runs 31 through 52. Re = 6.77x10, ß = 15°.

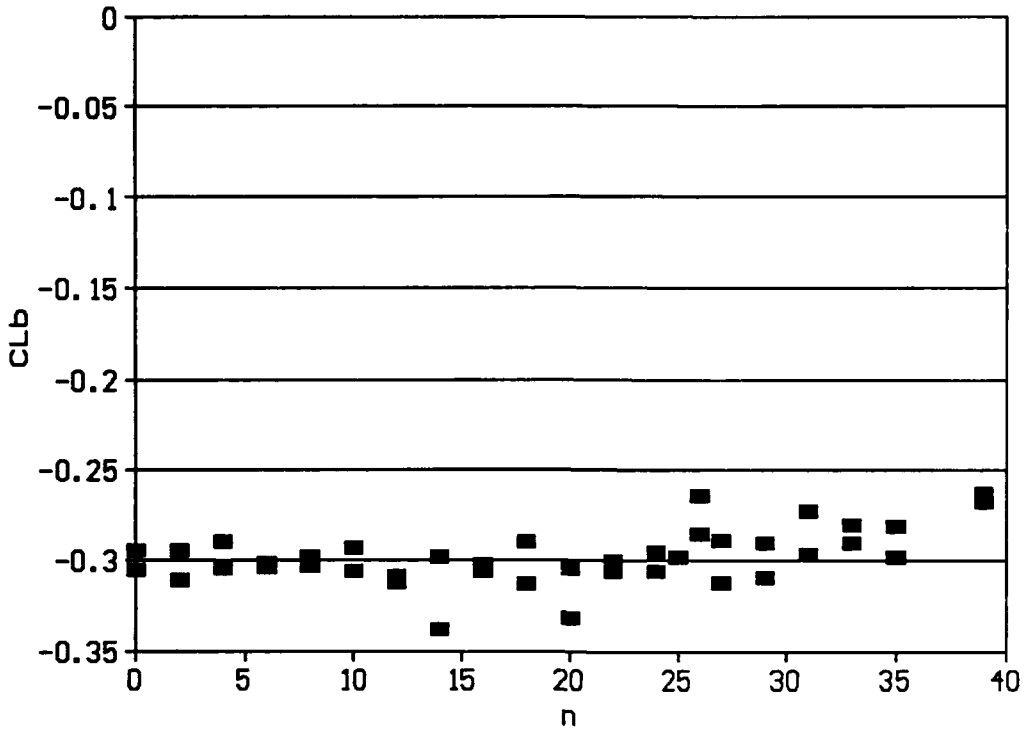

Figure 44. Roll moment coefficient versus number of vortex generators. Data from runs 31 through 52. Re = 6.77x10, ß = 15°.

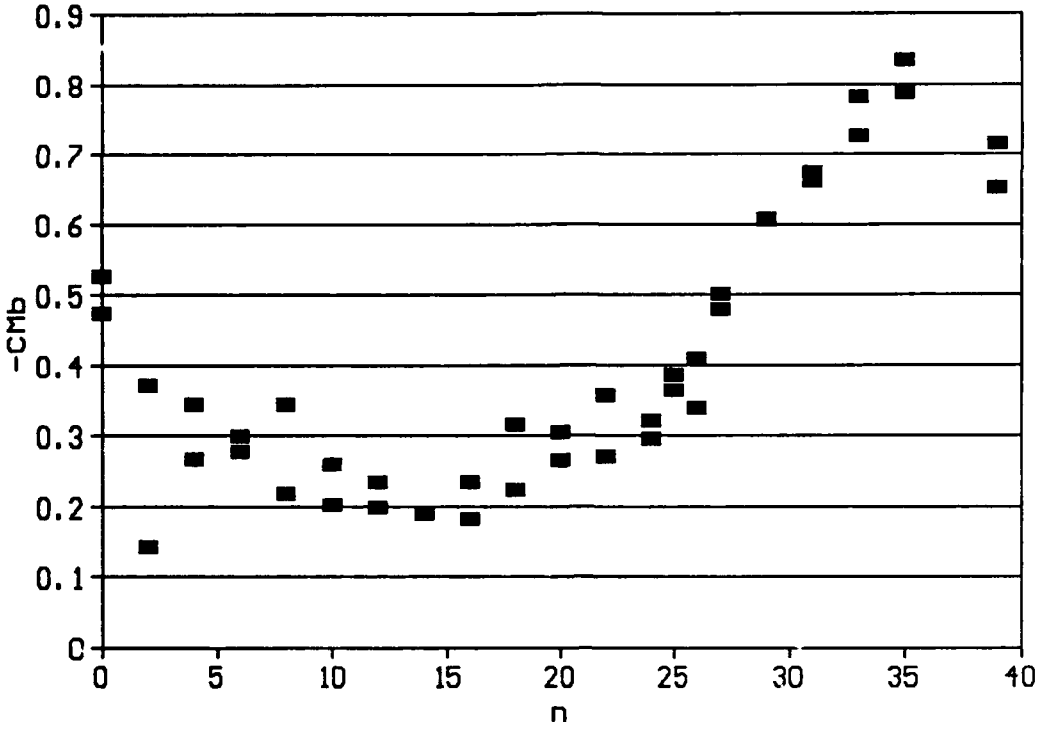

Figure 45. Pitching moment coefficient versus number of vortex generators. Data from runs 31 through 52. Re = 6.77x10, β = 15°.

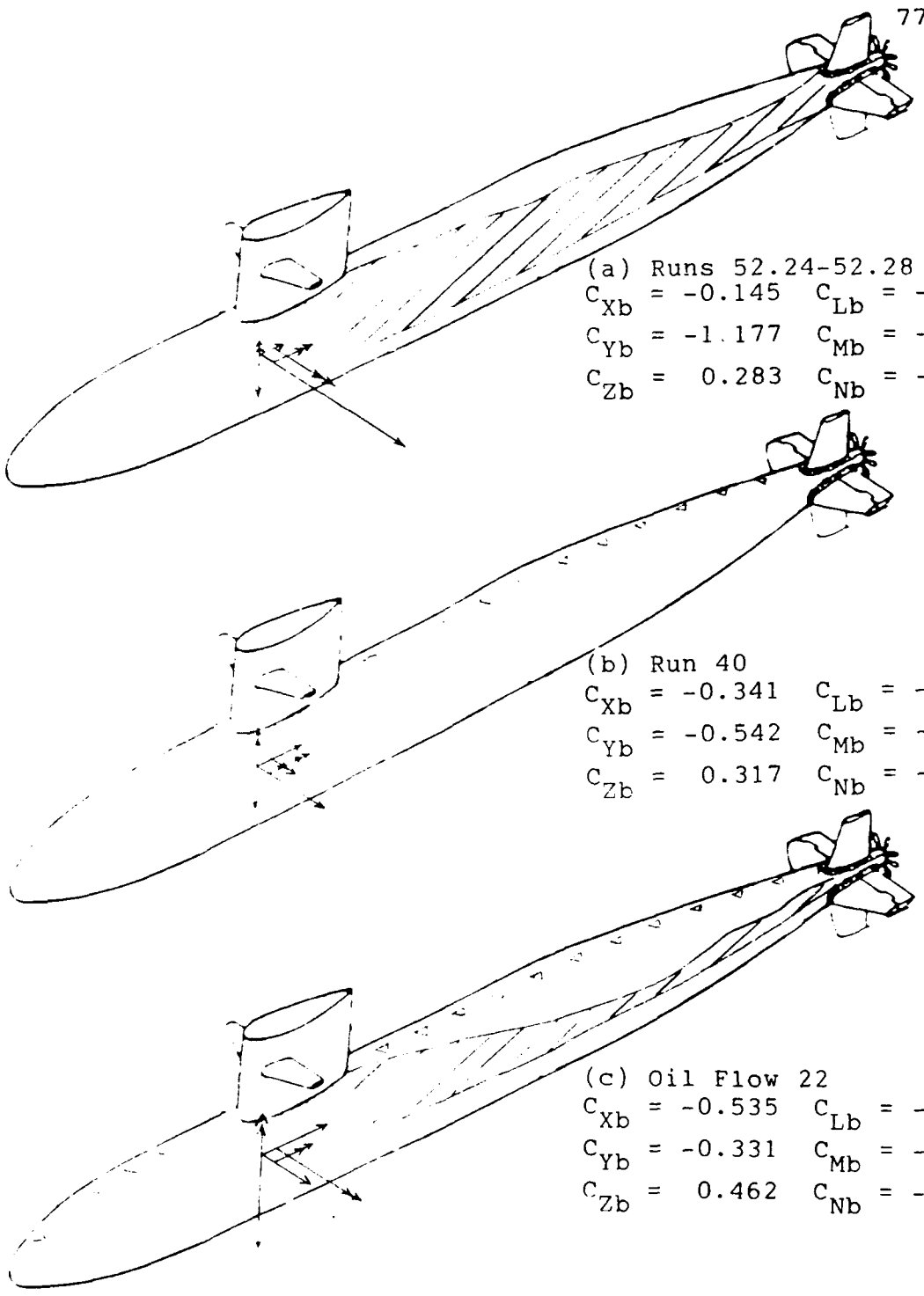

Figure 46. Pictorial summation of the forces and moments acting on the submarine for (a) no vortex generators, (b) vortex generators from stern to sail, and (c) vortex generators from stern to bow. Shaded areas represent areas of flow separation.

APPENDIX I Model Offsets

The following table presents the actual shape data of the wind tunnel model. The model diameters are given for the model at stations every four inches.

Body Dimensions: Los Angeles Class 688 Submarine Model

x, in.	x/L	Dh, in.	Dv, in.	Dh/L	Dv/L
4.00	0.0443	5.675	5.605	0.06288	0.06211
8.00	0.0886	7.485	7.475	0.08294	0.08283
12.00	0.1330	8.120	8.105	0.08997	0.08981
16.00	0.1773	8.215	8.225	0.09102	0.09114
20.00	0.2216	8.220	8.215	0.09108	0.09102
24.00	0.2659	8.225	8.220	0.09114	0.09108
28.00	0.3102	8.265	-	0.09158	0.00000
32.00	0.3546	8.250	8.225	0.09141	0.09114
36.00	0.3989	8.230	8.210	0.09119	0.09097
40.00	0.4432	8.215	8.215	0.09102	0.09102
44.00	0.4875	8.210	8.210	0.09097	0.09097
48.00	0.5319	8.220	8.240	0.09108	0.09130
52.00	0.5762	8.220	8.235	0.09108	0.09125
56.00	0.6205	8.325	8.235	0.09224	0.09125
60.00	0.6648	8.200	8.200	0.09086	0.09086
64.00	0.7091	8.000	8.025	0.08864	0.08892
68.00	0.7535	7.570	7.570	0.08388	0.08388
72.00	0.7978	7.065	7.090	0.07828	0.07856
76.00	0.8421	6.145	6.130	0.06809	0.06792
80.00	0.8864	4.870	4.900	0.05396	0.05429

Subamarine Model:
Nominally 90.25" long
Nominally 8.25" wide and high

Towed Array Housing:
Nominally 1.25" Wide
Height
Start at x = 11.815"
End at x = 79.975"
Each end is semicircular in top view, and blended into body

Sail:
1.665" wide
4.285" high
Leading edge at x = 24.635"
Trailing edge at x = 33.135"

All measurements +/- 0.005"

Manufacturer: The Scale Shipyard
5866 Orange Ave. #3
Long Beach, CA 90805-4146
(213)-428-5027

APPENDIX II Test Run History and Data Tabulation

The following tables contain specific run history information and data tabulation. The first set of runs are for the naked submarine. These runs include the last twenty force and moment runs and the first fifteen oil flows. The rest of the runs are for vortex generator configurations. All tables list the run and/or oil flow number.

Table IIA. Tabulated are run assignments, run conditions, data type collected, and general comments. "F&M" refer to whether or not forces and moments were recorded, and "Sep. Data" refers to whether or not separation line data was recorded. Oil flow numbers in italics indicate that the vortex generator configuration for that force and moment run is identical to the configuration used in the oil flow number listed.

Run #	Oil Flow	Re x10-6	ß, °	F&M?	Sep. Data?	Comments
52.00	14	4.640	0	X		*
52.01	12	4.585	5	X		*
52.02	8	4.530	10	X	X	*
52.03	5	4.540	15	X		*
52.04	10	4.540	15	X	X	N
52.10		5.670	0	X		A
52.11		5.600	5	X		K
52.12		5.565	10	X		E
52.13		5.560	15	X		D
52.20	13	6.900	0	X		
52.21	11	6.845	5	X		S
52.22	6	6.770	10	X	X	U
52.23	7	6.770	10	X	X	B
52.24	1	6.780	15	X		M
52.25	2	6.780	15	X		A
52.26	3	6.780	15	X		R
52.27	4	6.780	15	X		I
52.28	9	6.780	15	X	X	N
52.30		8.850	0	X		E
52.31		8.750	5	X		*
52.32		8.680	10	X		*
52.33		8.675	15	X		*
	15	6.869	15		X	1st vortex generator run
	16	6.785	15		X	small vortex generators ahead of towed array (at ϕ = -60°) on sail side
	17	6.805	15		X	sail side vortex generators moved to ϕ = -90°
	18	6.654	15	X		small vortex generators on sail side replaced with large ones; same separation line as 19
	19	6.480	15	X	X	
	20	6.430	15	X	X	
	21	6.650	15	X		separation line just before 20
	22	6.620	15	X		same as 21
	23	6.645	15	X		reversed α for 2 vortex generators on nose; 2 small vortex generators on sail; slightly worse than 22
	24	6.765	15	X		

Table IIA. Tabulated are run assignments, run conditions, data type collected, and general comments. "F&M" refer to whether or not forces and moments were recorded, and "Sep. Data" refers to whether or not separation line data was recorded. Oil flow numbers in italics indicate that the vortex generator configuration for that force and moment run is identical to the configuration used in the oil flow number listed.

Run #	Oil Flow	Re x10-6	ß, °	F& M?	Sep. Data?	Comments
30	*23*	6.775	15	X		
30	*23*	4.625	15	X		
31.00	*22*	4.600	0	X		
31.01		4.600	5	X		
31.02		4.605	10	X		
31.03		4.585	15	X		
31.10		5.610	0			
31.11		5.615	5			
31.12		5.620	10	X		
31.13		5.600	15	X		
31.20		6.825	0	X		
31.21		6.710	5	X		
31.22		6.730	10	X		
31.23		6.755	15	X		
32	*18*	6.825	15	X		
33		6.825	15	X		
34		6.825	15	X		
35		6.805	15	X		
36		6.820	15	X		
37		6.815	15	X		
38		6.820	15	X		
39		6.840	15	X		
40		6.835	15	X		
41		6.825	15	X		
42		6.820	15	X		
43		6.810	15	X		
44		6.805	15	X		
45		6.805	15	X		
46		6.800	15	X		
47		6.795	15	X		
48		6.795	15	X		
49		6.780	15	X		
50		6.785	15	X		
51		6.785	15	X		

Table IIB. Vortex generator configurations. A large X refers to a full size vortex generator, and a small x refers to a half size vortex generator. S refers to sail side, while B refers to bottom side.

Run #	Oil Flow	x, inches from nose 4	8	12	16	20	24	28	32	36	40	44	48	52	56	60	64	68	72	76	80
52	14																				
	15 S																				
	B						X	X	X	X	X	X	X	X	X	X	X	X	X		
	16 S			x	x	x	x	x	x	x	x	x	x	x	x	x	x	x	x	x	
	B						X	X	X	X	X	X	X	X	X	X	X	X	X		
	17 S			x	x	x				x	x	x	x	x	x	x	x	x	x	x	
	B			X	X	X	X	X	X	X	X	X	X	X	X	X	X	X	X	X	
	18 S		X	X	X	X				X	X	X	X	X	X	X	X	X	X	X	X
	B		X	X	X	X	X	X	X	X	X	X	X	X	X	X	X	X	X	X	X
	19 S		XX	X	X	X				X	X	X	X	X	X	X	X	X	X	X	X
	B		XX	X	X	X	X	X	X	X	X	X	X	X	X	X	X	X	X	X	X
	20 S		XX	X	X	X				X	X	X	X	X	X	X	X	X	X	X	X
	B		XX	X	X	X	X	X	X	X	X	X	X	X	X	X	X	X	X	X	X
	21 S	X	X	X	X	X				X	X	X	X	X	X	X	X	X	X	X	X
	B	X	X	X	X	X	X	X	X	X	X	X	X	X	X	X	X	X	X	X	X
	22 S	XX	X	X	X	X	X			X	X	X	X	X	X	X	X	X	X	X	X
	B	XX	X	X	X	X	X	X	X	X	X	X	X	X	X	X	X	X	X	X	X
	23 S	XX	X	X	X	X	Xxx			X	X	X	X	X	X	X	X	X	X	X	X
	B	XX	X	X	X	X	X	X	X	X	X	X	X	X	X	X	X	X	X	X	X
	24 S	X	X	X	X	X	Xxx			X	X	X	X	X	X	X	X	X	X	X	X
	B	X	X	X	X	X	X	X	X	X	X	X	X	X	X	X	X	X	X	X	X
30	*23* S	X	X	X	X	X	Xxx			X	X	X	X	X	X	X	X	X	X	X	X
	B	X	X	X	X	X	X	X	X	X	X	X	X	X	X	X	X	X	X	X	X
31	*22* S	XX	X	X	X	X	X			X	X	X	X	X	X	X	X	X	X	X	X
	B	XX	X	X	X	X	X	X	X	X	X	X	X	X	X	X	X	X	X	X	X
32	*18* S	X	X	X	X	X	X			X	X	X	X	X	X	X	X	X	X	X	X
	B	X	X	X	X	X	X	X	X	X	X	X	X	X	X	X	X	X	X	X	X
33	S		X	X	X	X	X			X	X	X	X	X	X	X	X	X	X	X	X
	B		X	X	X	X	X	X	X	X	X	X	X	X	X	X	X	X	X	X	X
34	S			X	X	X	X			X	X	X	X	X	X	X	X	X	X	X	X
	B			X	X	X	X	X	X	X	X	X	X	X	X	X	X	X	X	X	X
35	S				X	X	X			X	X	X	X	X	X	X	X	X	X	X	X
	B				X	X	X	X	X	X	X	X	X	X	X	X	X	X	X	X	X
36	S					X	X			X	X	X	X	X	X	X	X	X	X	X	X
	B					X	X	X	X	X	X	X	X	X	X	X	X	X	X	X	
37	S						X			X	X	X	X	X	X	X	X	X	X	X	X
	B						X	X	X	X	X	X	X	X	X	X	X	X	X	X	X
38	S									X	X	X	X	X	X	X	X	X	X	X	X
	B							X	X	X	X	X	X	X	X	X	X	X	X	X	X
39	S									X	X	X	X	X	X	X	X	X	X	X	X
	B								X	X	X	X	X	X	X	X	X	X	X	X	X
40	S									X	X	X	X	X	X	X	X	X	X	X	X
	B									X	X	X	X	X	X	X	X	X	X	X	X
41	S										X	X	X	X	X	X	X	X	X	X	X
	B										X	X	X	X	X	X	X	X	X	X	X
42	S											X	X	X	X	X	X	X	X	X	X
	B											X	X	X	X	X	X	X	X	X	X

Table IIB. Vortex generator configurations. A large X refers to a full size vortex generator, and a small x refers to a half size vortex generator. S refers to sail side, while B refers to bottom side.

Run #	Oil Flow	x, inches from nose 4	8	12	16	20	24	28	32	36	40	44	48	52	56	60	64	68	72	76	80
43	S												X	X	X	X	X	X	X	X	X
	B												X	X	X	X	X	X	X	X	X
44	S													X	X	X	X	X	X	X	X
	B													X	X	X	X	X	X	X	X
45	S														X	X	X	X	X	X	X
	B														X	X	X	X	X	X	X
46	S															X	X	X	X	X	X
	B															X	X	X	X	X	X
47	S																X	X	X	X	X
	B																X	X	X	X	X
48	S																	X	X	X	X
	B																	X	X	X	X
49	S																		X	X	X
	B																		X	X	X
50	S																			X	X
	B																			X	X
51	S																				X
	B																				X

Table IIC. Force and moment coefficients.

Run #	Oil Flow	CX	CY	CZ	CL	CM	CN
52.00	14	-0.166	-0.011	-0.001	0.012	0.090	0.055
52.01	12	-0.156	-0.274	0.061	-0.142	0.053	-0.038
52.02	8	-0.144	-0.748	0.256	-0.300	-0.164	-0.060
52.03	5	-0.155	-1.171	0.269	-0.299	-0.470	-0.046
52.04	10	-0.155	-1.171	0.269	-0.299	-0.470	-0.046
52.10		-0.163	-0.021	-0.010	0.010	0.112	0.057
52.11		-0.147	-0.283	0.073	-0.142	0.030	-0.040
52.12		-0.127	-0.742	0.255	-0.313	-0.227	-0.067
52.13		-0.155	-1.142	0.287	-0.297	-0.466	-0.043
52.20	13	-0.149	-0.020	0.001	0.001	0.120	0.050
52.21	11	-0.142	-0.278	0.071	-0.145	0.031	-0.043
52.22	6	-0.195	-0.749	0.264	-0.312	-0.292	-0.070
52.23	7	-0.195	-0.749	0.264	-0.312	-0.292	-0.070
52.24	1	-0.145	-1.177	0.283	-0.300	-0.499	-0.035
52.25	2	-0.145	-1.177	0.283	-0.300	-0.499	-0.035
52.26	3	-0.145	-1.177	0.283	-0.300	-0.499	-0.035
52.27	4	-0.145	-1.177	0.283	-0.300	-0.499	-0.035
52.28	9	-0.145	-1.177	0.283	-0.300	-0.499	-0.035
52.30		-0.017	0.000	-0.001	-0.001	0.115	0.048
52.31		-0.140	-0.283	0.073	-0.142	0.006	-0.046
52.32		-0.111	-0.756	0.264	-0.315	-0.309	-0.073
52.33		-0.141	-1.147	0.241	-0.307	-0.468	-0.056
	18	-0.490	-0.332	0.441	-0.207	-0.444	-0.246
	19	-0.495	-0.310	0.381	-0.248	-0.281	-0.249
	20	-0.504	-0.291	0.481	-0.228	-0.562	-0.241
	21	-0.501	-0.336	0.493	-0.219	-0.569	-0.239
	22	-0.535	-0.331	0.462	-0.222	-0.496	-0.220
	23	-0.490	-0.470	0.633	-0.297	-0.877	-0.224
	24	-0.469	-0.566	0.733	-0.351	-0.931	-0.200
30	*23*	-0.445	-0.666	0.895	-0.449	-0.975	-0.193
	23	-0.470	-0.506	0.680	-0.319	-0.819	-0.215
31.00	*22*	-0.386	0.173	0.042	0.003	0.068	0.085
31.01		-0.383	-0.034	0.157	-0.153	0.176	-0.045
31.02		-0.427	-0.330	0.648	-0.307	0.263	-0.128
31.03		-0.505	-0.394	0.546	-0.263	-0.592	-0.224
31.10		-0.385	0.165	0.046	0.001	0.053	0.086
31.11		-0.383	-0.035	0.169	-0.155	0.109	-0.047
31.12		-0.429	-0.336	0.675	-0.304	0.082	-0.123
31.13		-0.487	-0.440	0.628	-0.281	-0.696	-0.213
31.20		-0.374	0.175	0.035	-0.010	0.074	0.080
31.21		-0.384	-0.040	0.179	-0.155	0.094	-0.045
31.22		-0.421	-0.340	0.685	-0.301	0.130	-0.126
31.23		-0.499	-0.390	0.589	-0.271	-0.644	-0.231
32	*18*	-0.478	-0.422	0.629	-0.302	-0.796	-0.231
33		-0.460	-0.432	0.630	-0.291	-0.811	-0.238
34		-0.448	-0.440	0.619	-0.286	-0.755	-0.248
35		-0.421	-0.457	0.592	-0.285	-0.667	-0.257
36		-0.404	-0.485	0.563	-0.301	-0.607	-0.262
37		-0.377	-0.489	0.492	-0.301	-0.490	-0.275

Table IIC. Force and moment coefficients.

Run #	Oil Flow	CX	CY	CZ	CL	CM	CN
38		-0.374	-0.517	0.418	-0.274	-0.374	-0.280
39		-0.354	-0.531	0.389	-0.298	-0.374	-0.275
40		-0.341	-0.542	0.317	-0.301	-0.308	-0.277
41		-0.339	-0.581	0.299	-0.303	-0.313	-0.278
42		-0.315	-0.644	0.313	-0.319	-0.284	-0.257
43		-0.291	-0.694	0.312	-0.302	-0.269	-0.251
44		-0.275	-0.740	0.310	-0.304	-0.208	-0.242
45		-0.261	-0.796	0.301	-0.319	-0.190	-0.224
46		-0.245	-0.844	0.321	-0.310	-0.216	-0.204
47		-0.224	-0.890	0.323	-0.300	-0.230	-0.181
48		-0.197	-0.957	0.323	-0.301	-0.280	-0.157
49		-0.177	-1.026	0.305	-0.303	-0.288	-0.130
50		-0.166	-1.076	0.283	-0.298	-0.305	-0.098
51		-0.148	-1.121	0.279	-0.303	-0.354	-0.069

Table IID. Separation line data.

Run #	Oil Flow	ϕ',° Sail	Bottom	ϕ_x',° Sail	Bottom
52.02	8	113.54	108.86	93.56	88.44
52.04	10	99.48	101.63	73.33	80.54
52.22	6		116.24		98.51
52.23	7	130.09	119.45	116.75	102.24
52.28	9	99.85	108.75	80.54	89.06
	15		139.44		129.76
	16	105.71	139.53	88.93	129.58
	17	112.58	144.85	97.99	135.36
	19	128.57	144.74	120.07	135.28
	20	128.46	146.82	120.17	137.06

APPENDIX III Oil Flow Photos for the Submarine Without Vortex Generators

The first 60 photos document the oil flows for the naked submarine at Re = 6.77×10^6 and 5°, 10°, and 15° of sideslip. Indicated for each photo is the orientation of the photo with respect to the entire submarine, the flow direction, and the separation lines, if any. The photos were all taken roughly normal to the body surface at about ϕ = 135°, which is the longitudinal grid line in all of the photos.

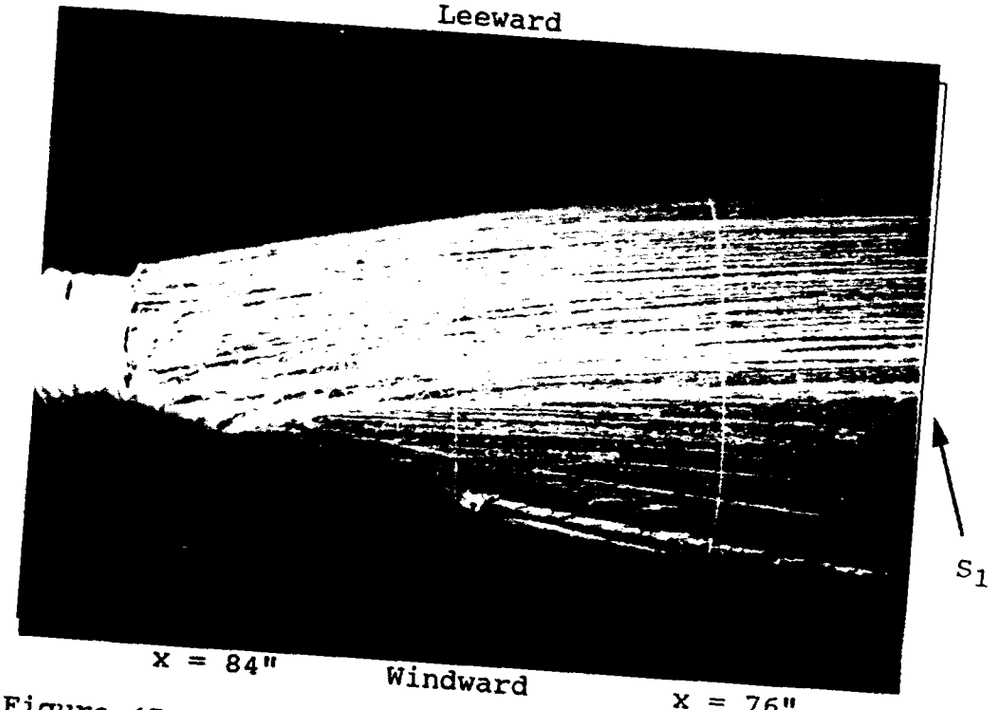

Figure 47. Oil flow 11, naked submarine, sail side, Re = 6.85×10^6, ß = 5°.

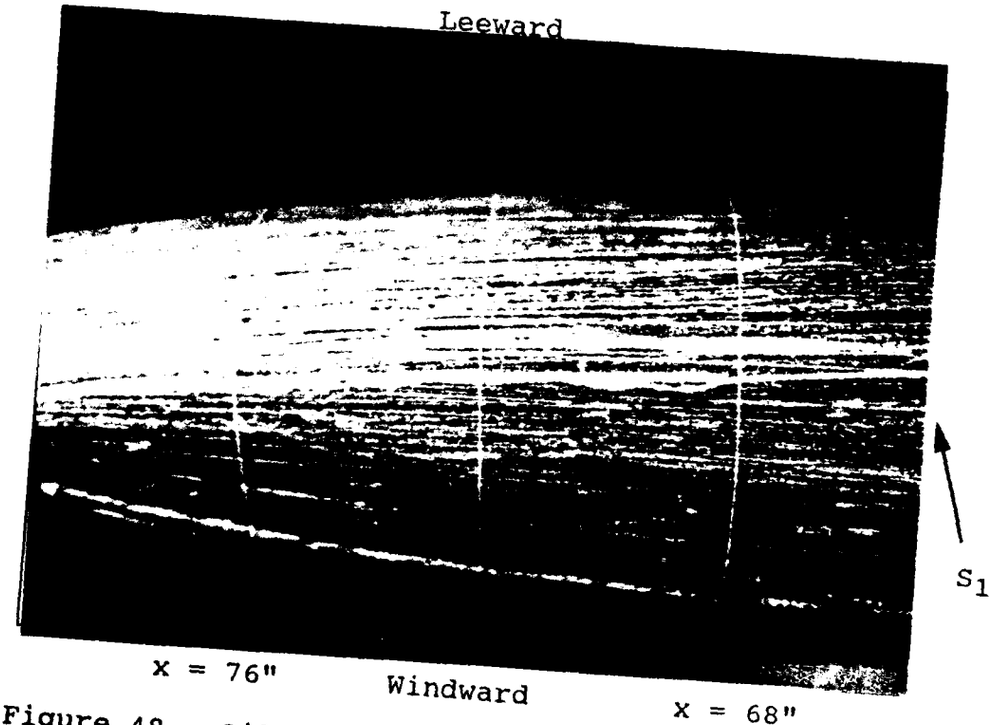

Figure 48. Oil flow 11, naked submarine, sail side, Re = 6.85×10^6, ß = 5°.

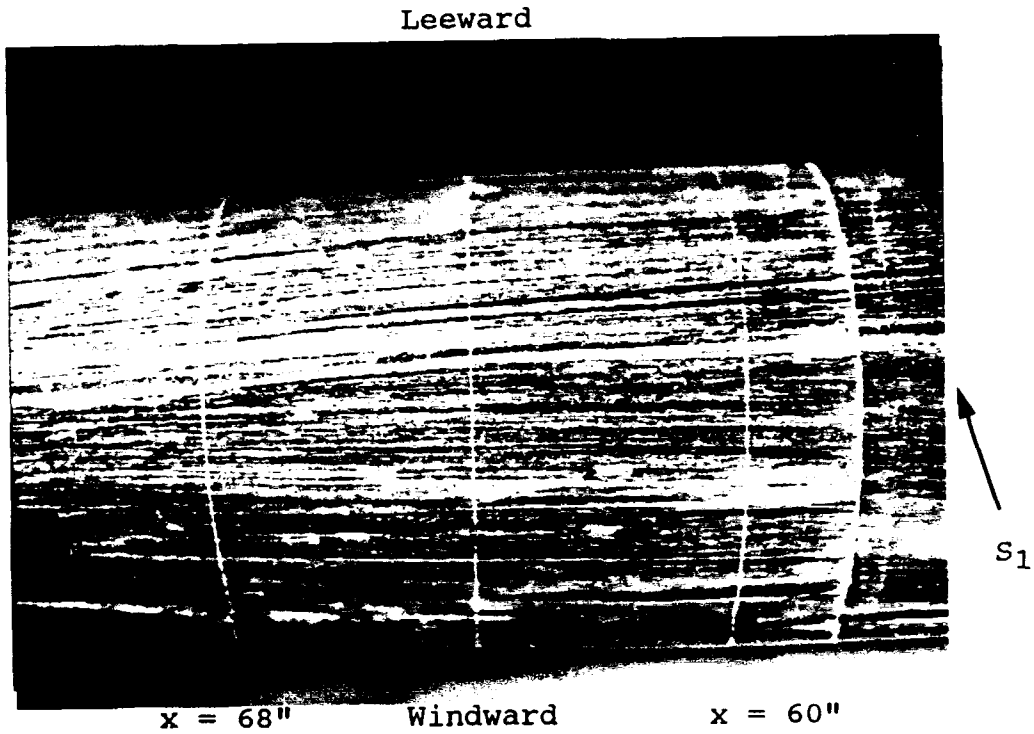

Figure 49. Oil flow 11, naked submarine, sail side, Re = 6.85×10^6, $\beta = 5°$.

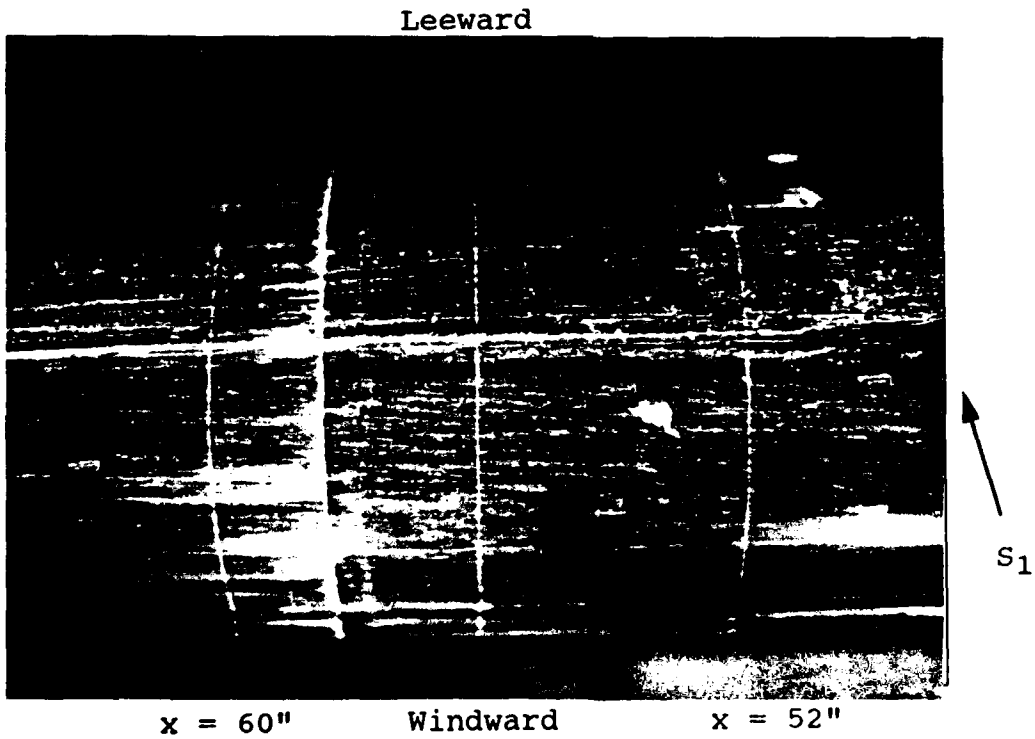

Figure 50. Oil flow 11, naked submarine, sail side, Re = 6.85×10^6, $\beta = 5°$.

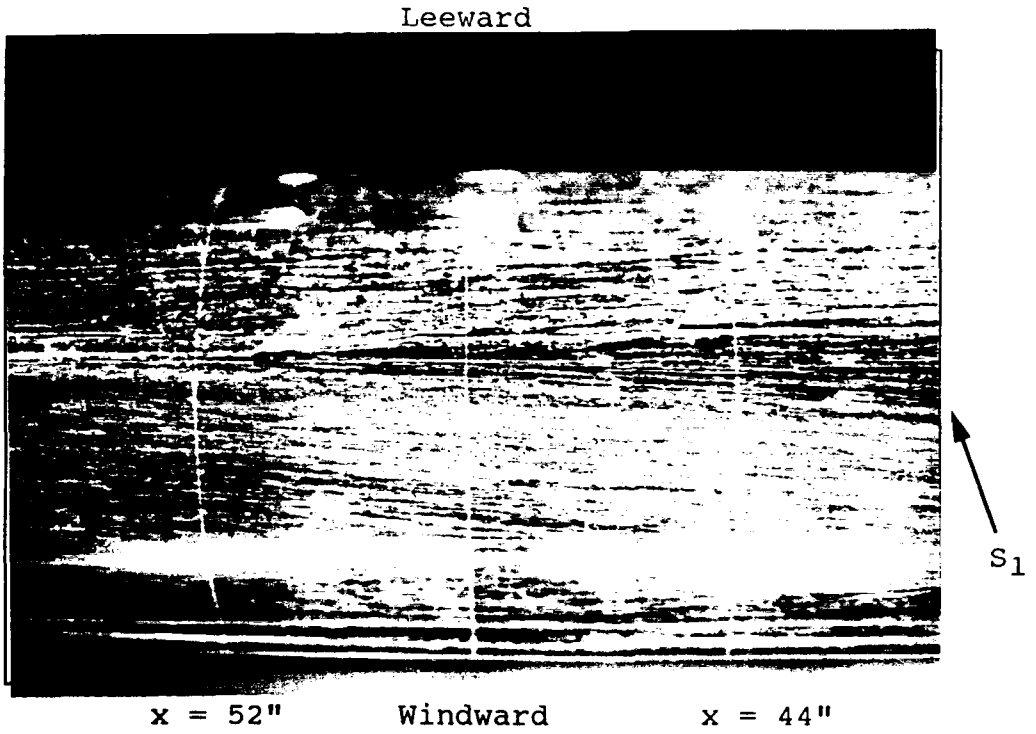

Figure 51. Oil flow 11, naked submarine, sail side, Re = 6.85×10^6, $\beta = 5°$.

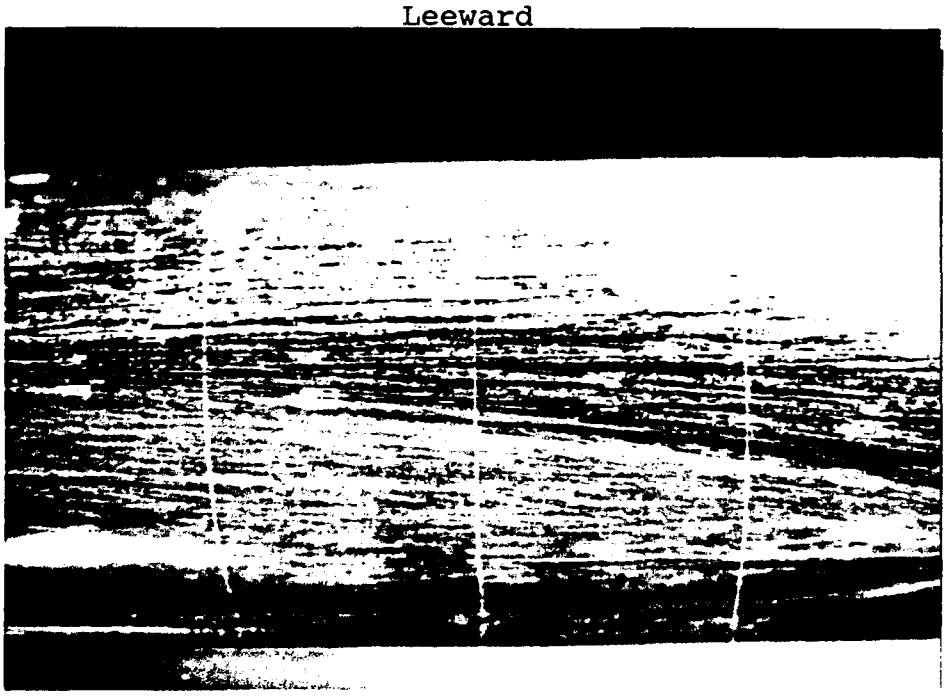

Figure 52. Oil flow 11, naked submarine, sail side, Re = 6.85×10^6, $\beta = 5°$.

Leeward

x = 36" Windward x = 28"

Figure 53. Oil flow 11, naked submarine, sail side, Re = 6.85×10^6, ß = 5°.

Leeward

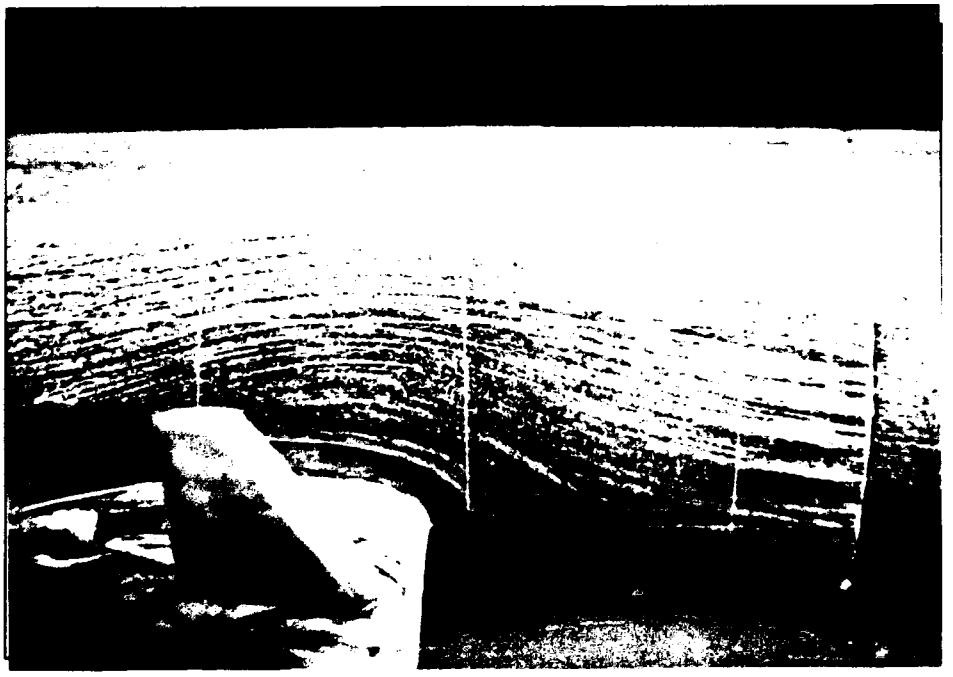

x = 28" Windward x = 20"

Figure 54. Oil flow 11, naked submarine, sail side, Re = 6.85×10^6, ß = 5°.

AD-A249 629 THE EFFECT OF VORTEX GENERATORS ON CROSSFLOW SEPARATION 2/2
ON A SUBMARINE IN A TURNING MANEUVER(U) VIRGINIA
POLYTECHNIC INST AND STATE UNIV BLACKSBURG DEPT OF..
UNCLASSIFIED T G WETZEL ET AL. 28 FEB 92 VPI-AOE-186 NL

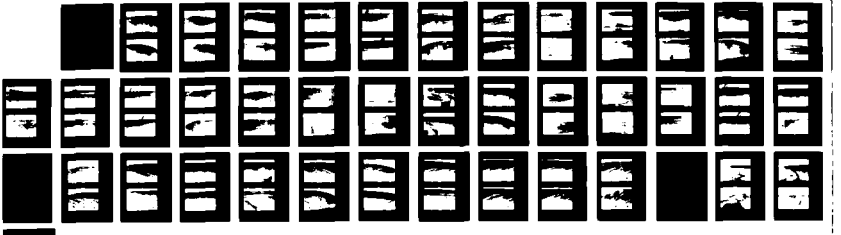

END
FILMED
DTIC

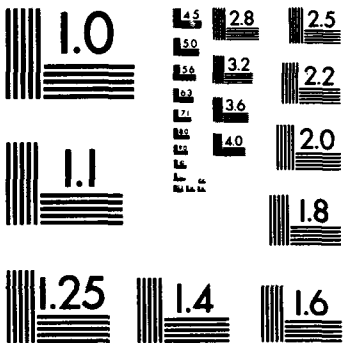

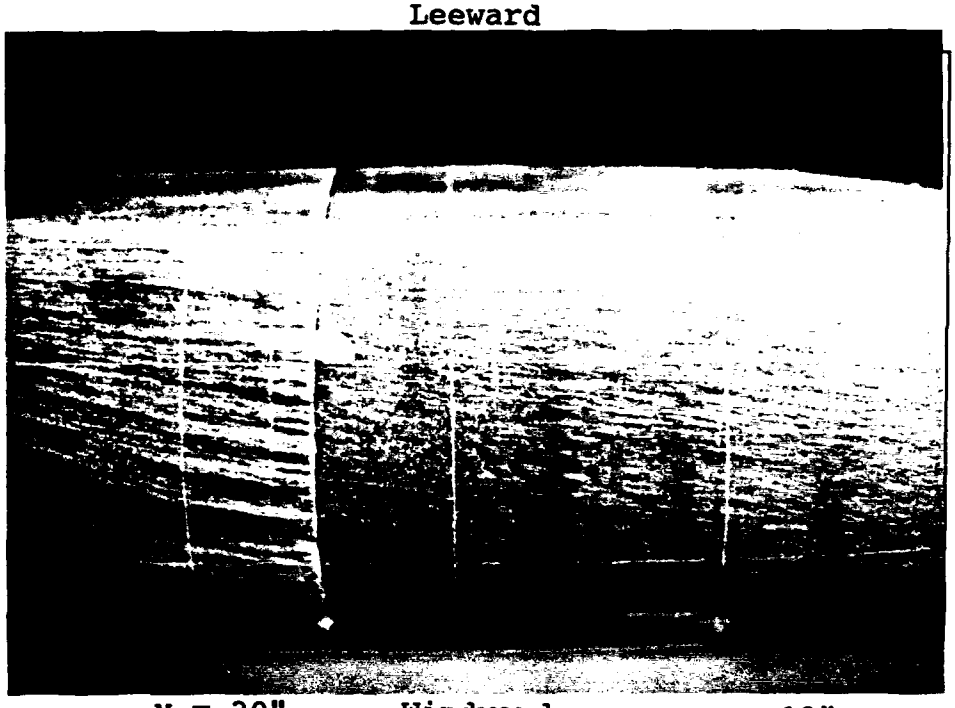

Figure 55. Oil flow 11, naked submarine, sail side, Re = 6.85×10^6, $\beta = 5°$.

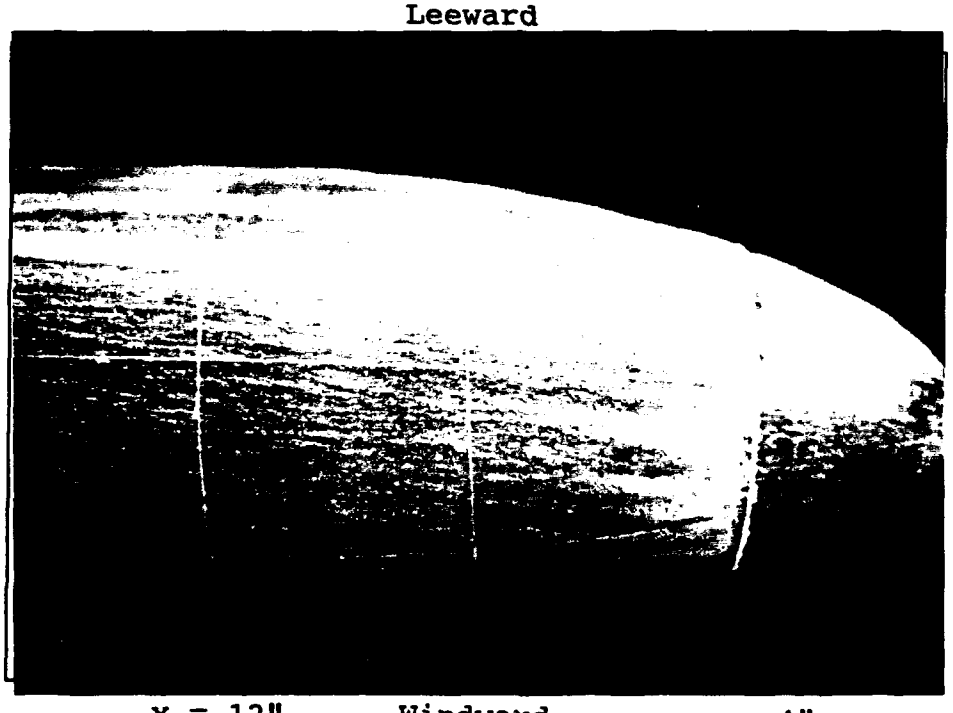

Figure 56. Oil flow 11, naked submarine, sail side, Re = 6.85×10^6, $\beta = 5°$.

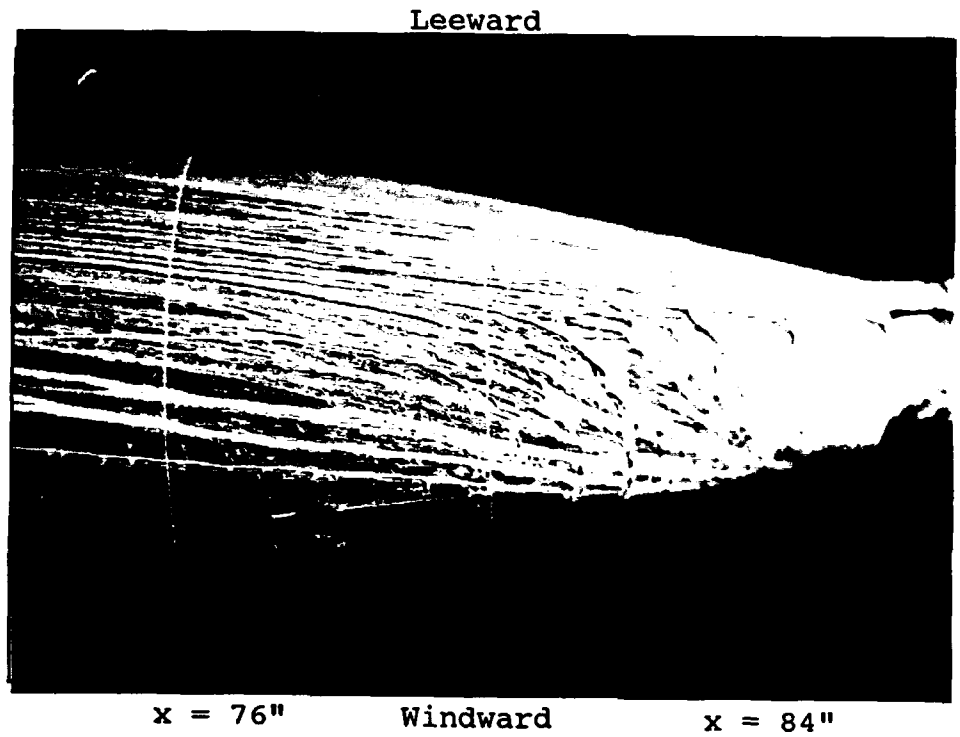

Figure 57. Oil flow 11, naked submarine, bottom side, Re = 6.85×10^6, $\beta = 5°$.

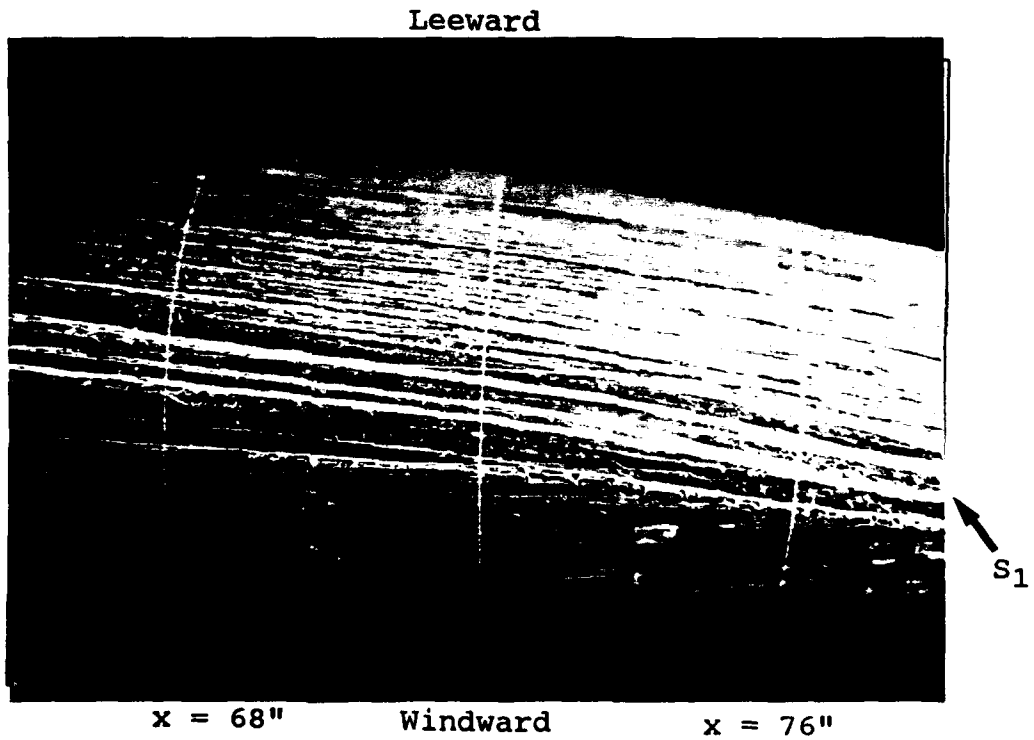

Figure 58. Oil flow 11, naked submarine, bottom side, Re = 6.85×10^6, $\beta = 5°$.

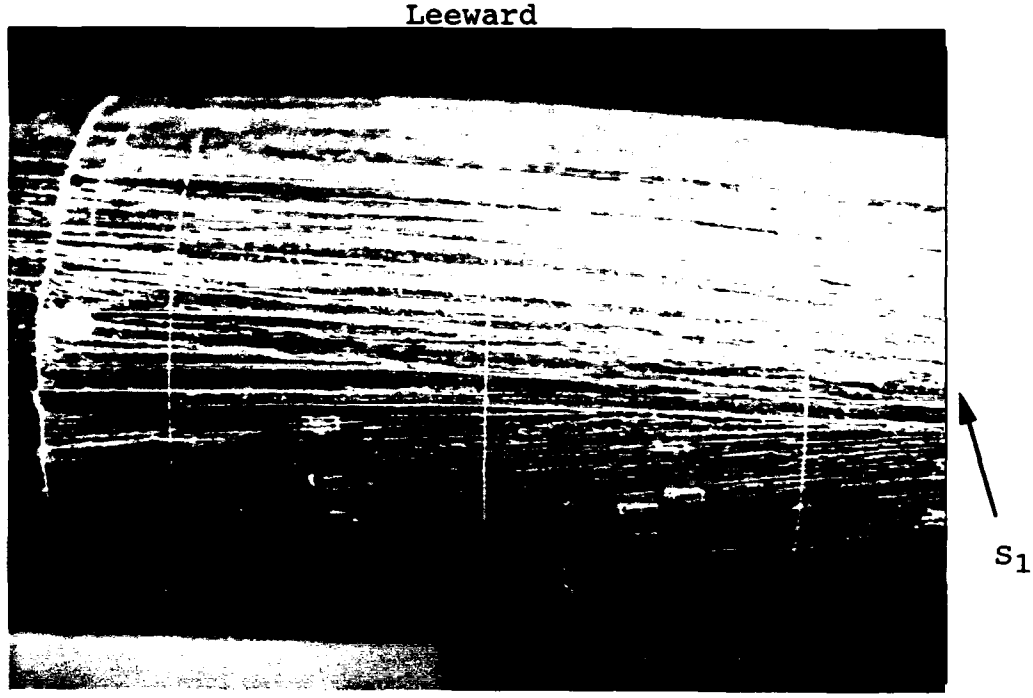

Figure 59. Oil flow 11, naked submarine, bottom side, Re = 6.85×10^6, $\beta = 5°$.

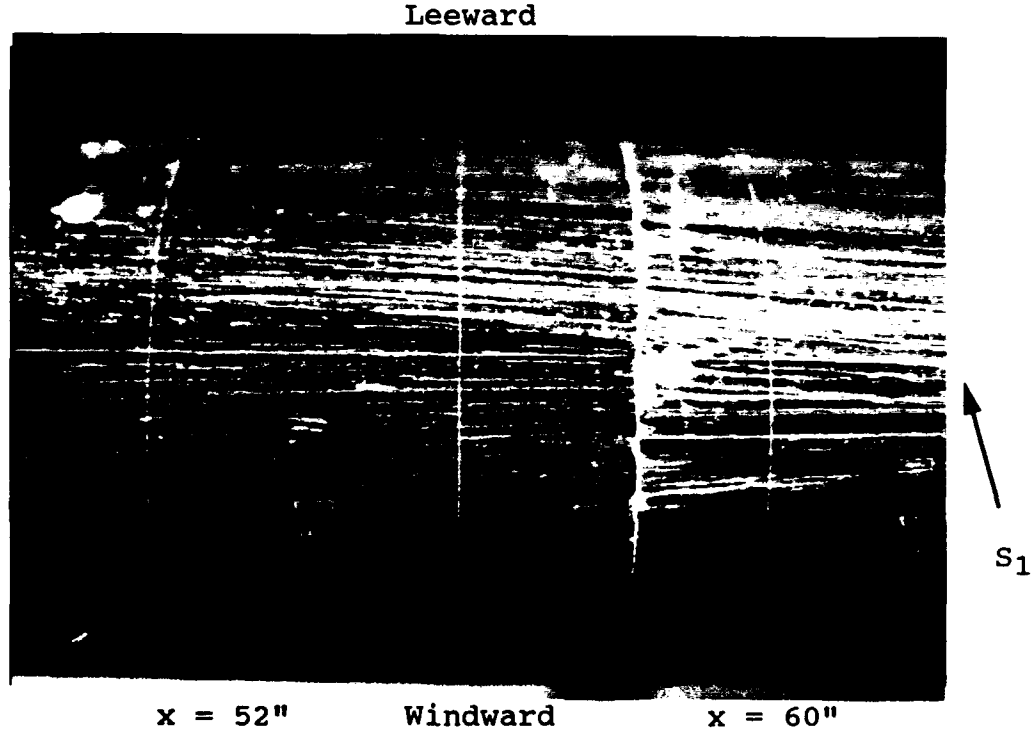

Figure 60. Oil flow 11, naked submarine, bottom side, Re = 6.85×10^6, $\beta = 5°$.

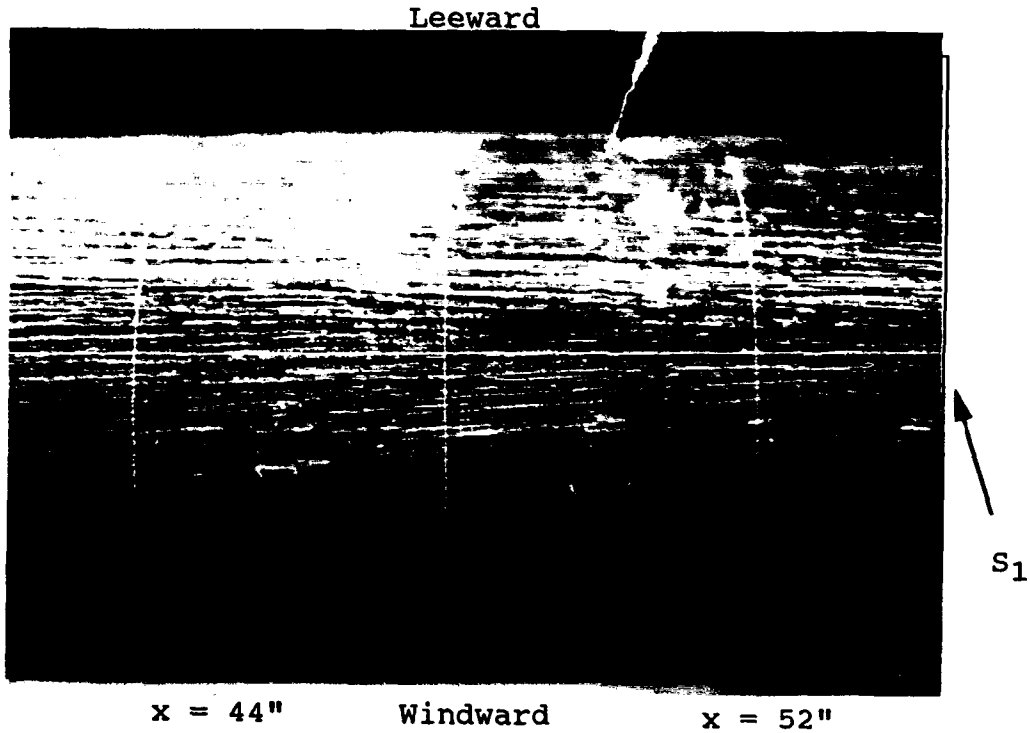

Figure 61. Oil flow 11, naked submarine, bottom side, Re = 6.85×10^6, $\beta = 5°$.

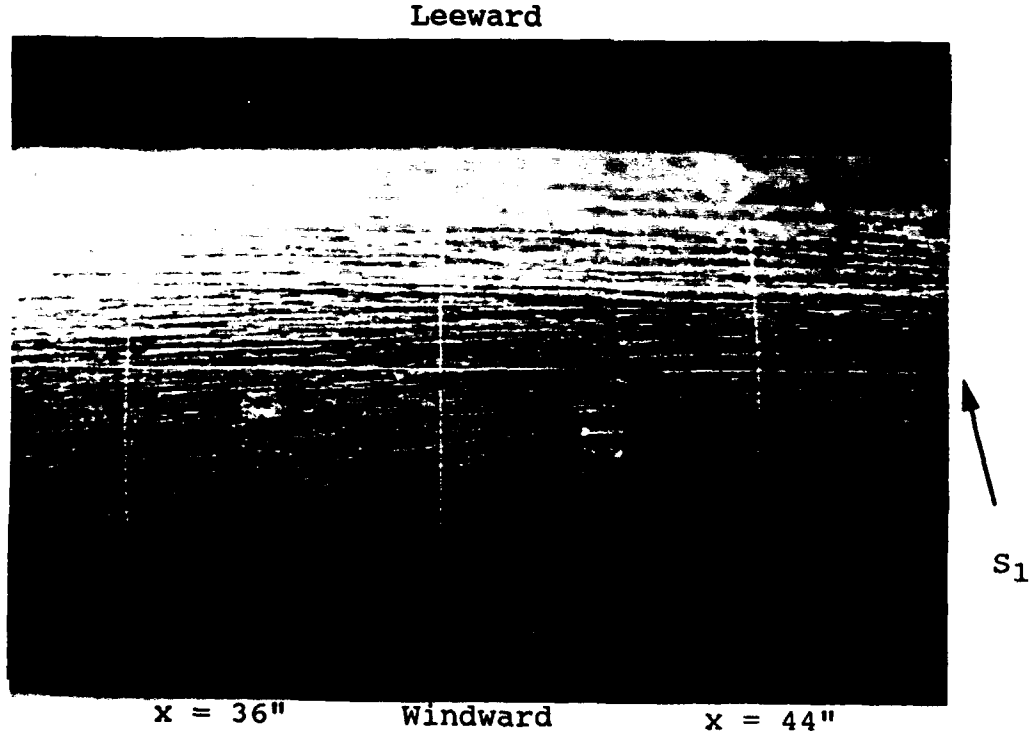

Figure 62. Oil flow 11, naked submarine, bottom side, Re = 6.85×10^6, $\beta = 5°$.

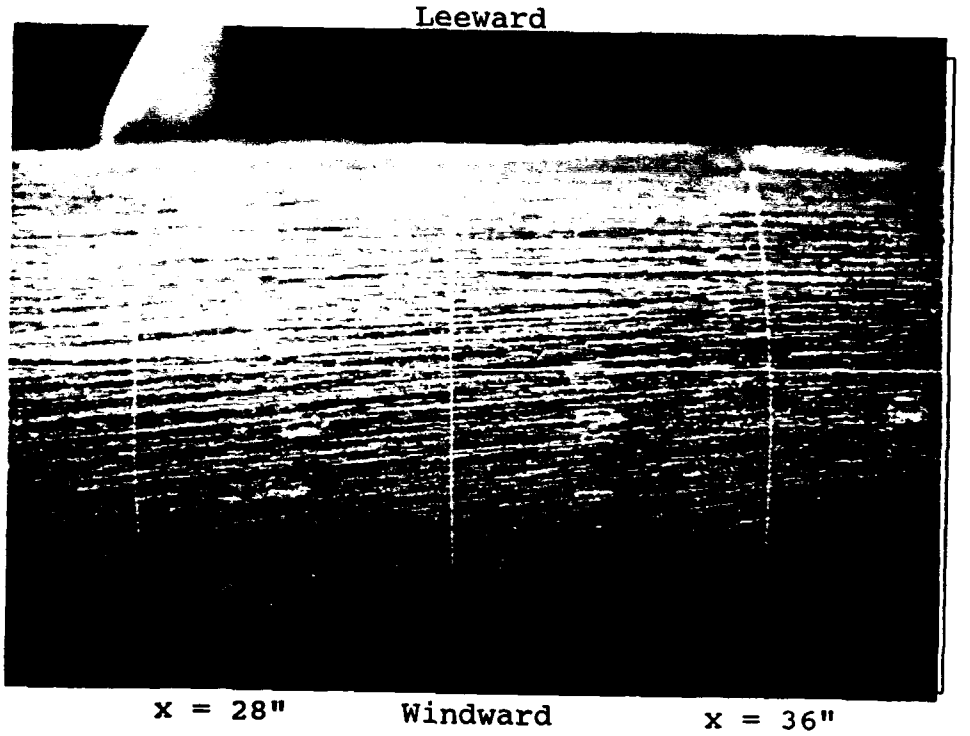

Figure 63. Oil flow 11, naked submarine, bottom side, Re = 6.85×10^6, $\beta = 5°$.

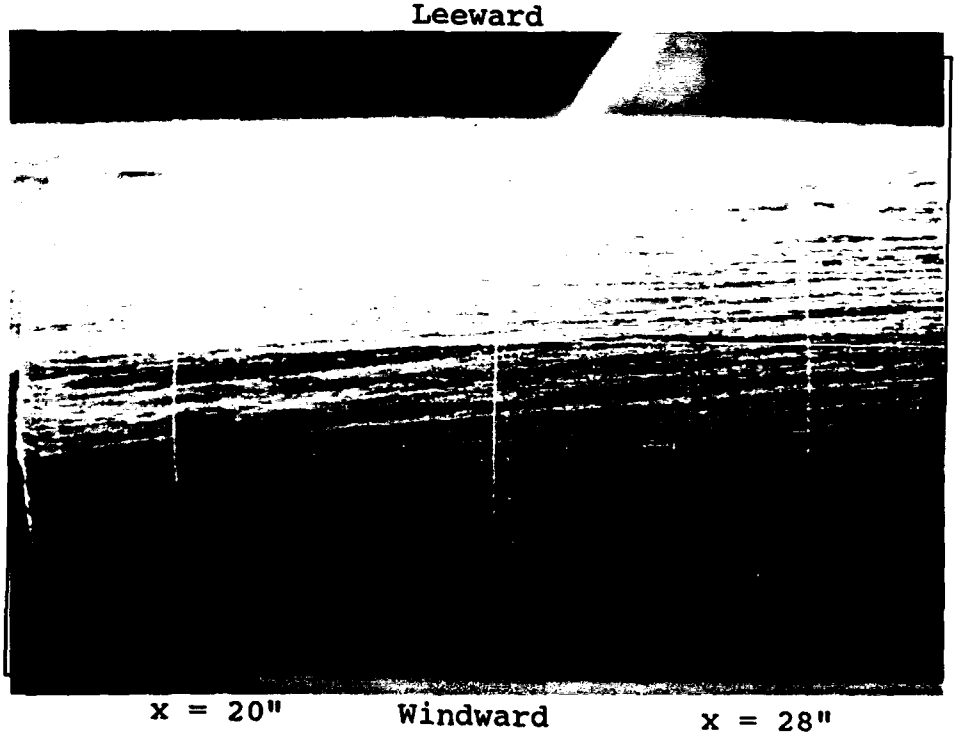

Figure 64. Oil flow 11, naked submarine, bottom side, Re = 6.85×10^6, $\beta = 5°$.

Leeward

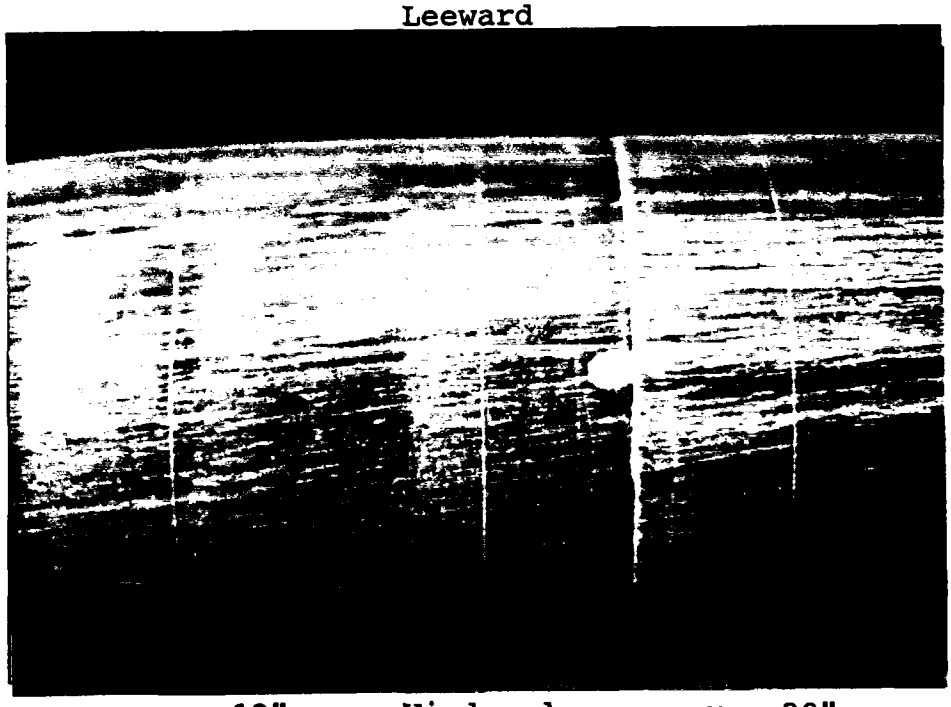

x = 12" Windward x = 20"

Figure 65. Oil flow 11, naked submarine, bottom side, Re = 6.85×10^6, ß = 5°.

Leeward

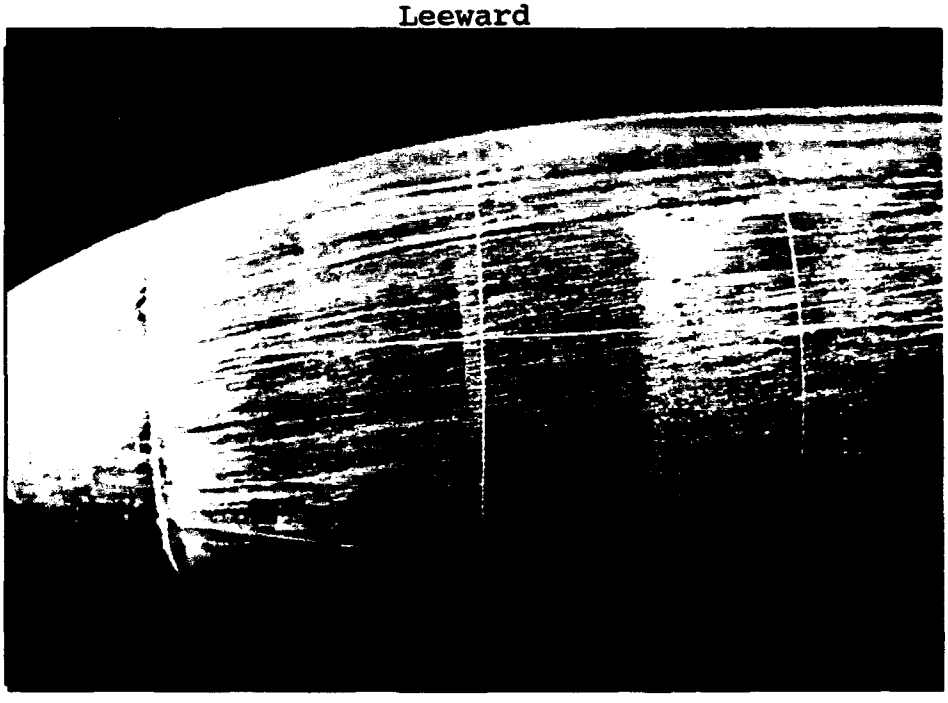

x = 4" Windward x = 12"

Figure 66. Oil flow 11, naked submarine, bottom side, Re = 6.85×10^6, ß = 5°.

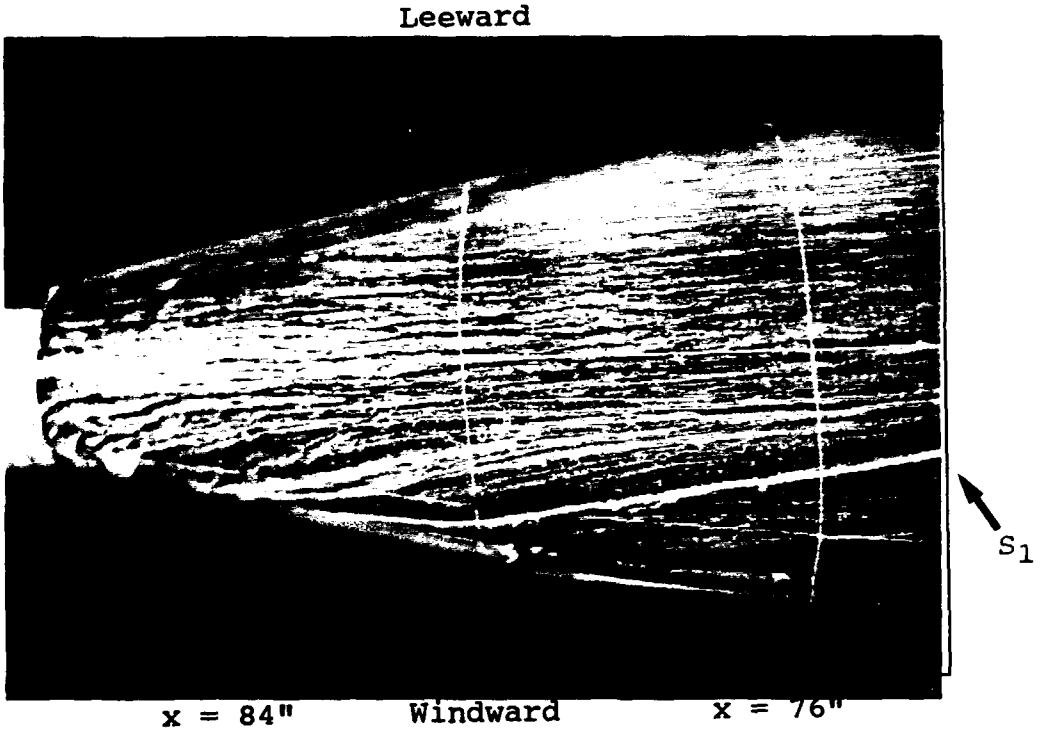

Figure 67. Oil flow 7, naked submarine, sail side, Re = 6.77×10^6, $\beta = 10°$.

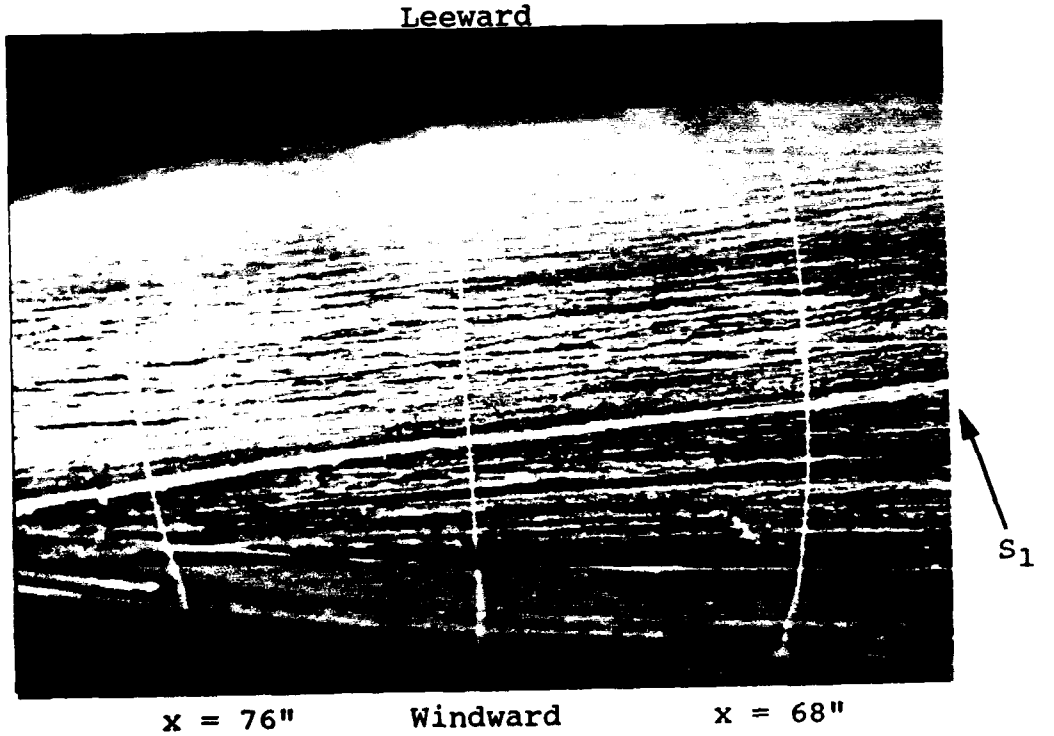

Figure 68. Oil flow 7, naked submarine, sail side, Re = 6.77×10^6, $\beta = 10°$.

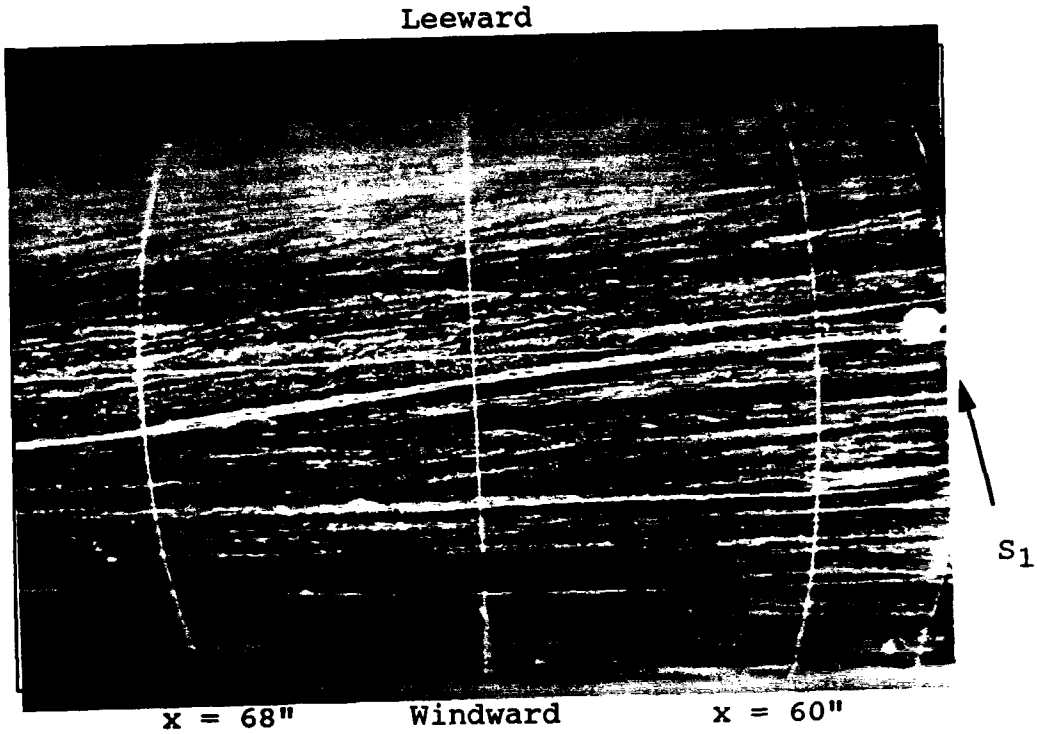

Figure 69. Oil flow 7, naked submarine, sail side, Re = 6.77×10^6, $\beta = 10°$.

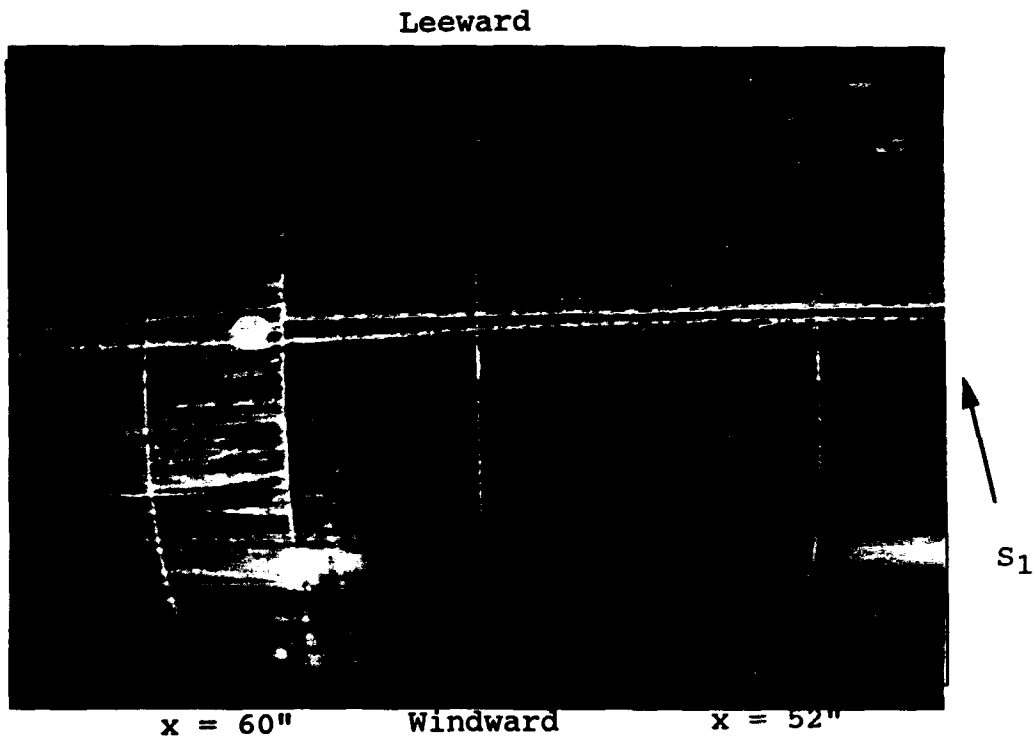

Figure 70. Oil flow 7, naked submarine, sail side, Re = 6.77×10^6, $\beta = 10°$.

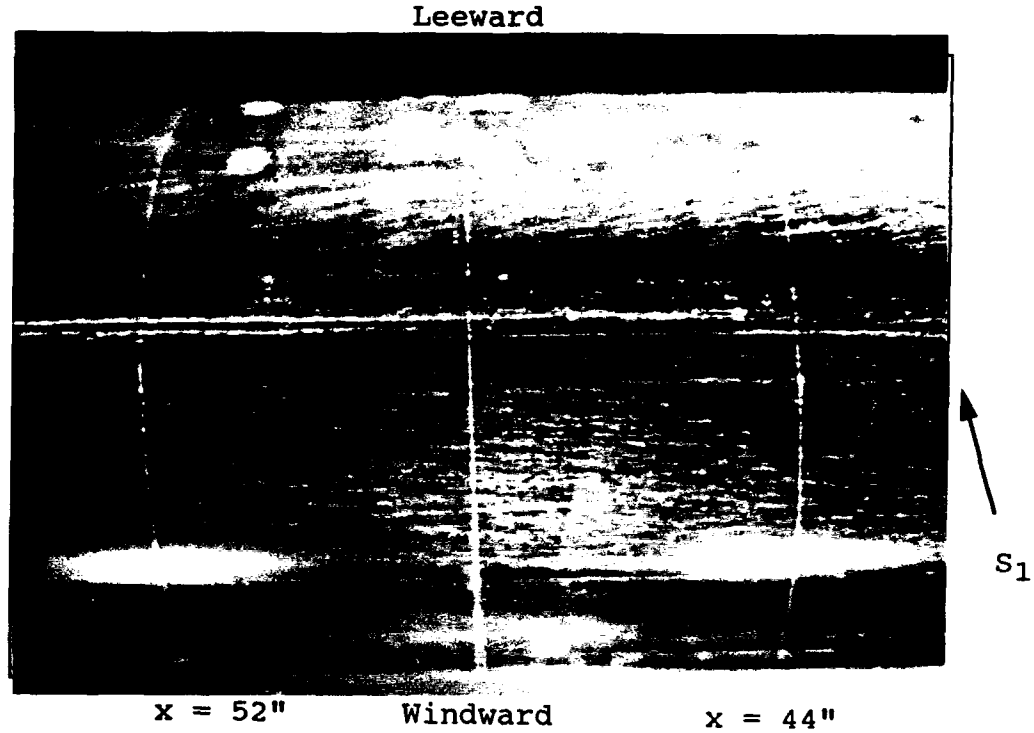

Figure 71. Oil flow 7, naked submarine, sail side, Re = 6.77×10^6, $\beta = 10°$.

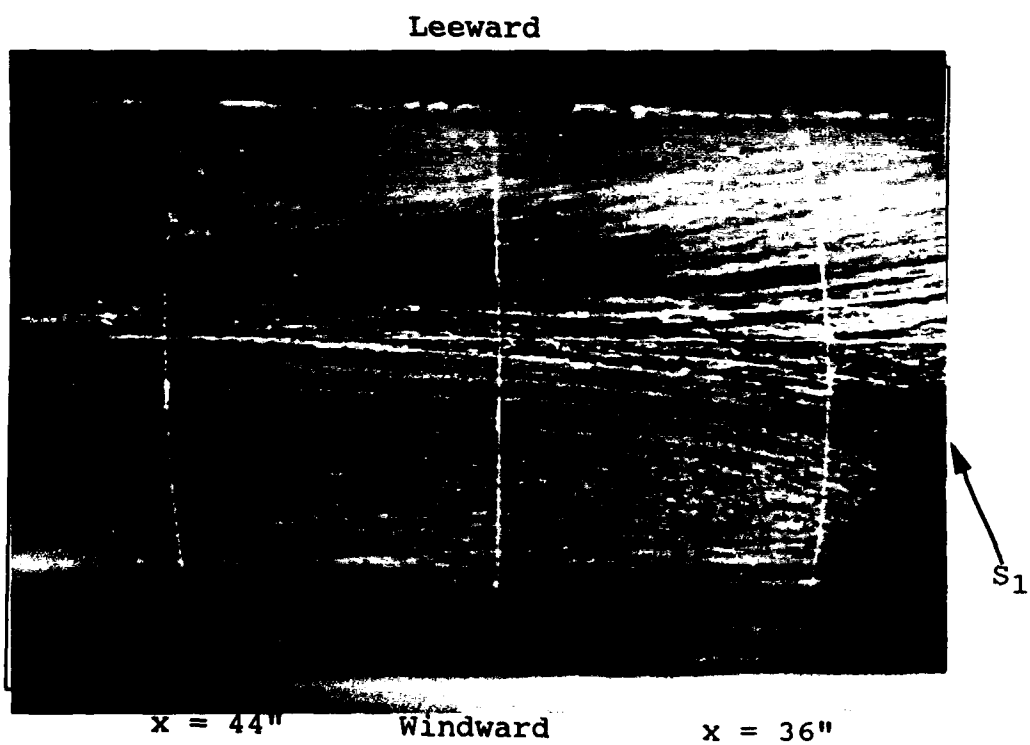

Figure 72. Oil flow 7, naked submarine, sail side, Re = 6.77×10^6, $\beta = 10°$.

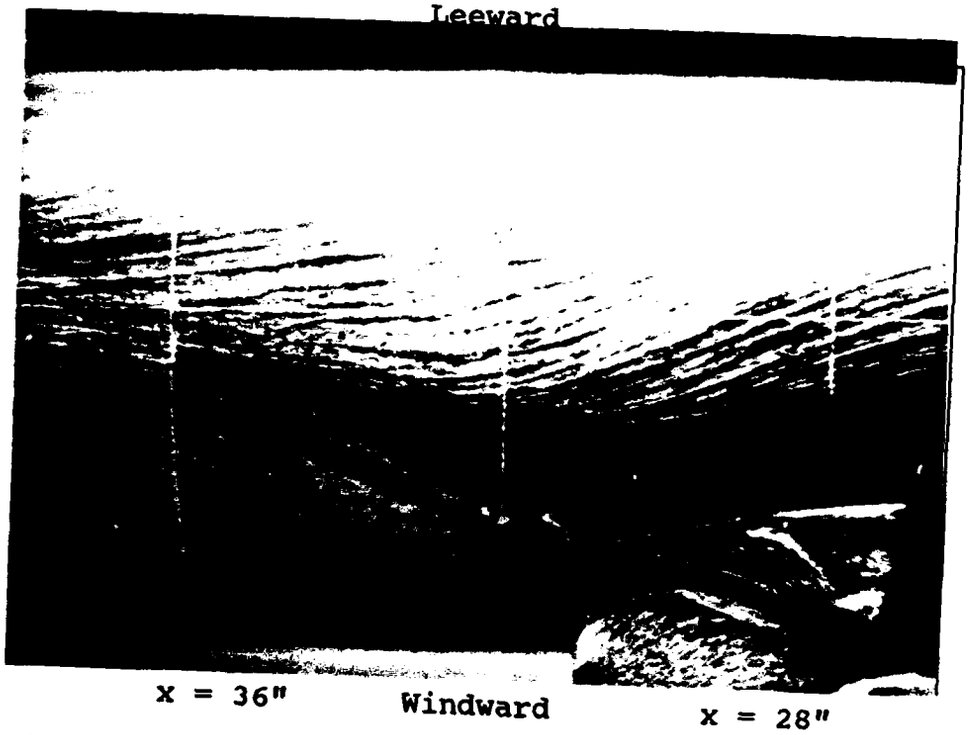

Figure 73. Oil flow 7, naked submarine, sail side, Re = 6.77×10^6, $\beta = 10°$.

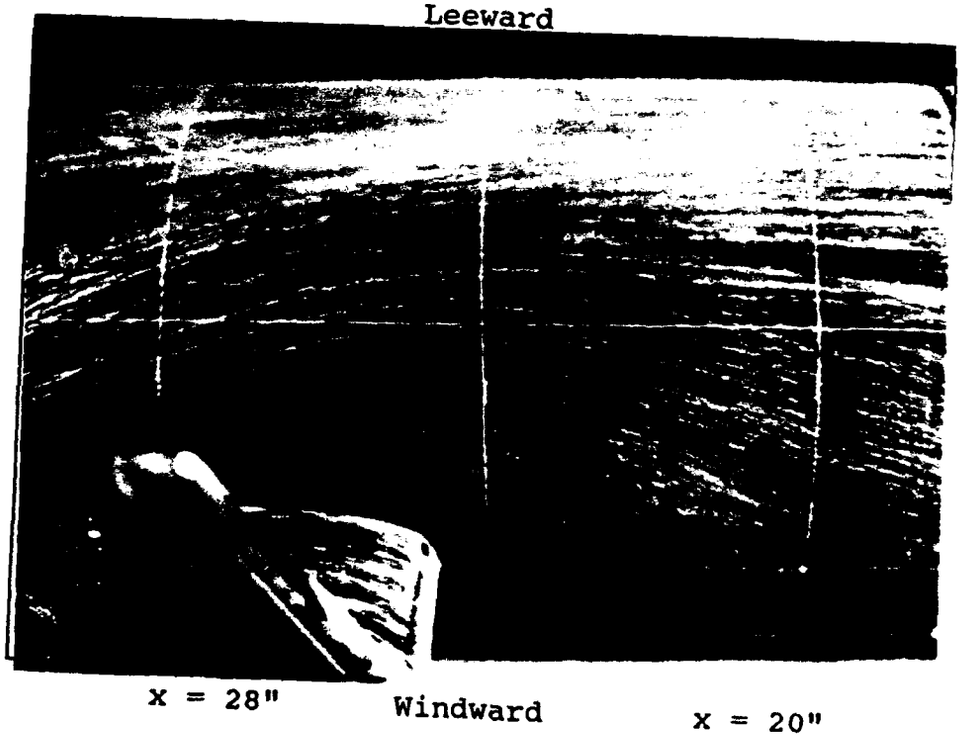

Figure 74. Oil flow 7, naked submarine, sail side, Re = 6.77×10^6, $\beta = 10°$.

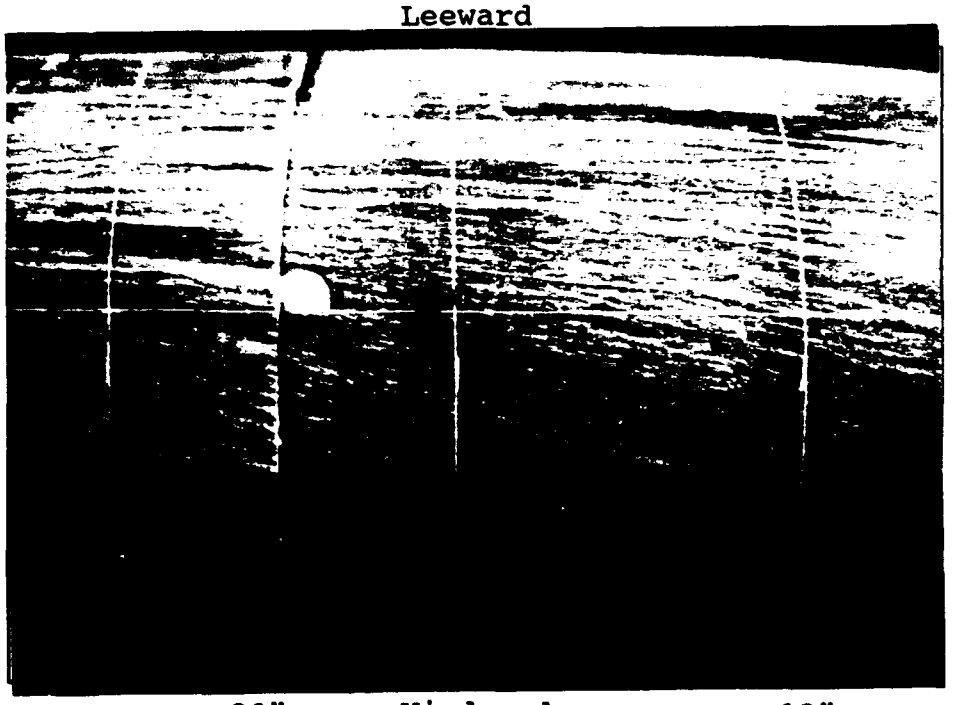

Figure 75. Oil flow 7, naked submarine, sail side, Re = 6.77×10^6, ß = 10°.

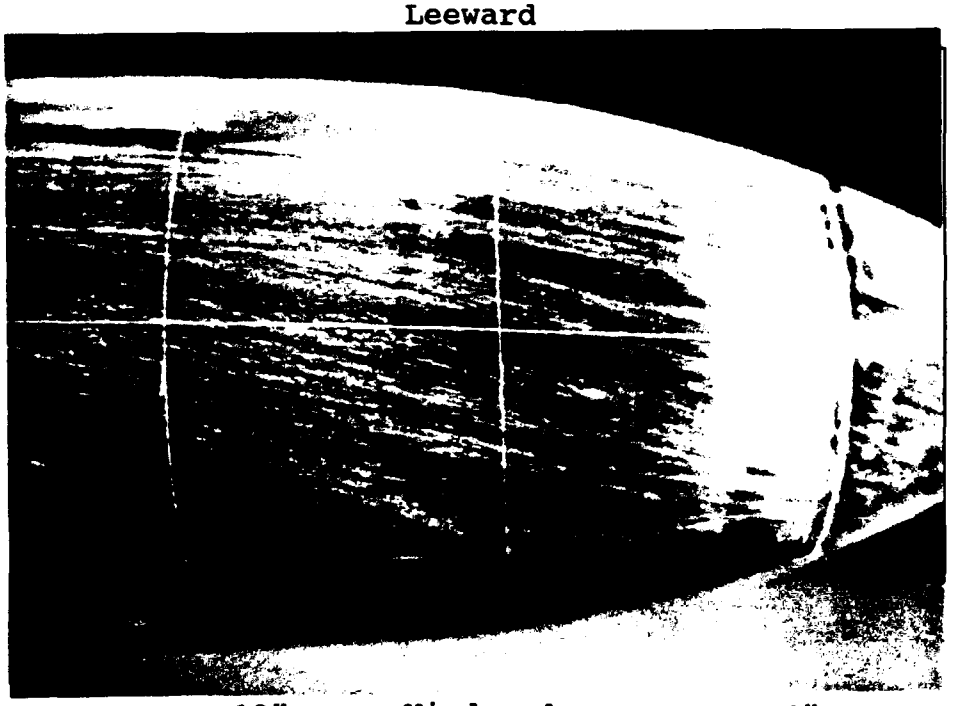

Figure 76. Oil flow 7, naked submarine, sail side, Re = 6.77×10^6, ß = 10°.

Leeward

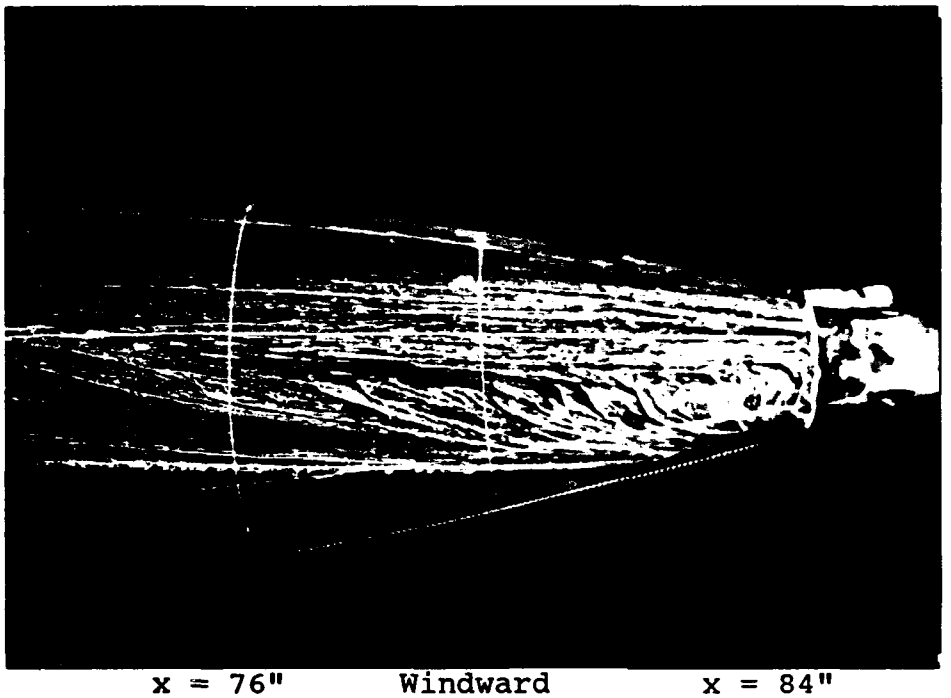

x = 76" Windward x = 84"

Figure 77. Oil flow 7, naked submarine, bottom side, Re = 6.77×10^6, ß = 10°.

Leeward

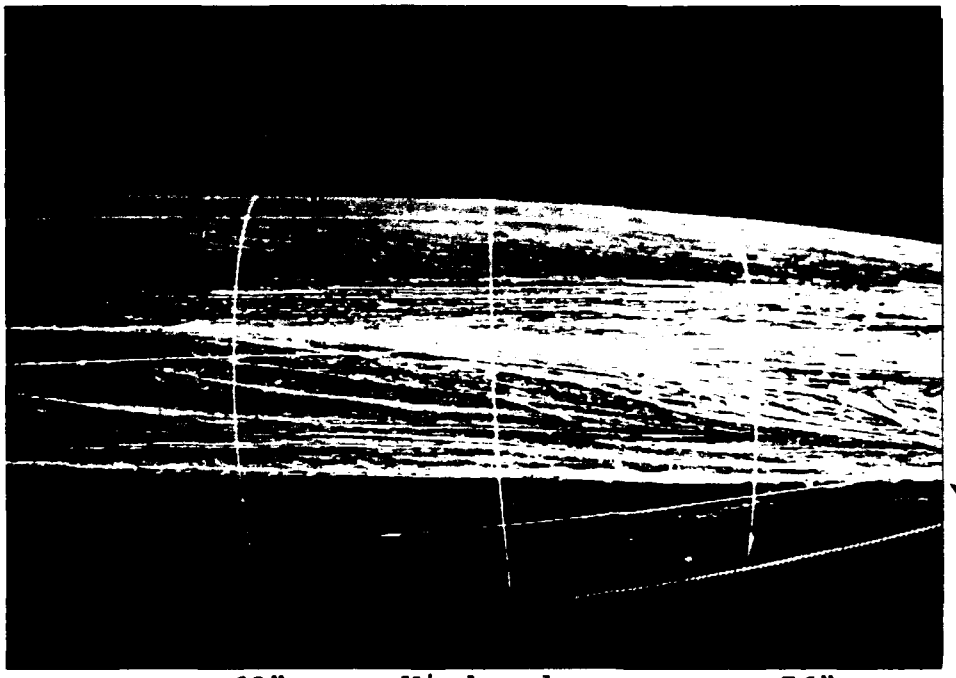

x = 68" Windward x = 76"

Figure 78. Oil flow 7, naked submarine, bottom side, Re = 6.77×10^6, ß = 10°.

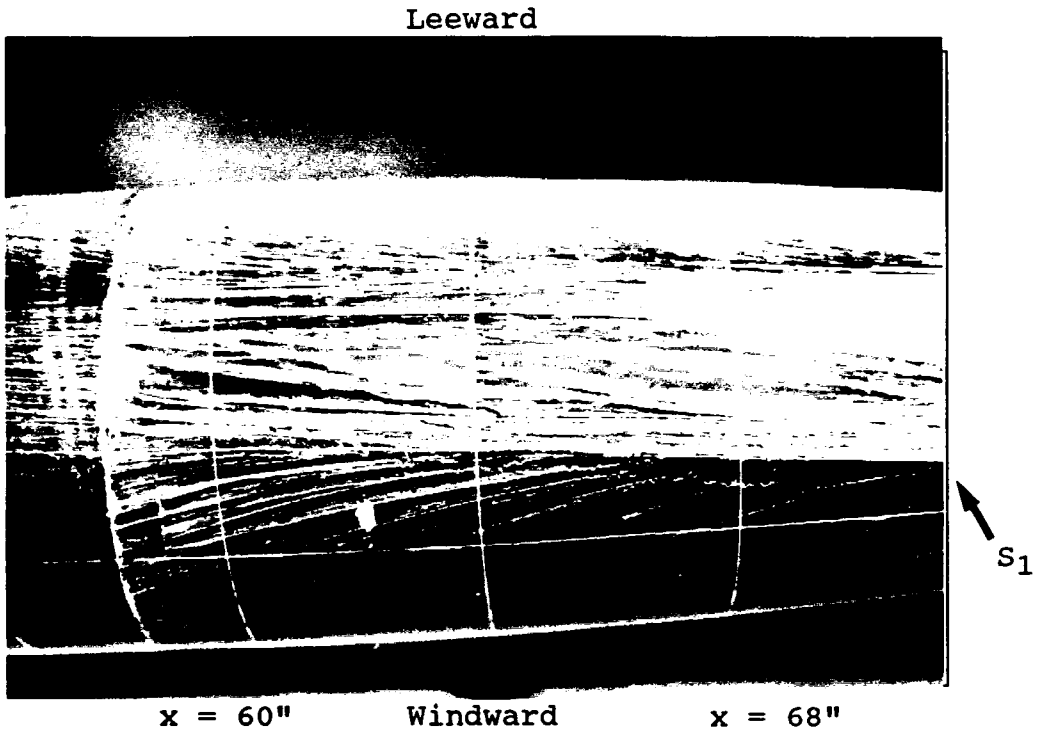

Figure 79. Oil flow 7, naked submarine, bottom side, Re = 6.77×10^6, ß = 10°.

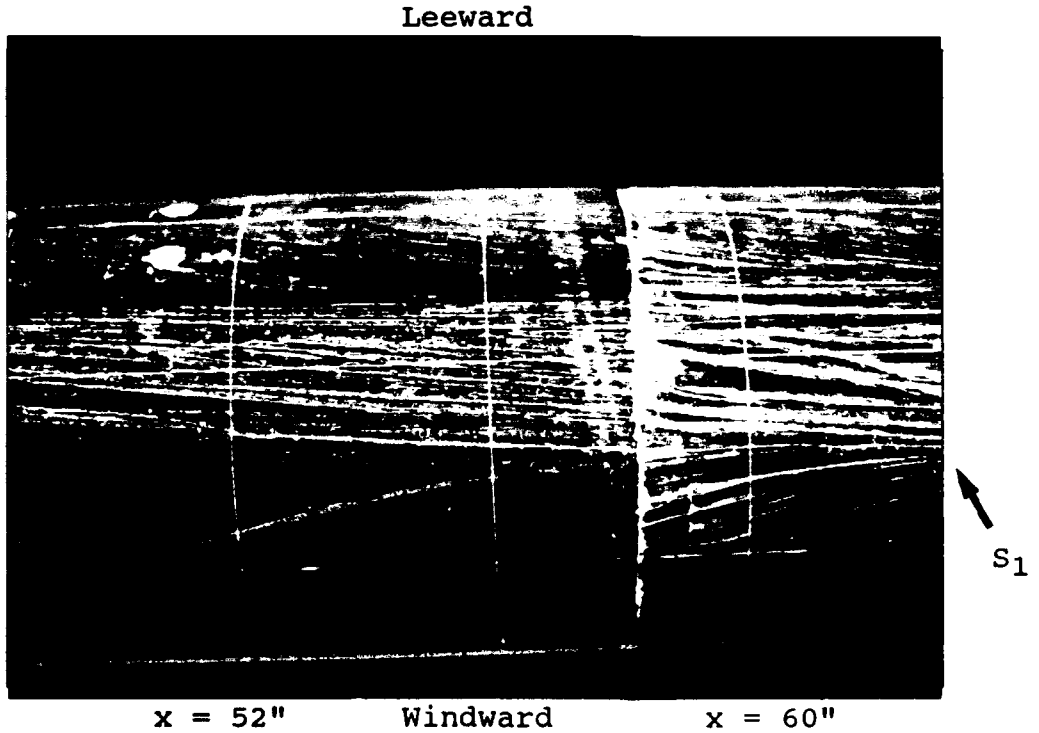

Figure 80. Oil flow 7, naked submarine, bottom side, Re = 6.77×10^6, ß = 10°.

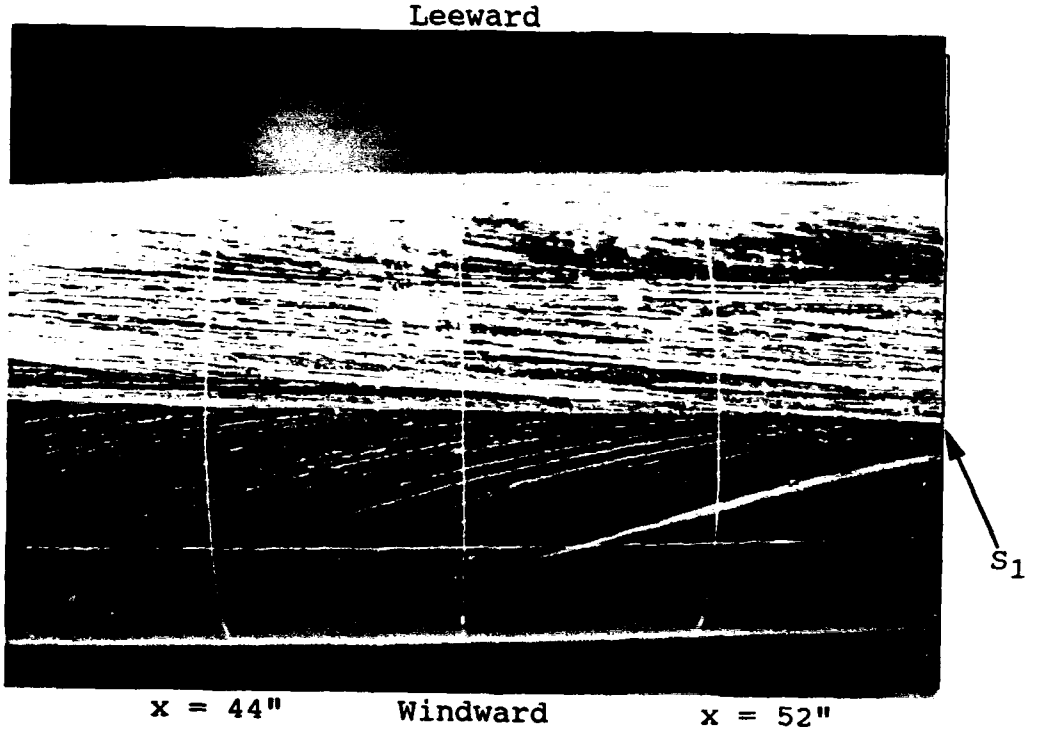

Figure 81. Oil flow 7, naked submarine, bottom side, Re = 6.77×10^6, $\beta = 10°$.

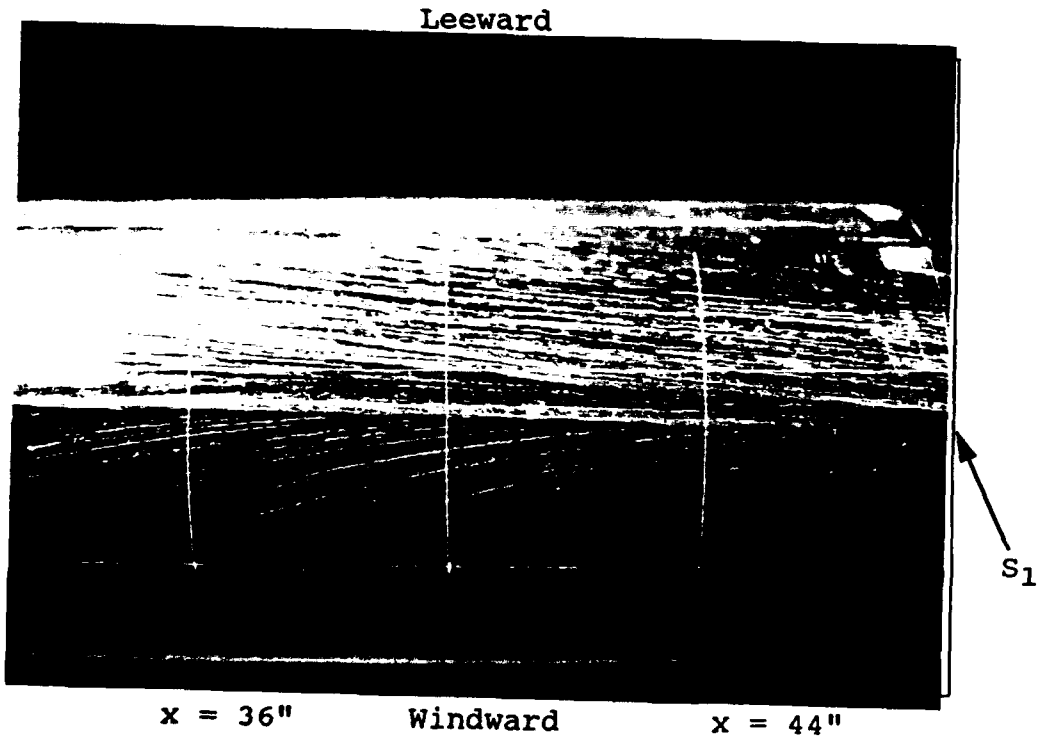

Figure 82. Oil flow 7, naked submarine, bottom side, Re = 6.77×10^6, $\beta = 10°$.

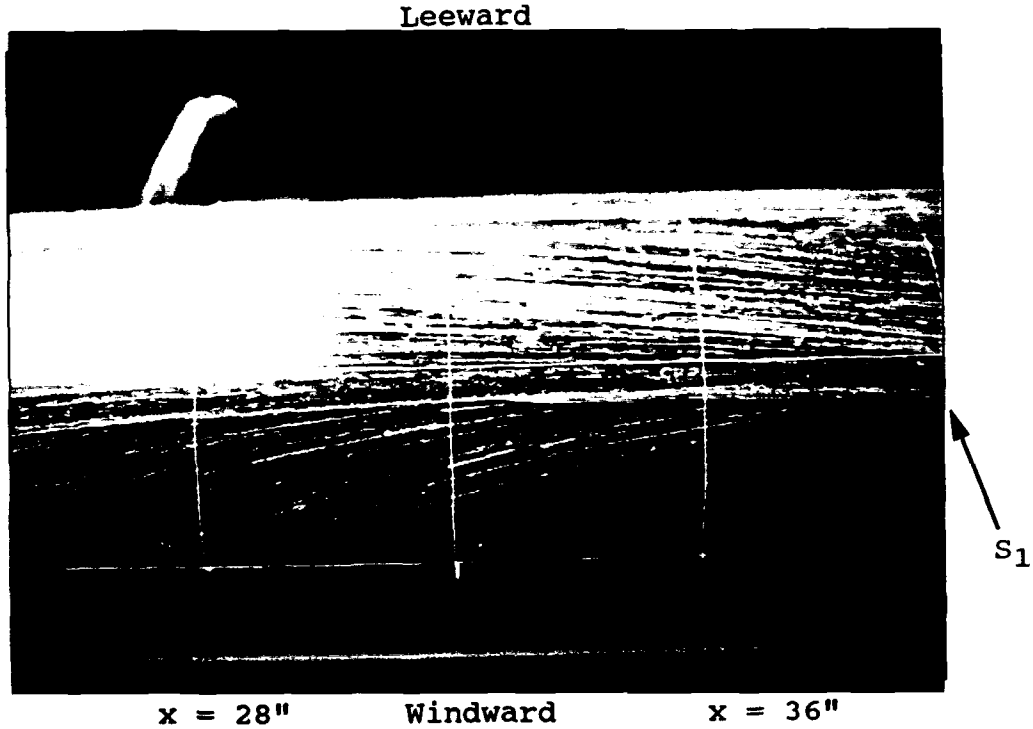

Figure 83. Oil flow 7, naked submarine, bottom side, Re = 6.77×10^6, $\beta = 10°$.

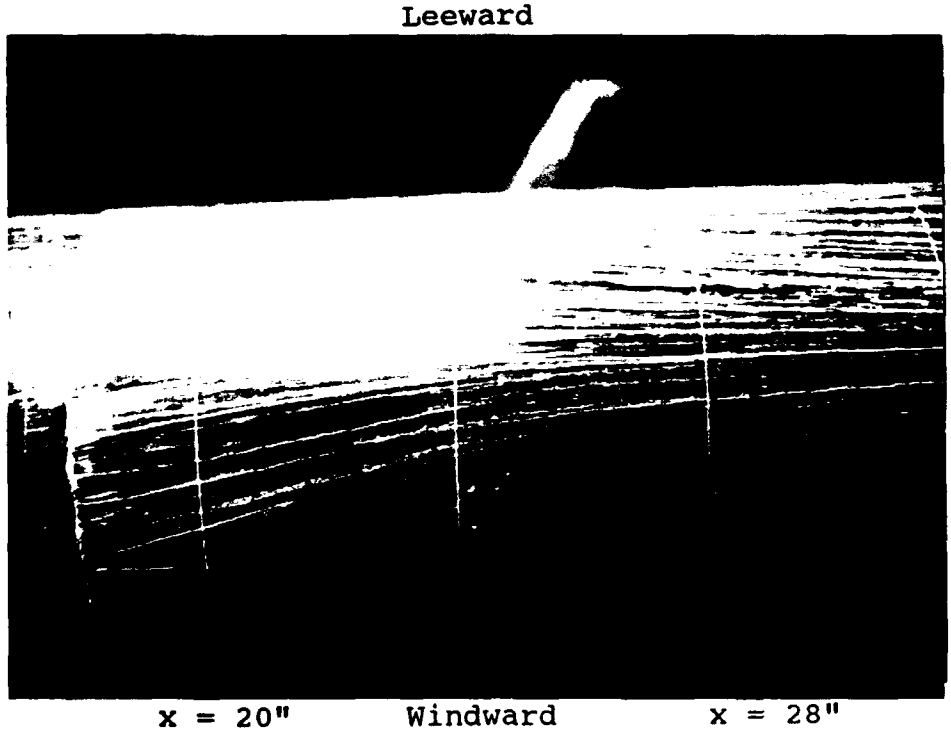

Figure 84. Oil flow 7, naked submarine, bottom side, Re = 6.77×10^6, $\beta = 10°$.

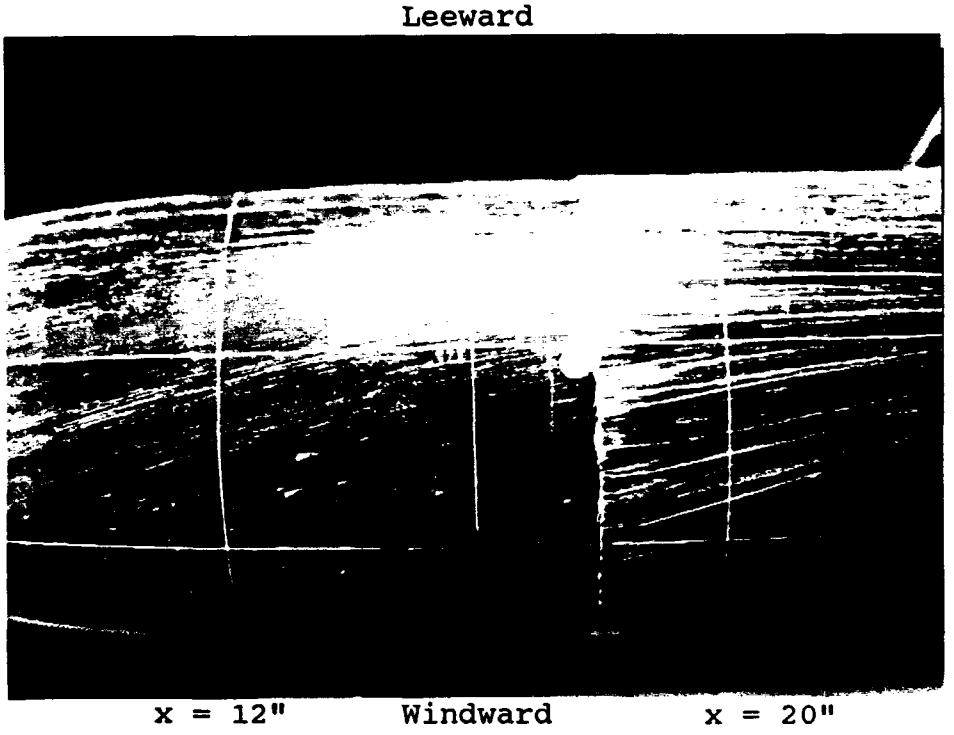

Figure 85. Oil flow 7, naked submarine, sail side, Re = 6.77×10^6, β = 10°.

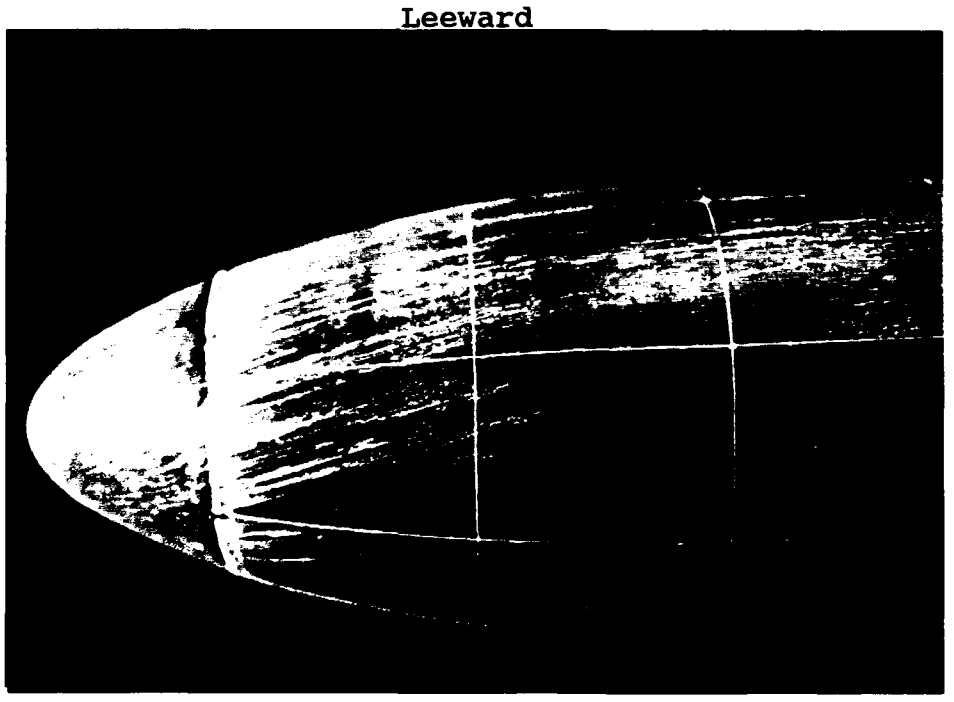

Figure 86. Oil flow 7, naked submarine, sail side, Re = 6.77×10^6, β = 10°.

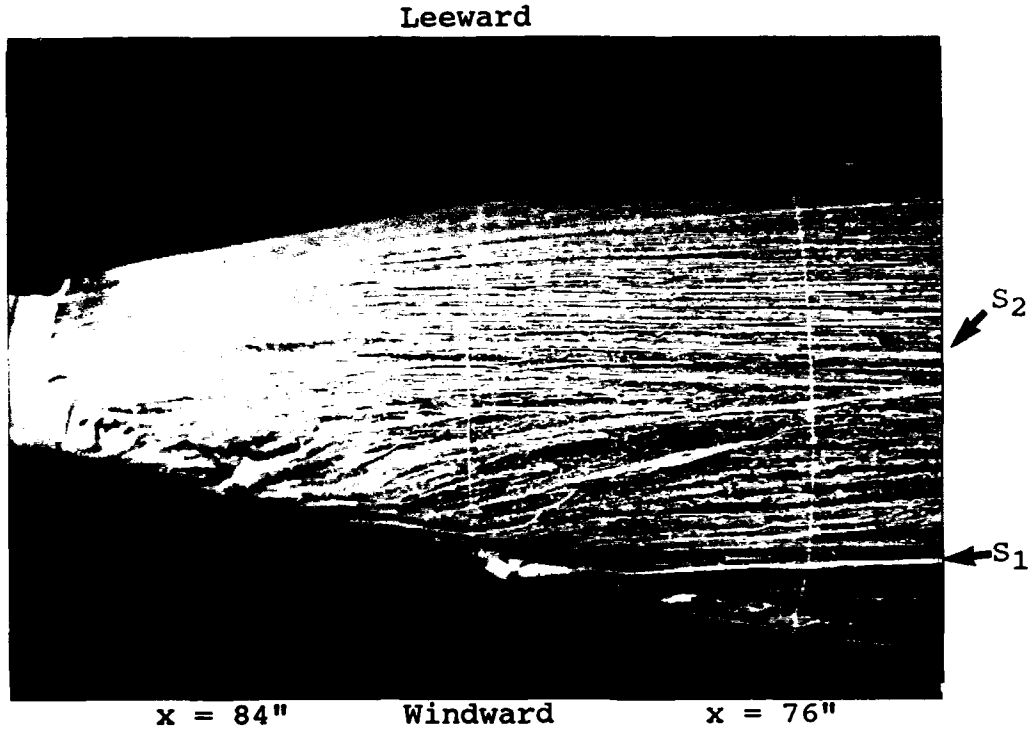

Figure 87. Oil flow 2, naked submarine, sail side, Re = 6.78×10^6, $\beta = 15°$.

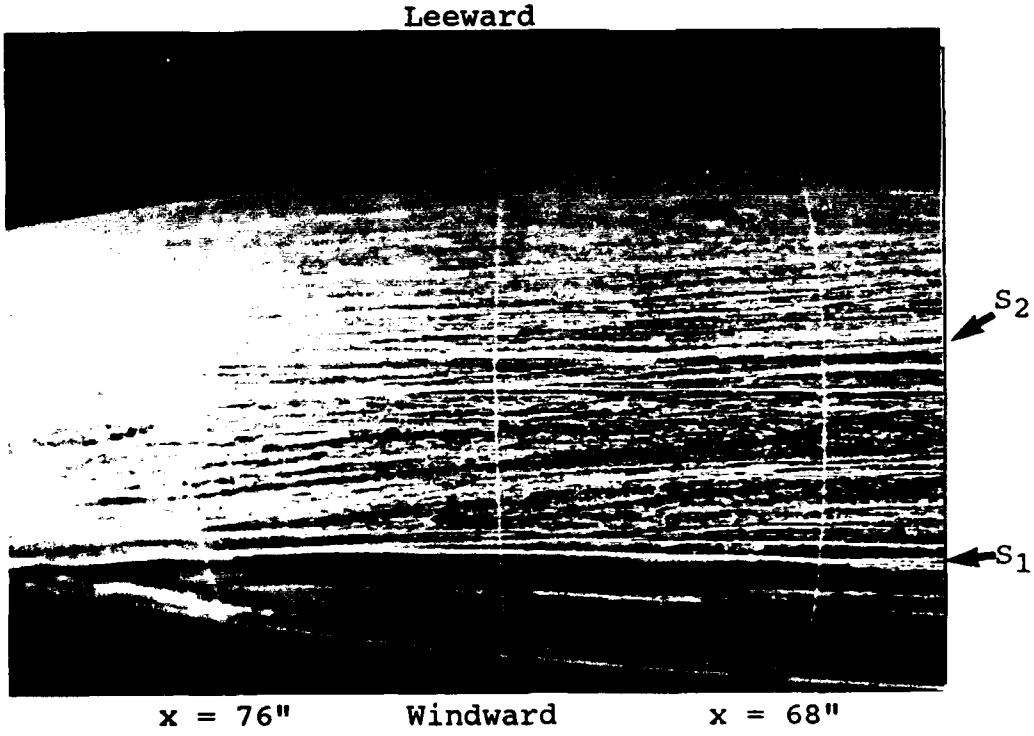

Figure 88. Oil flow 2, naked submarine, sail side, Re = 6.78×10^6, $\beta = 15°$.

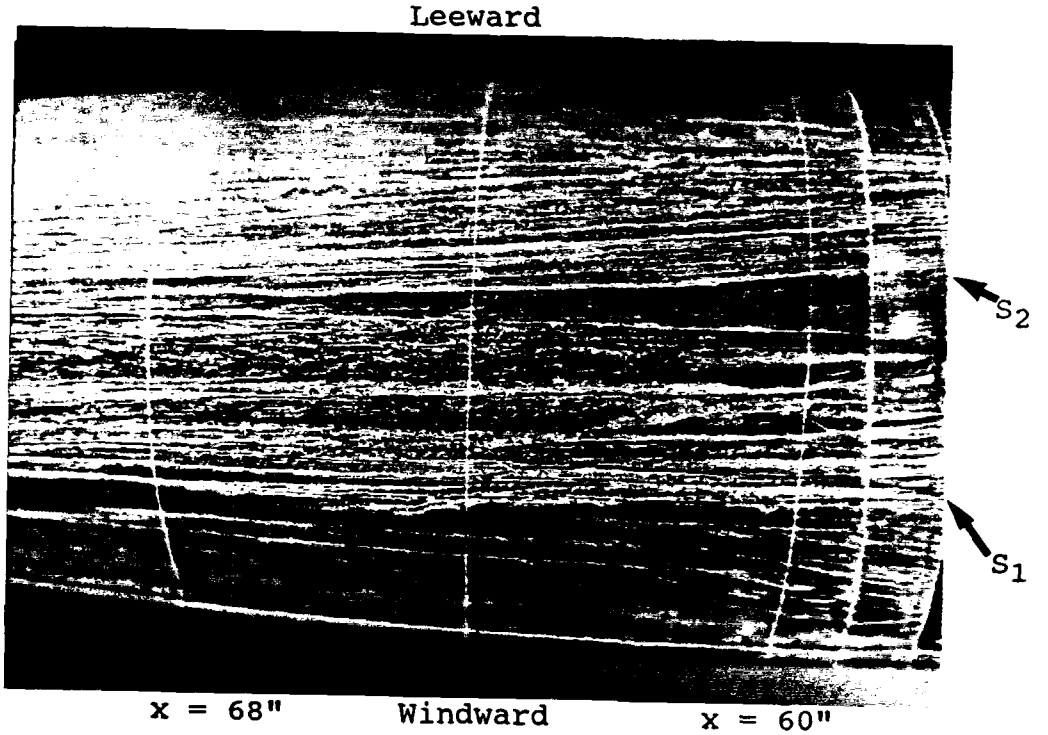

Figure 89. Oil flow 2, naked submarine, sail side, Re = 6.78×10^6, $\beta = 15°$.

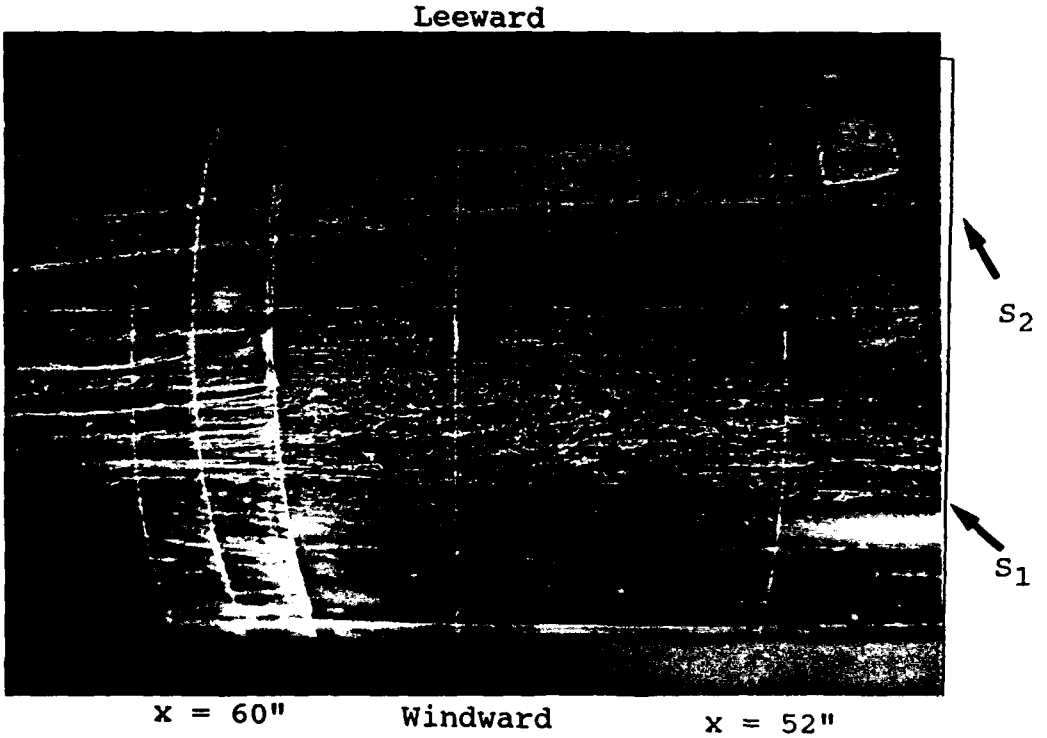

Figure 90. Oil flow 2, naked submarine, sail side, Re = 6.78×10^6, $\beta = 15°$.

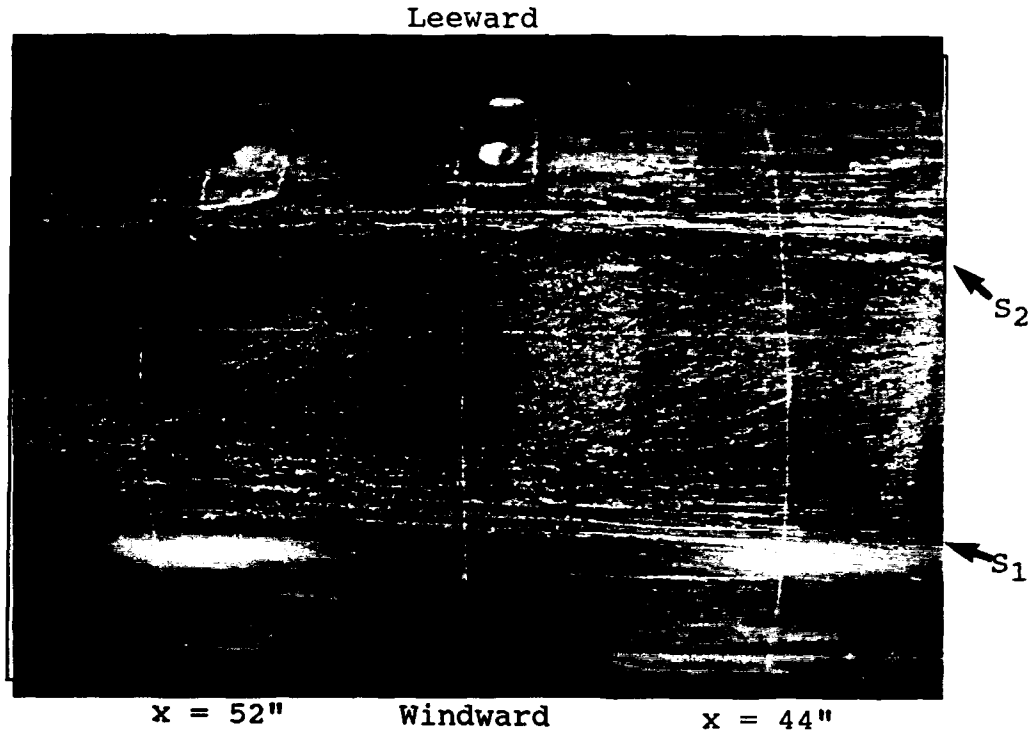

Figure 91. Oil flow 2, naked submarine, sail side, Re = 6.78×10^6, $\beta = 15°$.

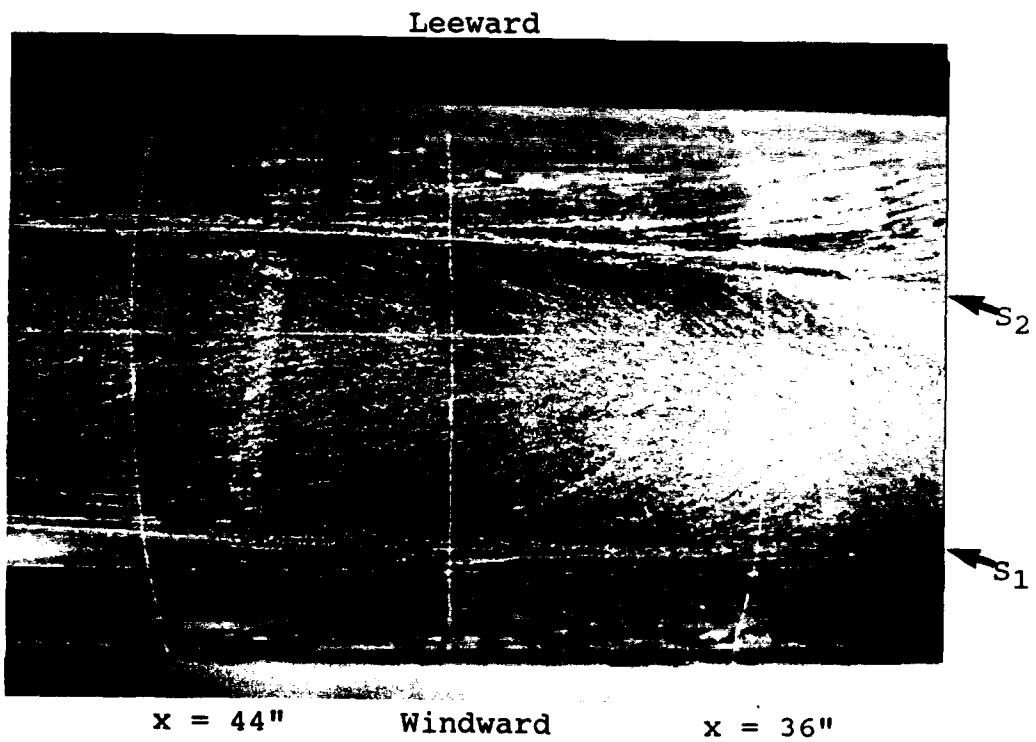

Figure 92. Oil flow 2, naked submarine, sail side, Re = 6.78×10^6, $\beta = 15°$.

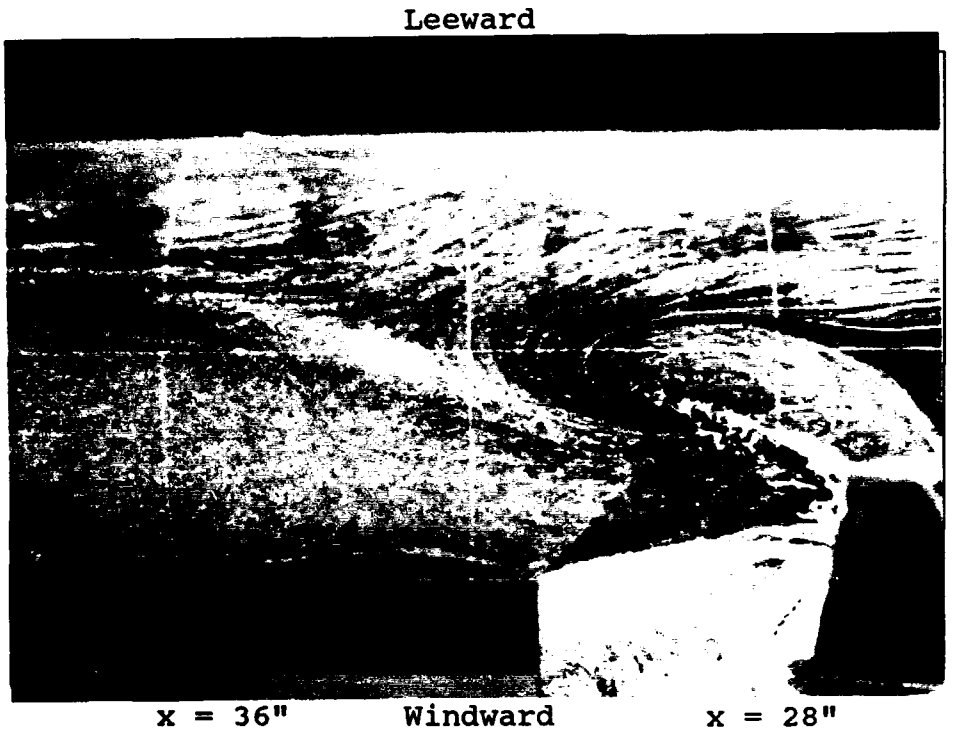

Figure 93. Oil flow 2, naked submarine, sail side, Re = 6.78×10^6, ß = 15°.

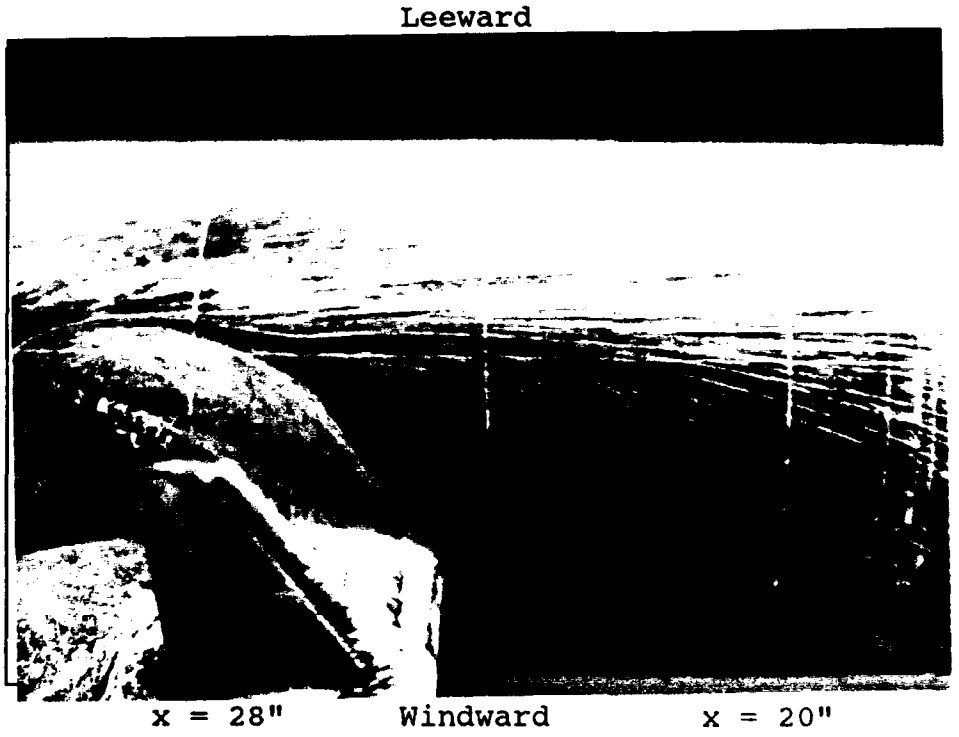

Figure 94. Oil flow 2, naked submarine, sail side, Re = 6.78×10^6, ß = 15°.

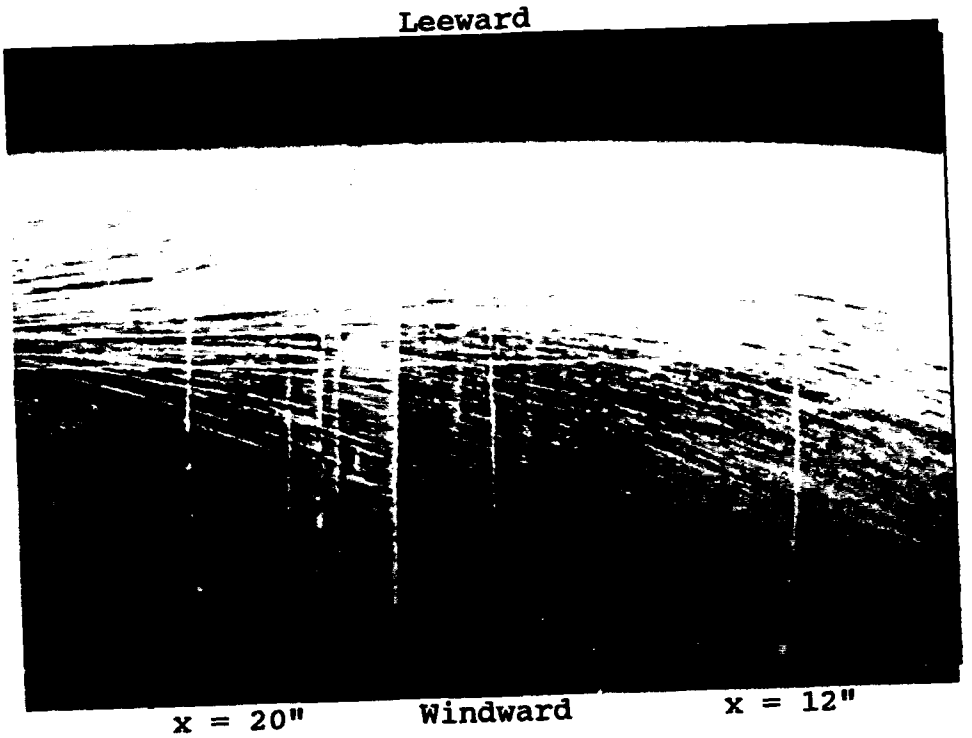

Figure 95. Oil flow 2, naked submarine, sail side, Re = 6.78×10^6, $\beta = 15°$.

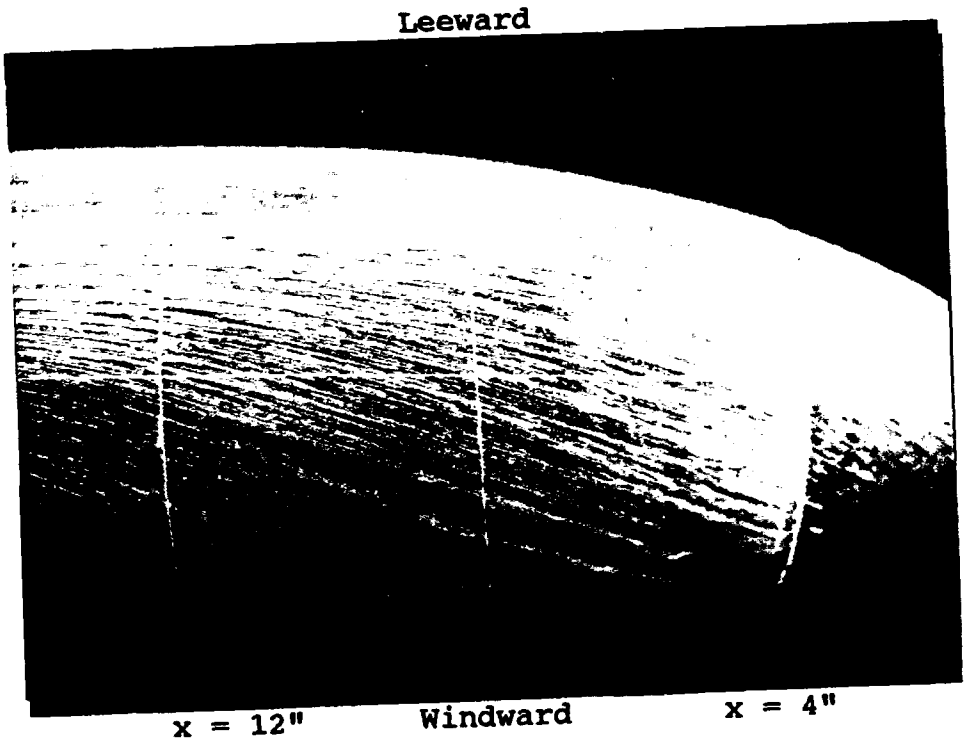

Figure 96. Oil flow 2, naked submarine, sail side, Re = 6.78×10^6, $\beta = 15°$.

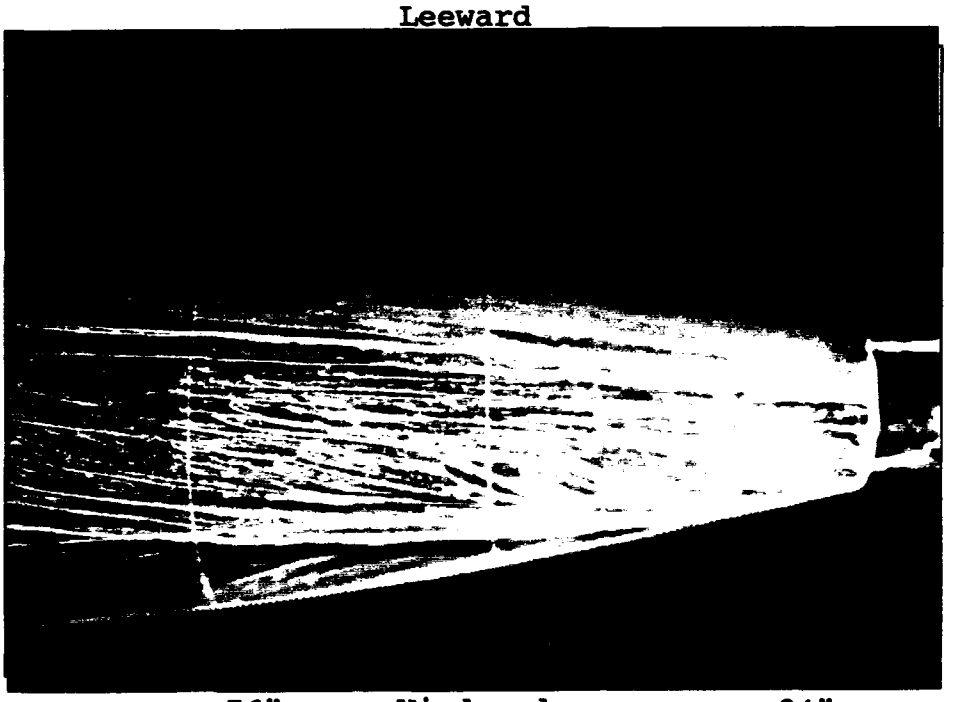

Figure 97. Oil flow 2, naked submarine, bottom side, Re = 6.78×10^6, β = 15°.

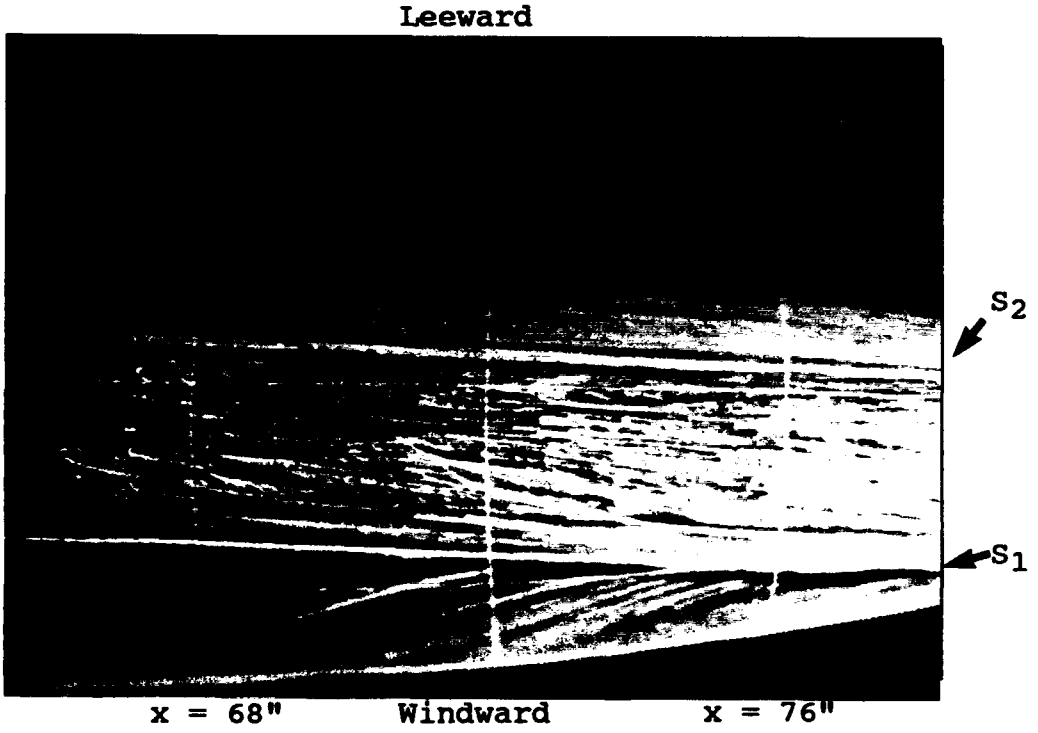

Figure 98. Oil flow 2, naked submarine, bottom side, Re = 6.78×10^6, β = 15°.

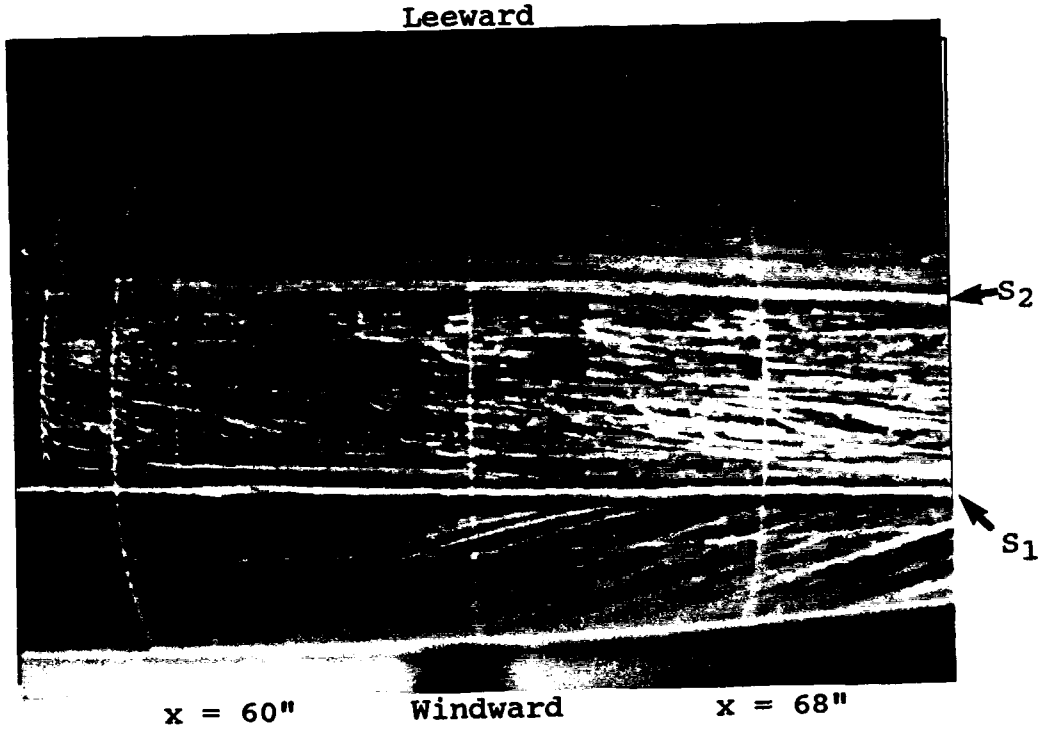

Figure 99. Oil flow 2, naked submarine, bottom side, Re = 6.78×10^6, β = 15°.

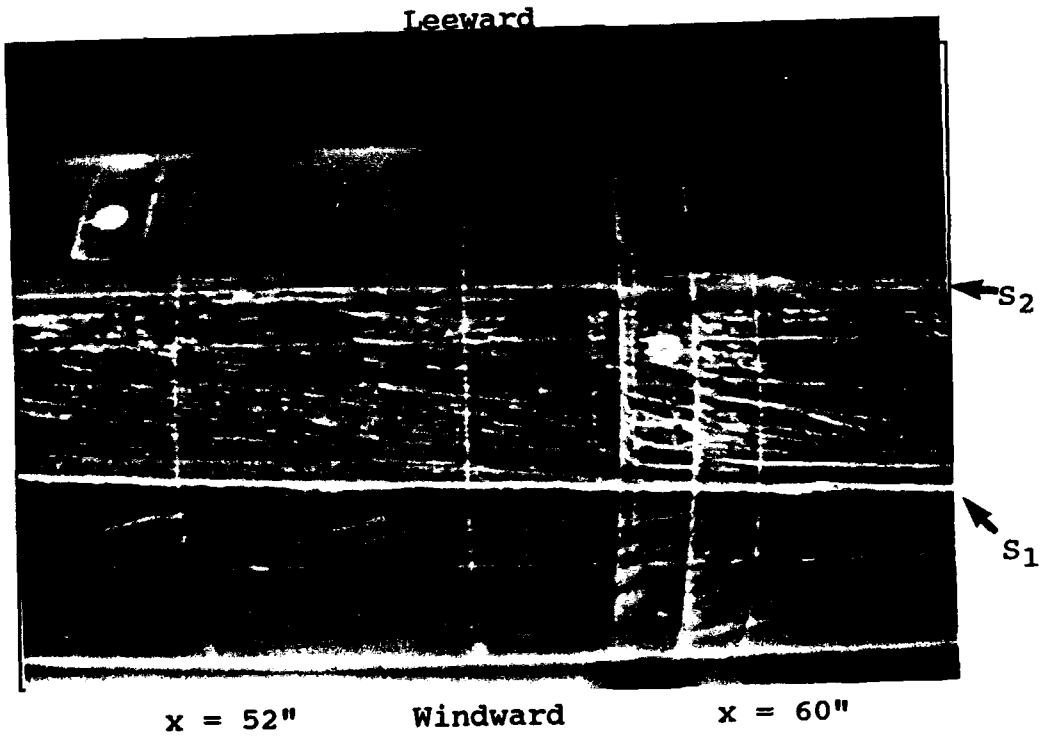

Figure 100. Oil flow 2, naked submarine, bottom side, Re = 6.78×10^6, β = 15°.

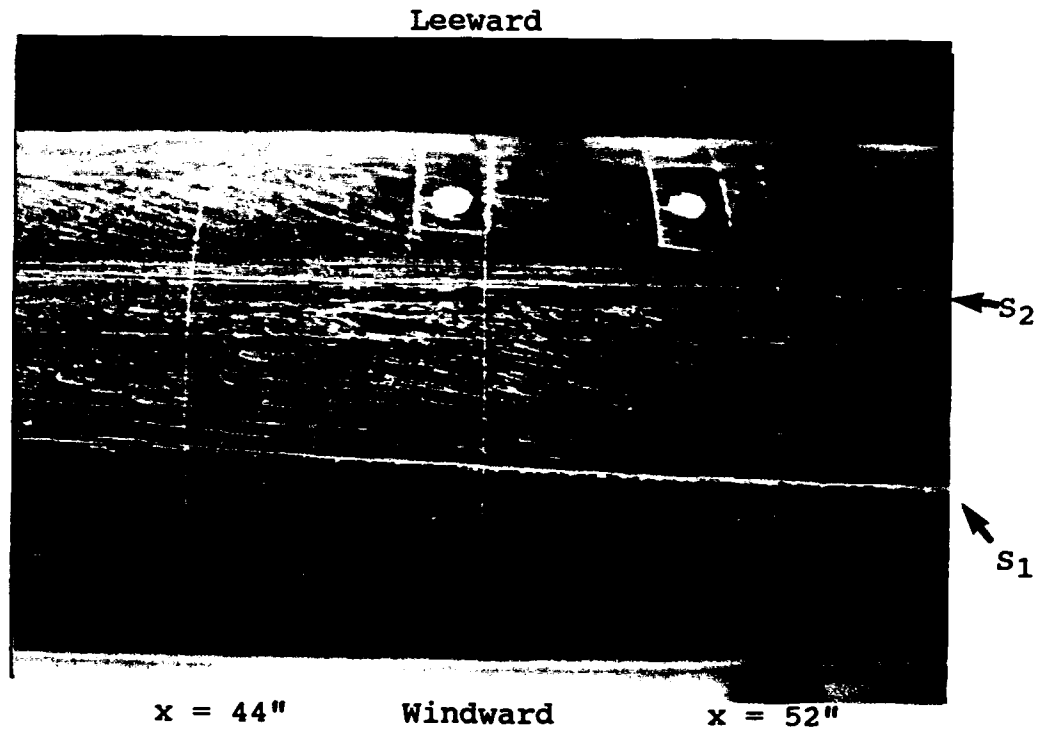

Figure 101. Oil flow 2, naked submarine, bottom side, Re = 6.78×10^6, β = 15°.

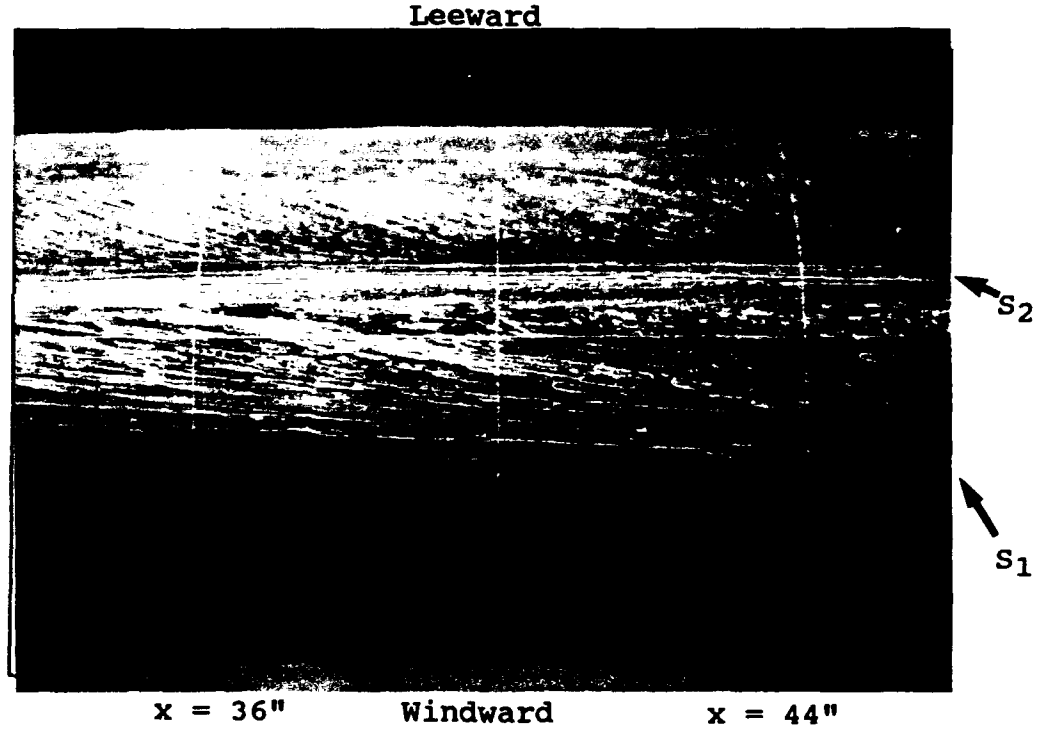

Figure 102. Oil flow 2, naked submarine, bottom side, Re = 6.78×10^6, β = 15°.

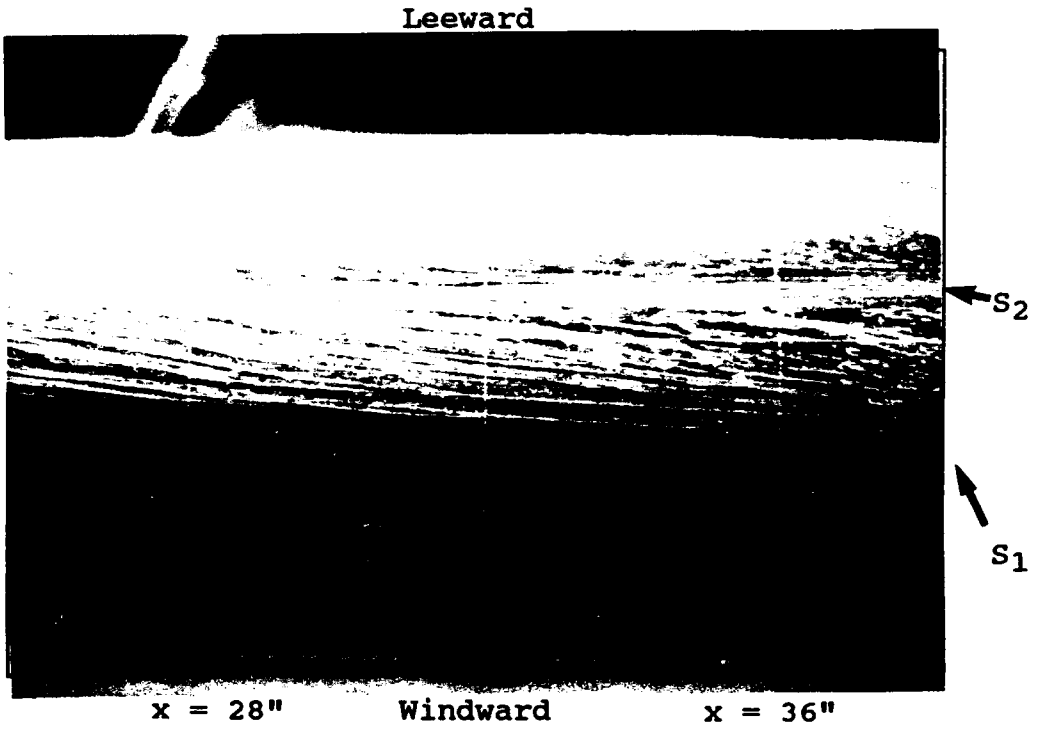

Figure 103. Oil flow 2, naked submarine, bottom side, Re = 6.78×10^6, $\beta = 15°$.

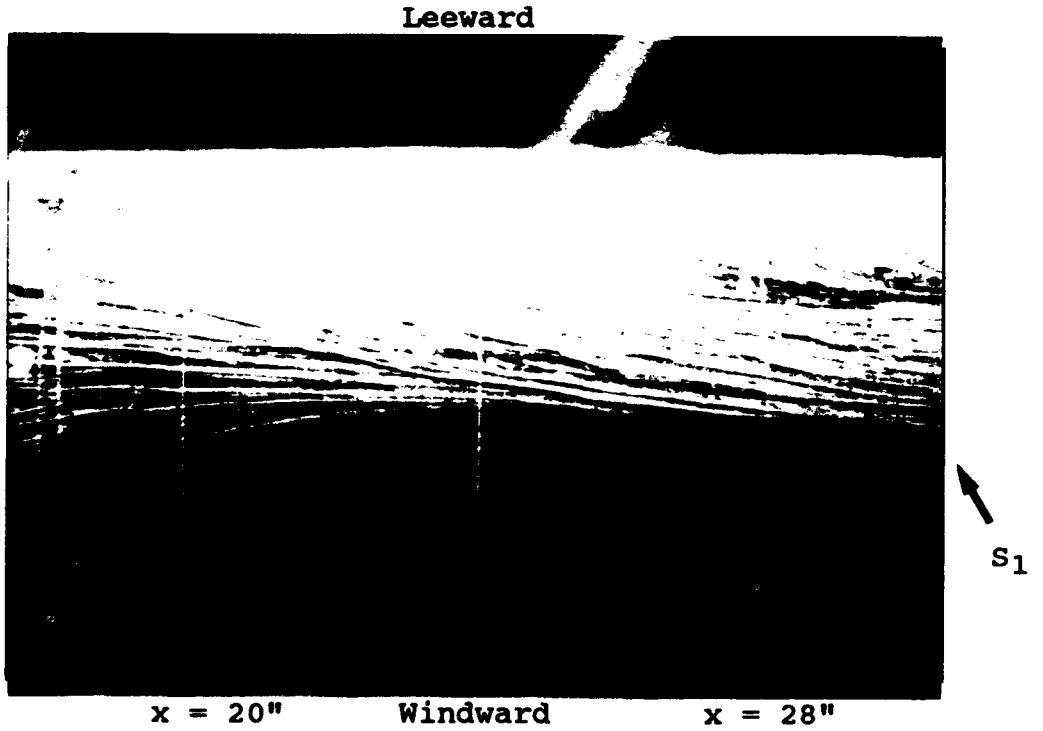

Figure 104. Oil flow 2, naked submarine, bottom side, Re = 6.78×10^6, $\beta = 15°$.

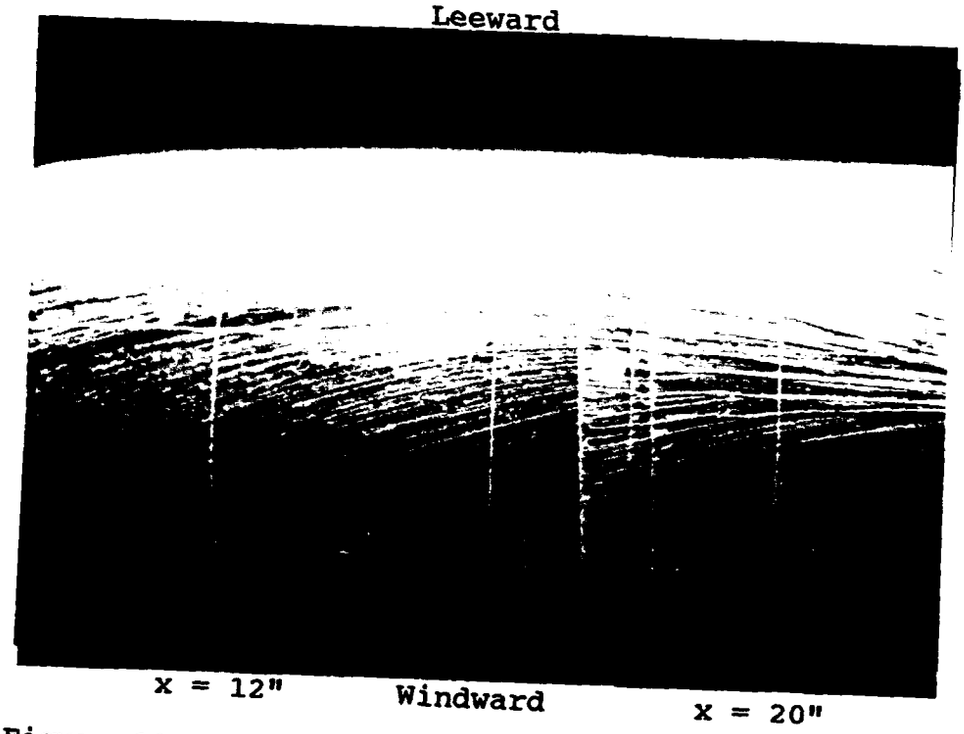

Figure 105. Oil flow 2, naked submarine, bottom side, Re = 6.78×10^6, $\beta = 15°$.

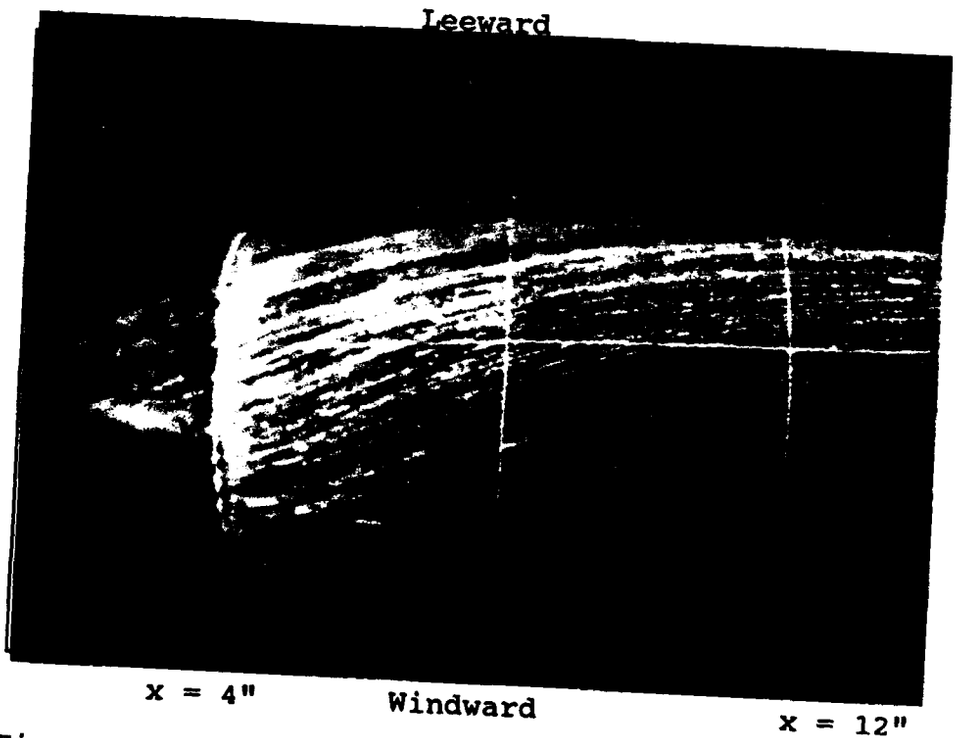

Figure 106. Oil flow 2, naked submarine, bottom side, Re = 6.78×10^6, $\beta = 15°$.

APPENDIX IV Oil Flow Photos for the Submarine With Vortex Generators

The next 20 photos document the oil flow for the most successful vortex generation configuration, oil flow #20, at 15° of sideslip and Re = 6.77×10^6. Note the delayed separation as compared to the naked submarine example.

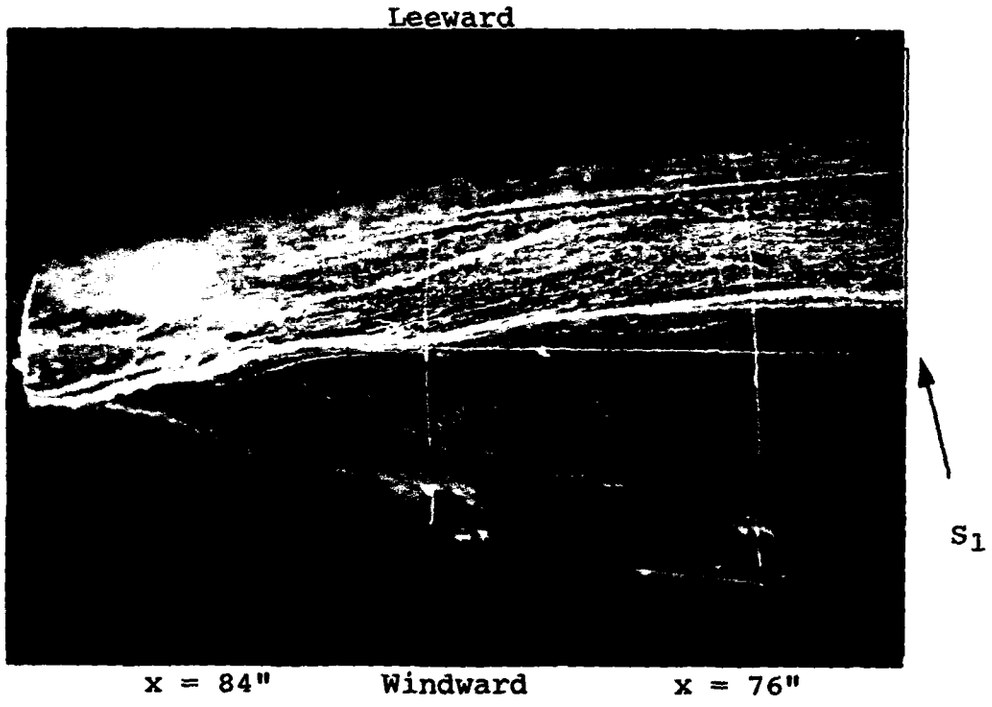

Figure 107. Oil flow 20, submarine with vortex generators, sail side, Re = 6.43×10^6, β = 15°.

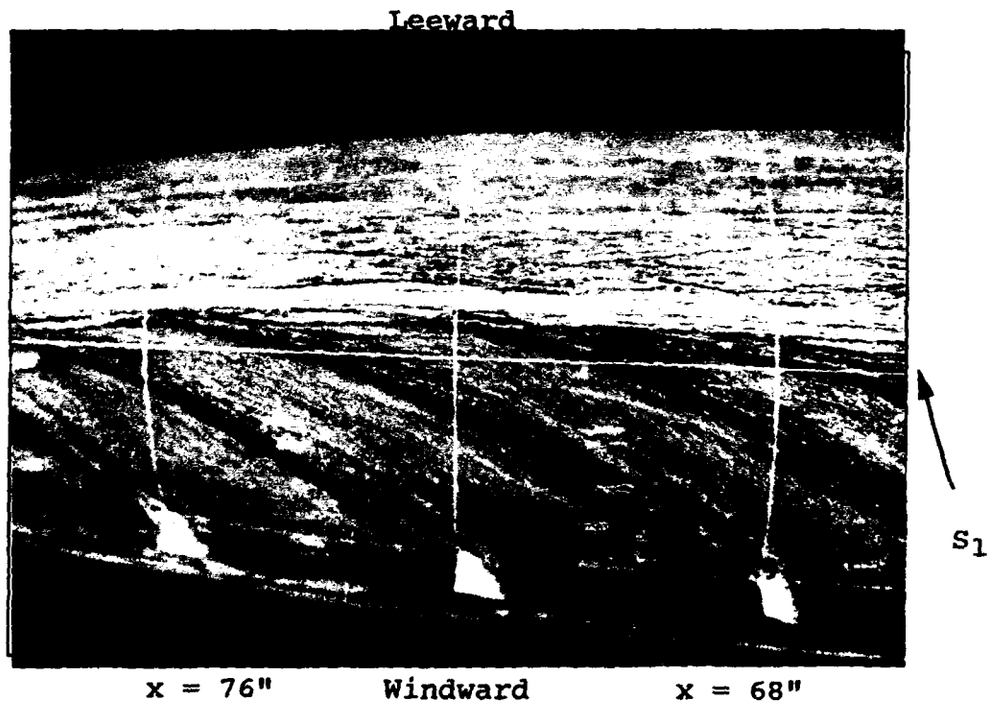

Figure 108. Oil flow 20, submarine with vortex generators, sail side, Re = 6.43×10^6, β = 15°.

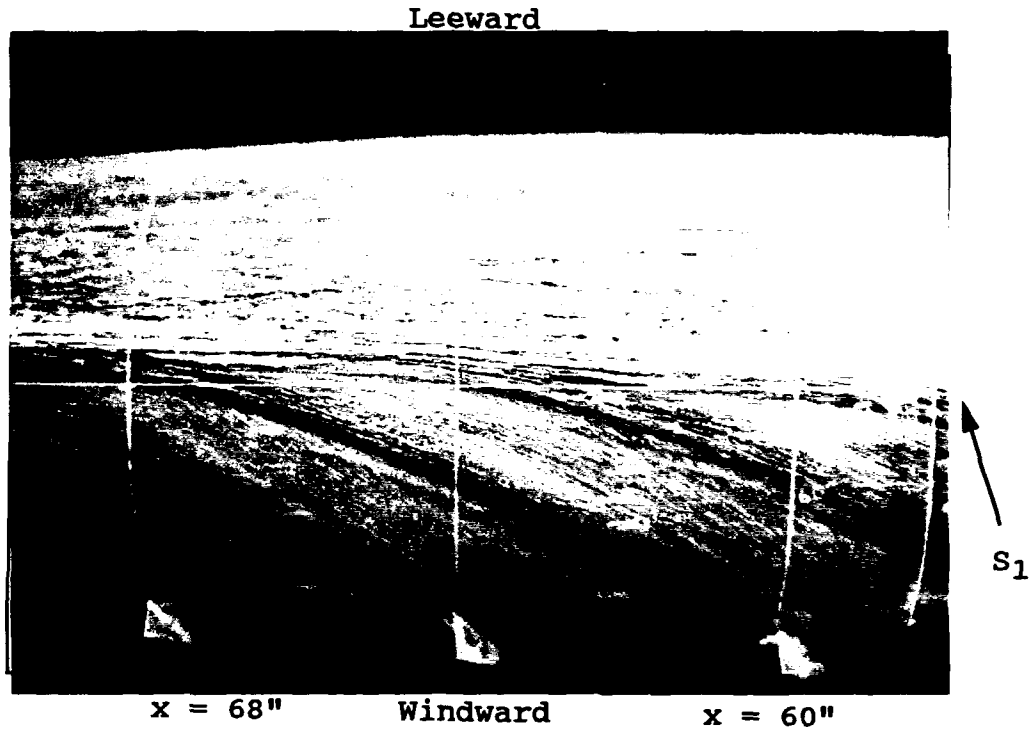

Figure 109. Oil flow 20, submarine with vortex generators, sail side, Re = 6.43×10^6, β = 15°.

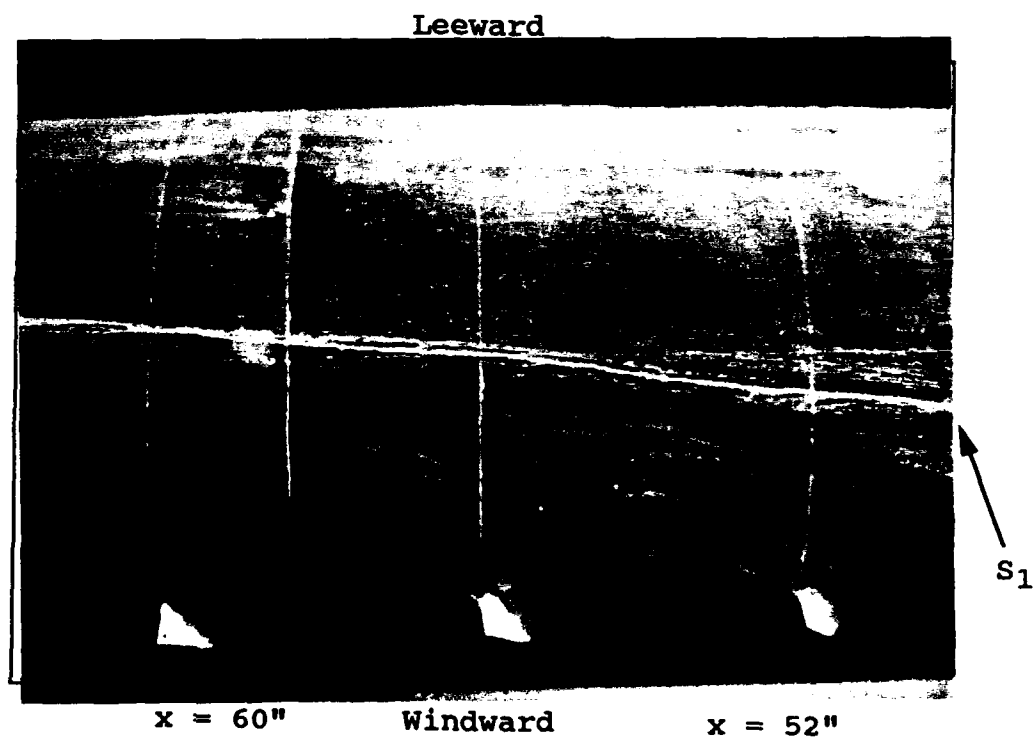

Figure 110. Oil flow 20, submarine with vortex generators, sail side, Re = 6.43×10^6, β = 15°.

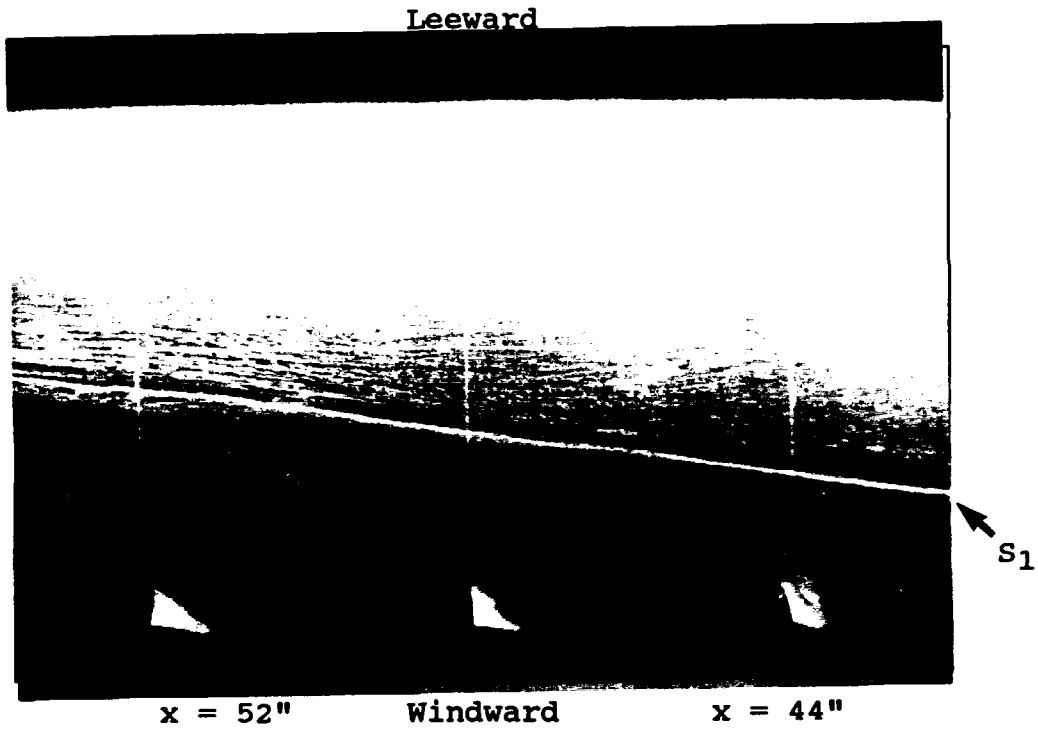

Figure 111. Oil flow 20, submarine with vortex generators, sail side, Re = 6.43×10^6, β = 15°.

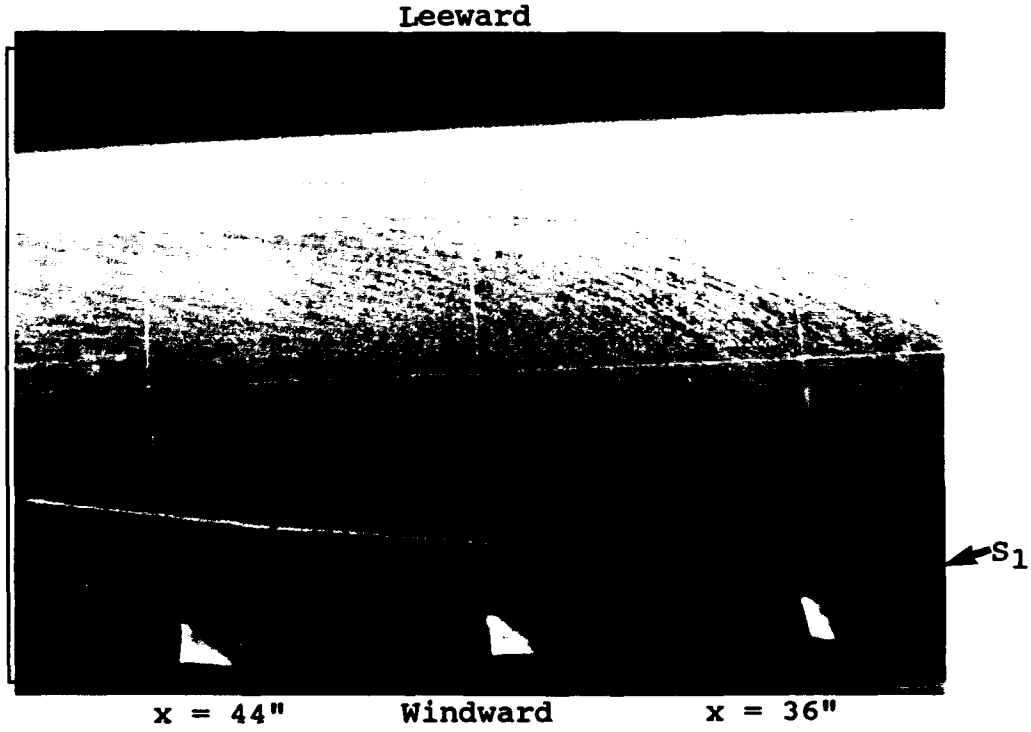

Figure 112. Oil flow 20, submarine with vortex generators, sail side, Re = 6.43×10^6, β = 15°.

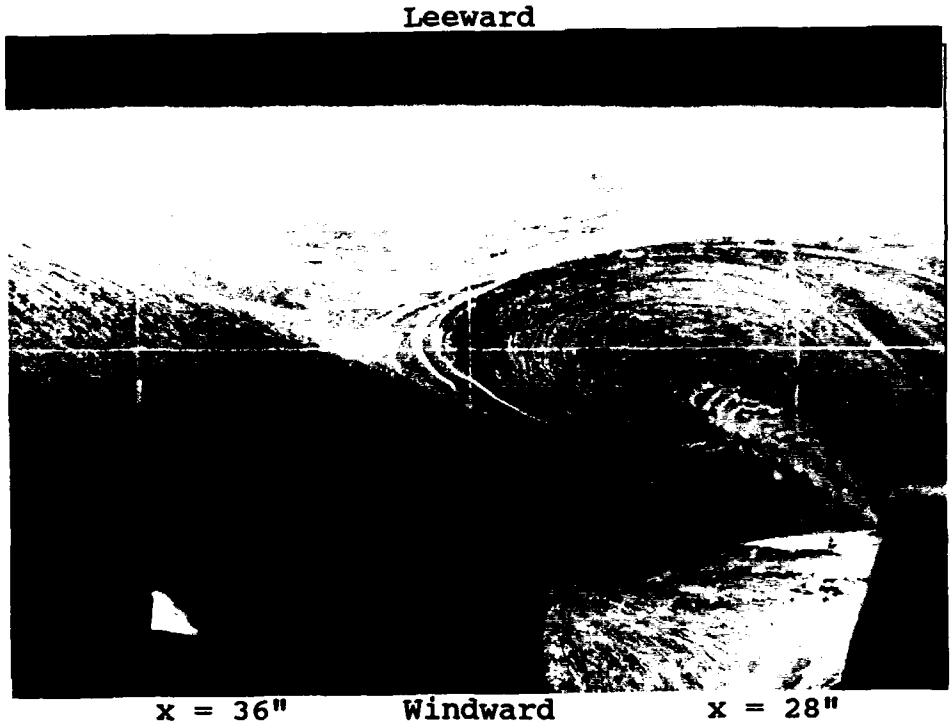

Figure 113. Oil flow 20, submarine with vortex generators, sail side, Re = 6.43×10^6, $\beta = 15°$.

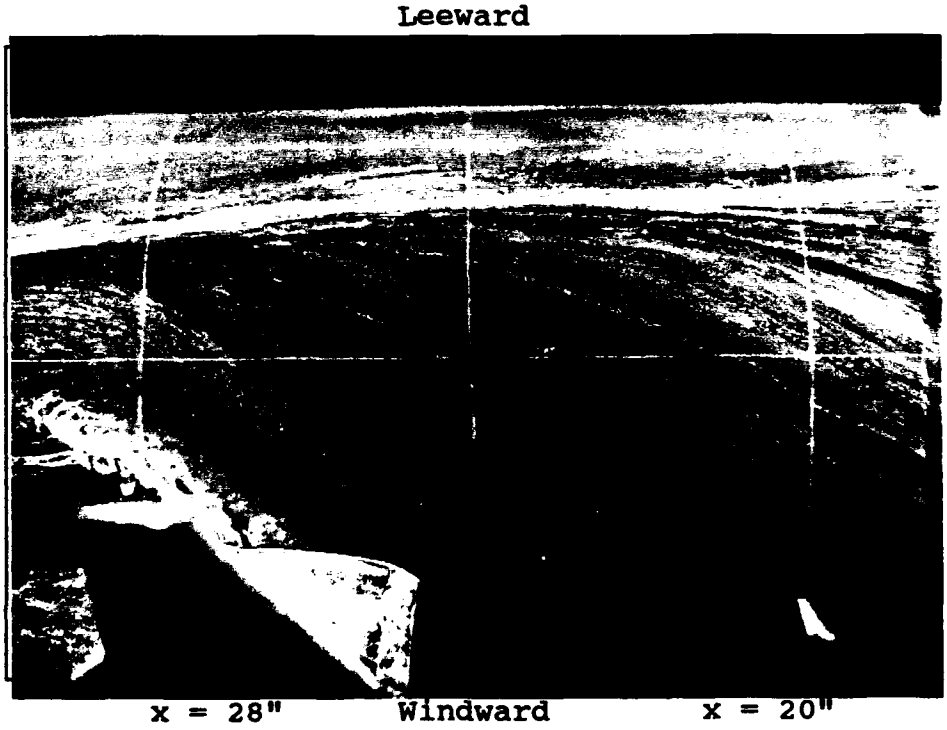

Figure 114. Oil flow 20, submarine with vortex generators, sail side, Re = 6.43×10^6, $\beta = 15°$.

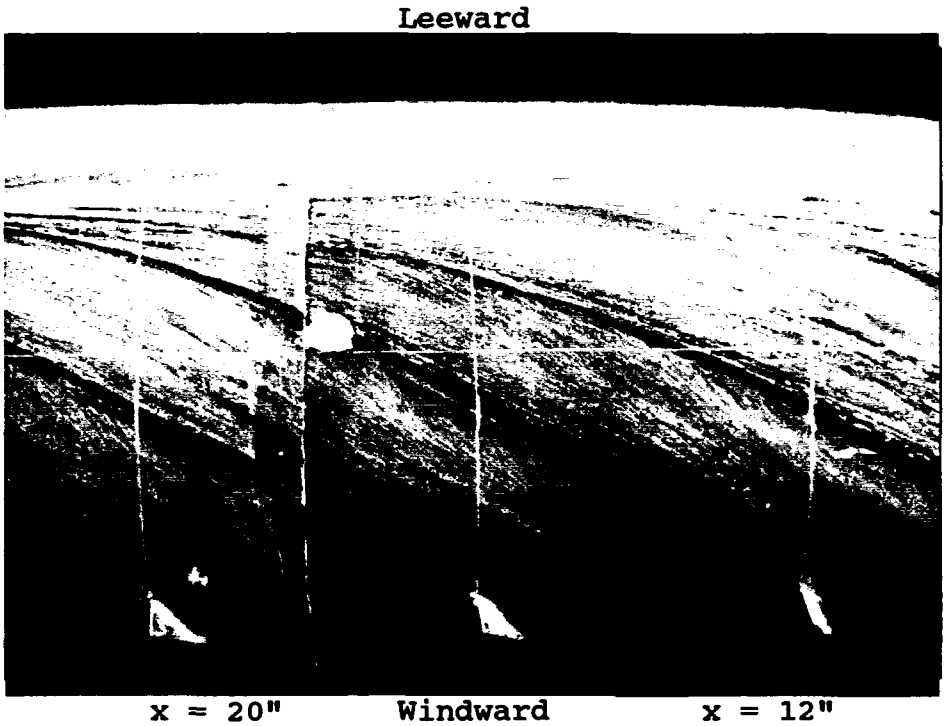

Figure 115. Oil flow 20, submarine with vortex generators, sail side, Re = 6.43×10^6, β = 15°.

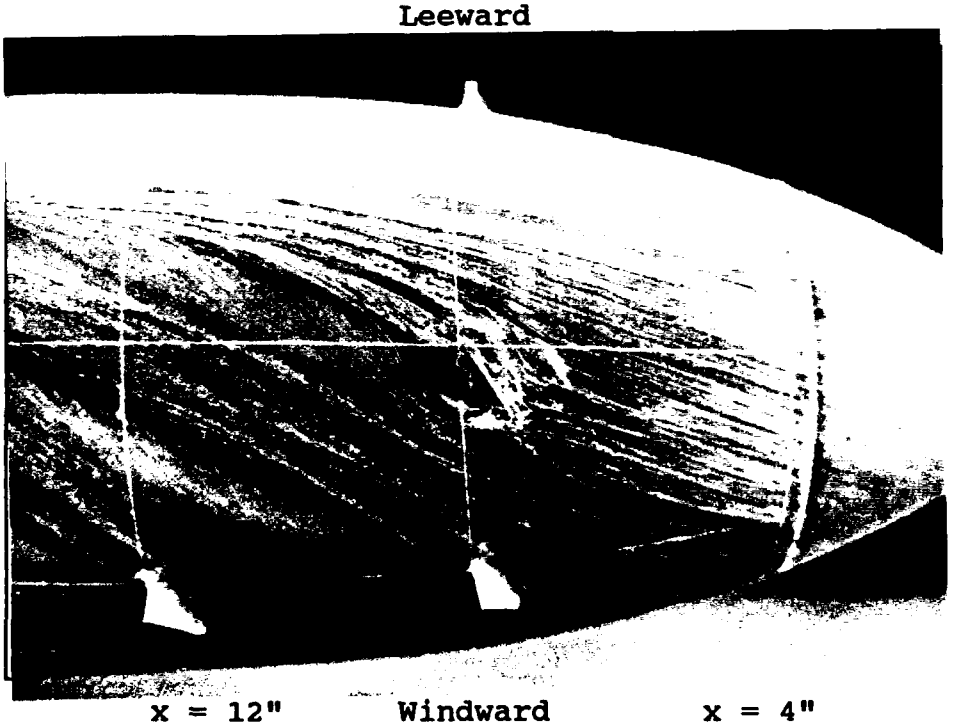

Figure 116. Oil flow 20, submarine with vortex generators, sail side, Re = 6.43×10^6, β = 15°.

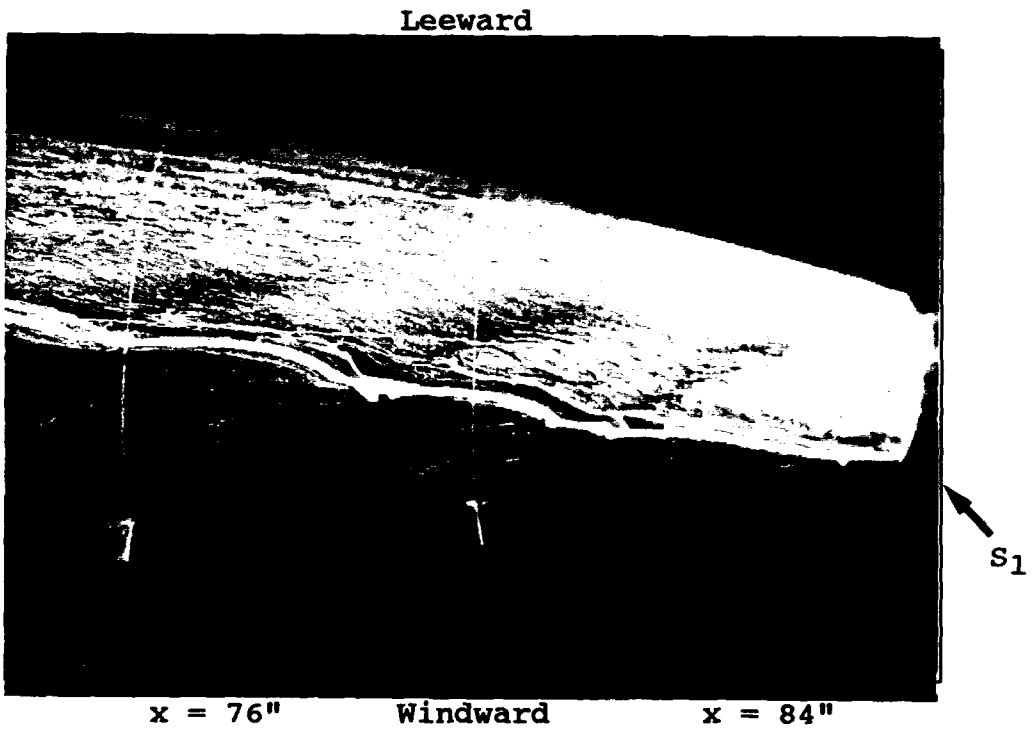

Figure 117. Oil flow 20, submarine with vortex generators, bottom side, Re = 6.43×10^6, $\beta = 15°$.

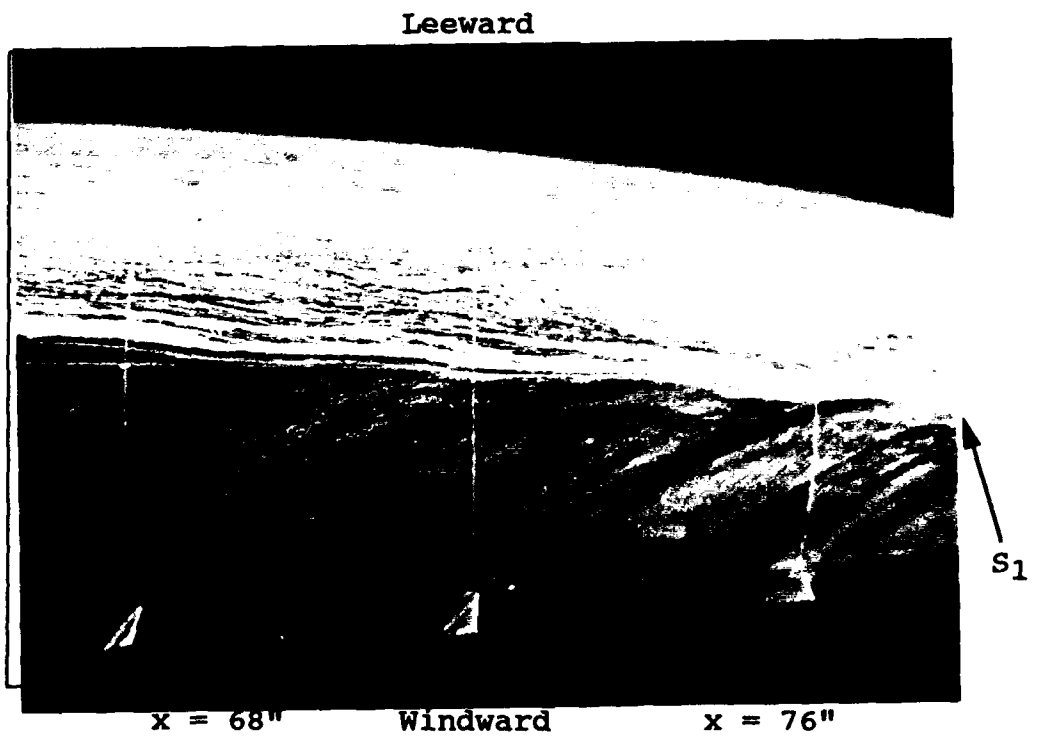

Figure 118. Oil flow 20, submarine with vortex generators, bottom side, Re = 6.43×10^6, $\beta = 15°$.

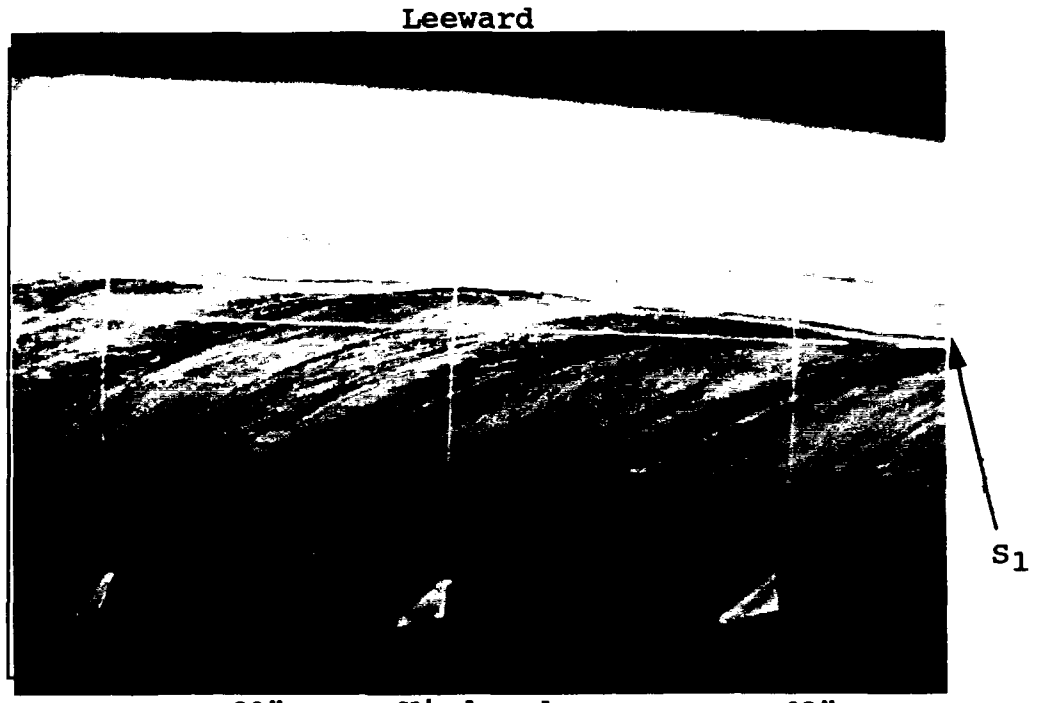

Figure 119. Oil flow 20, submarine with vortex generators, bottom side, Re = 6.43×10^6, β = 15°.

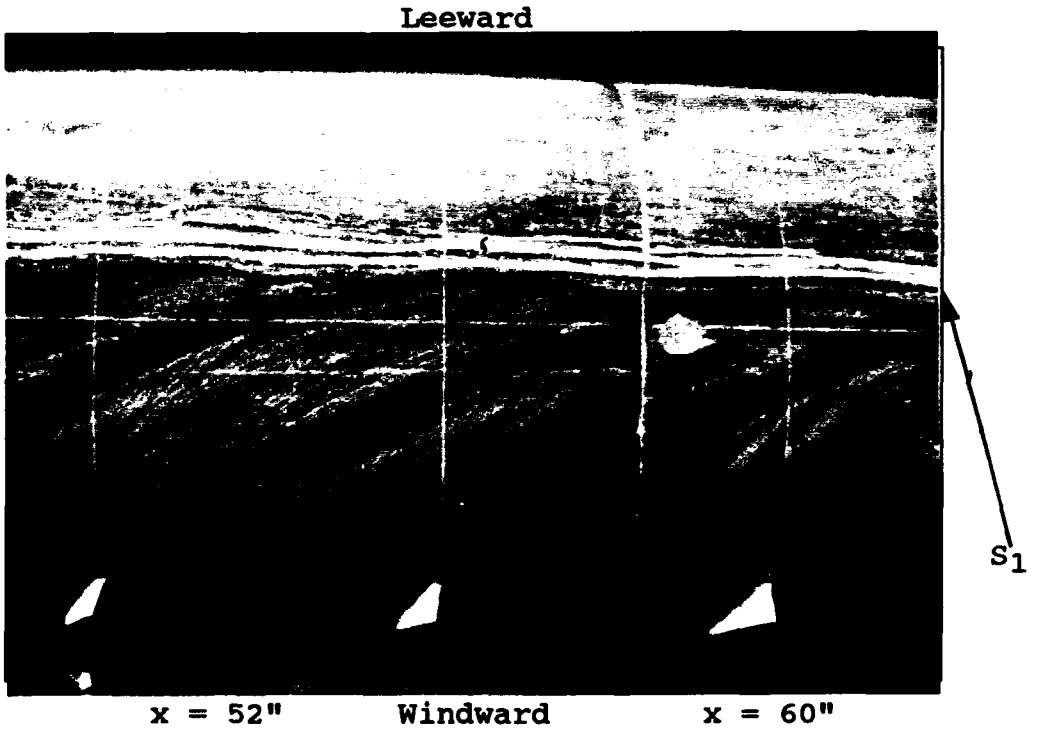

Figure 120. Oil flow 20, submarine with vortex generators, bottom side, Re = 6.43×10^6, β = 15°.

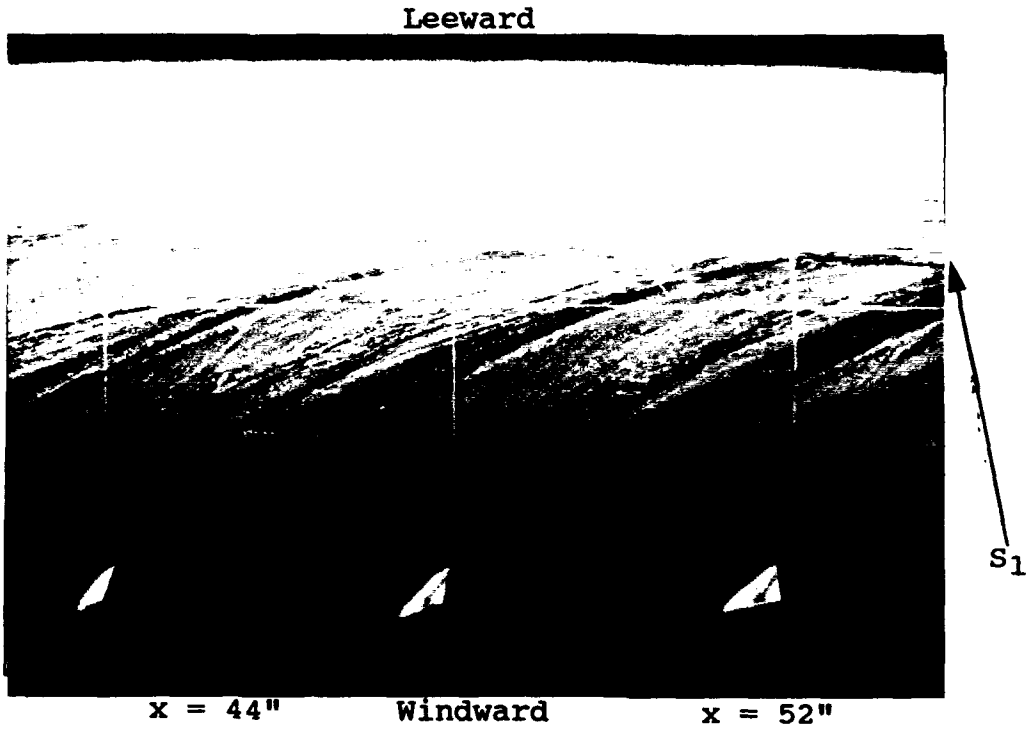

Figure 121. Oil flow 20, submarine with vortex generators, bottom side, Re = 6.43×10^6, β = 15°.

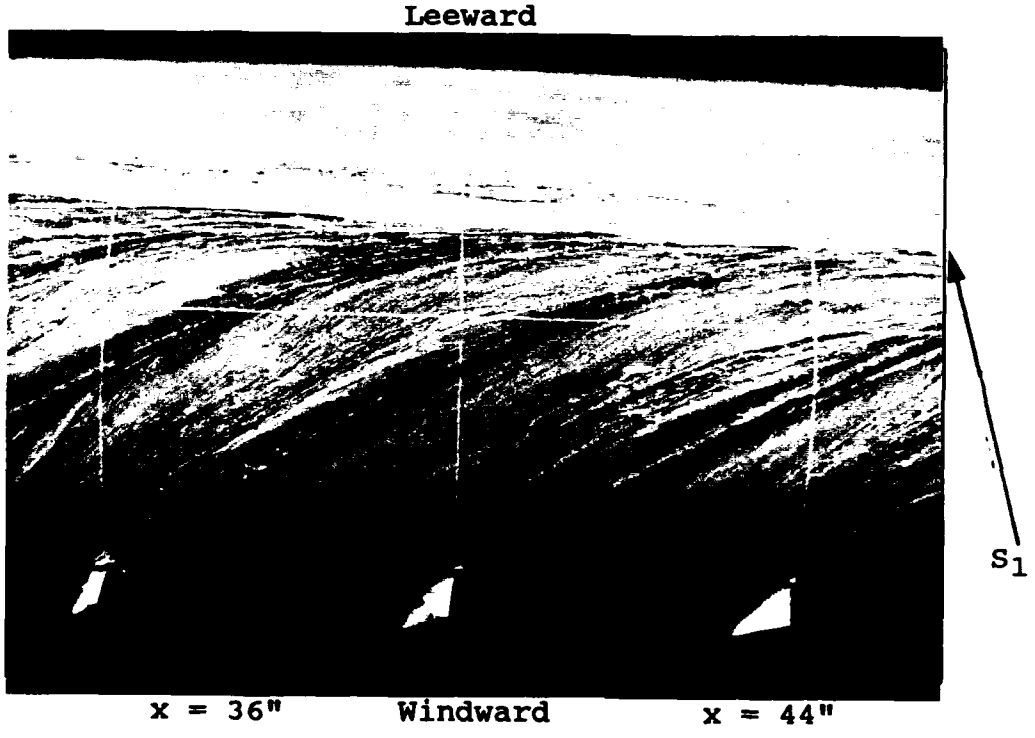

Figure 122. Oil flow 20, submarine with vortex generators, bottom side, Re = 6.43×10^6, β = 15°.

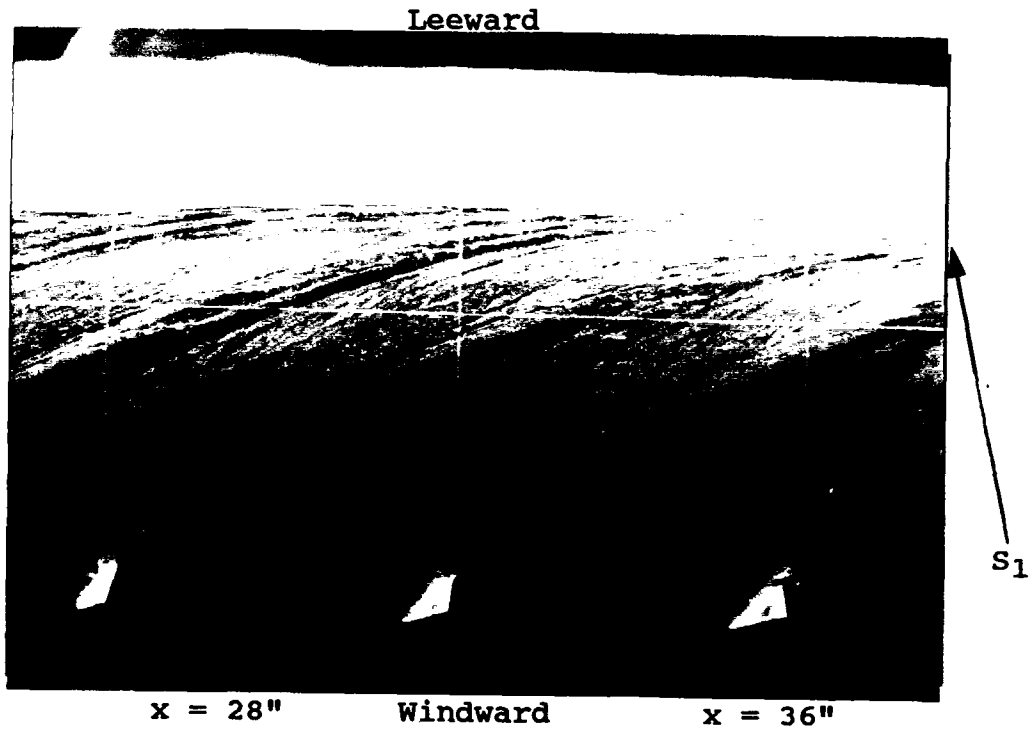

Figure 123. Oil flow 20, submarine with vortex generators, bottom side, Re = 6.43×10^6, β = 15°.

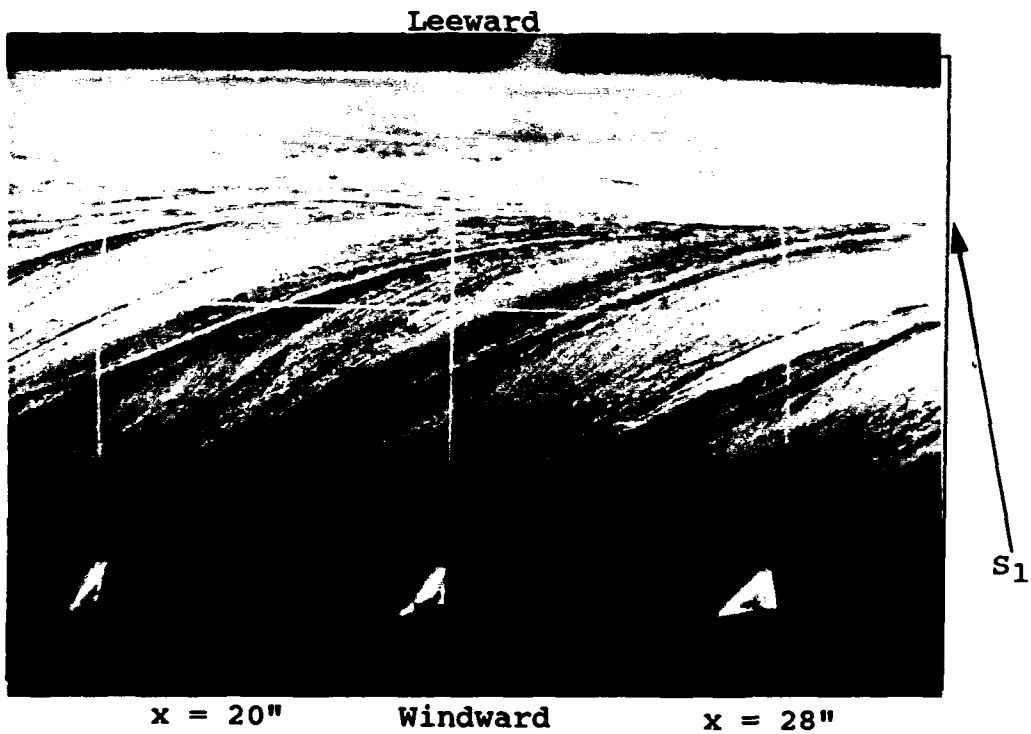

Figure 124. Oil flow 20, submarine with vortex generators, bottom side, Re = 6.43×10^6, β = 15°.

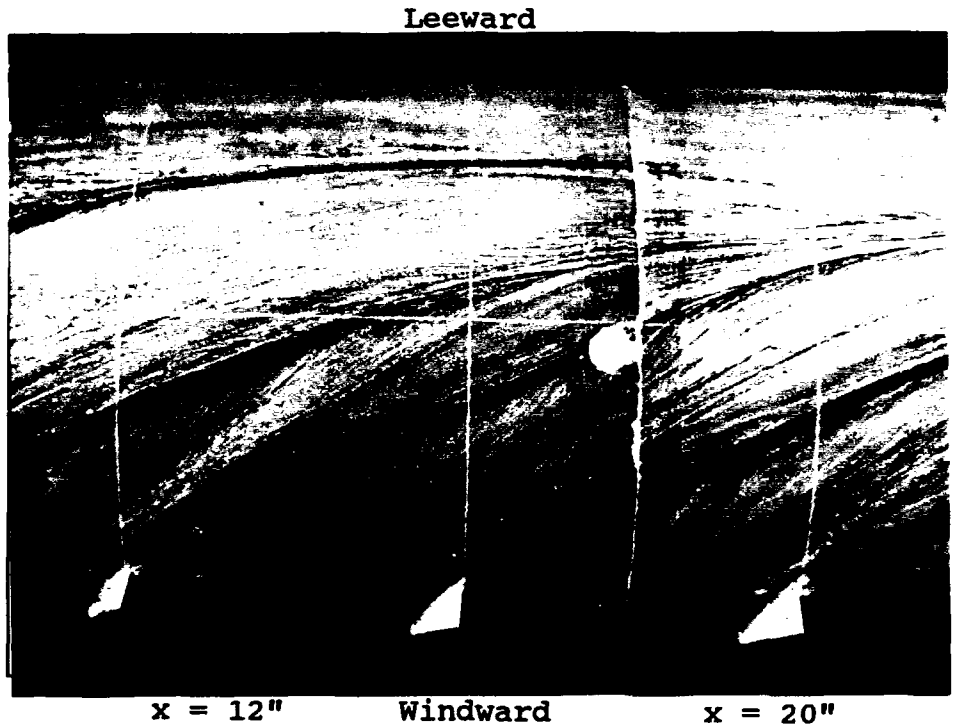

Figure 125. Oil flow 20, submarine with vortex generators, bottom side, Re = 6.43×10^6, $\beta = 15°$.

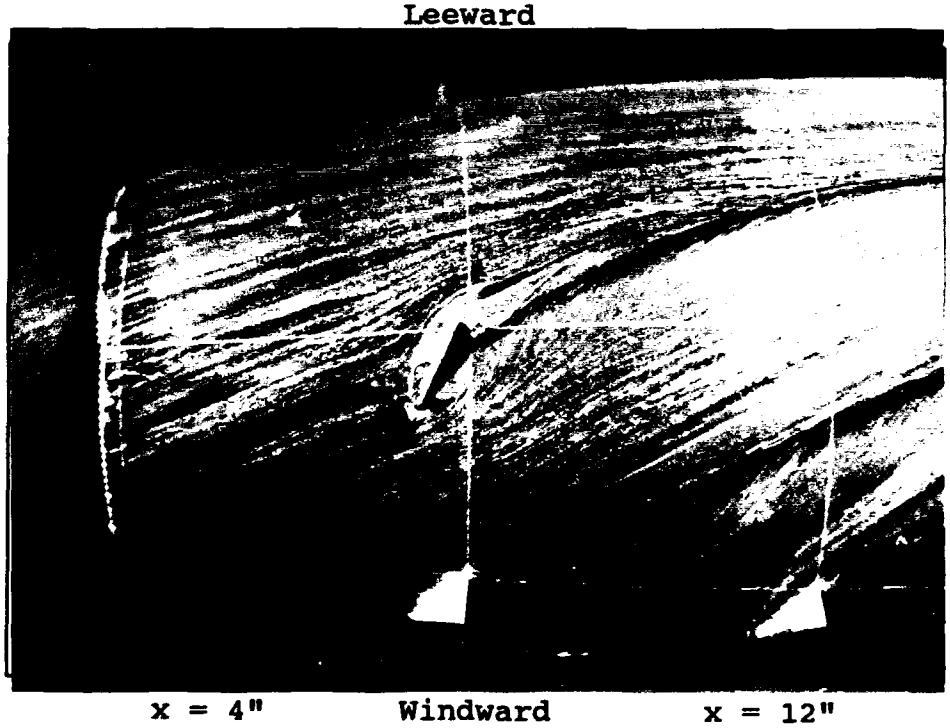

Figure 126. Oil flow 20, submarine with vortex generators, bottom side, Re = 6.43×10^6, $\beta = 15°$.

APPENDIX V Sail Flow Phenomena

These last four photos show the sail flow phenomena at different angles of sideslip. Note the development of the sail vortices, saddle points, and stagnation points.

Leeward

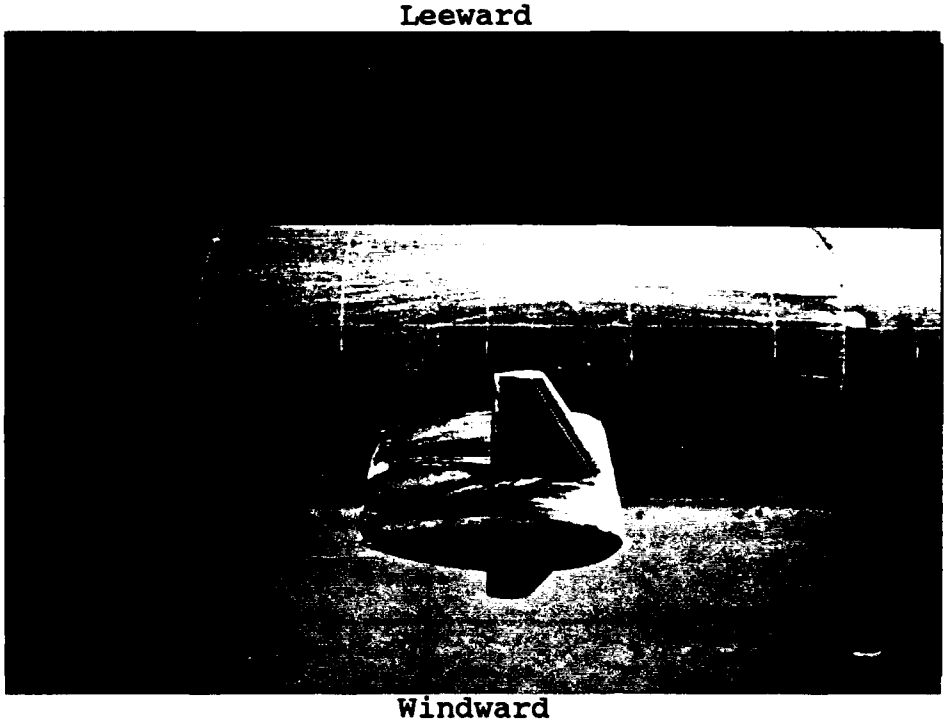

Windward

Figure 127. Oil flow 13, naked submarine, Re = 6.90×10^6, β = 0°.

Leeward

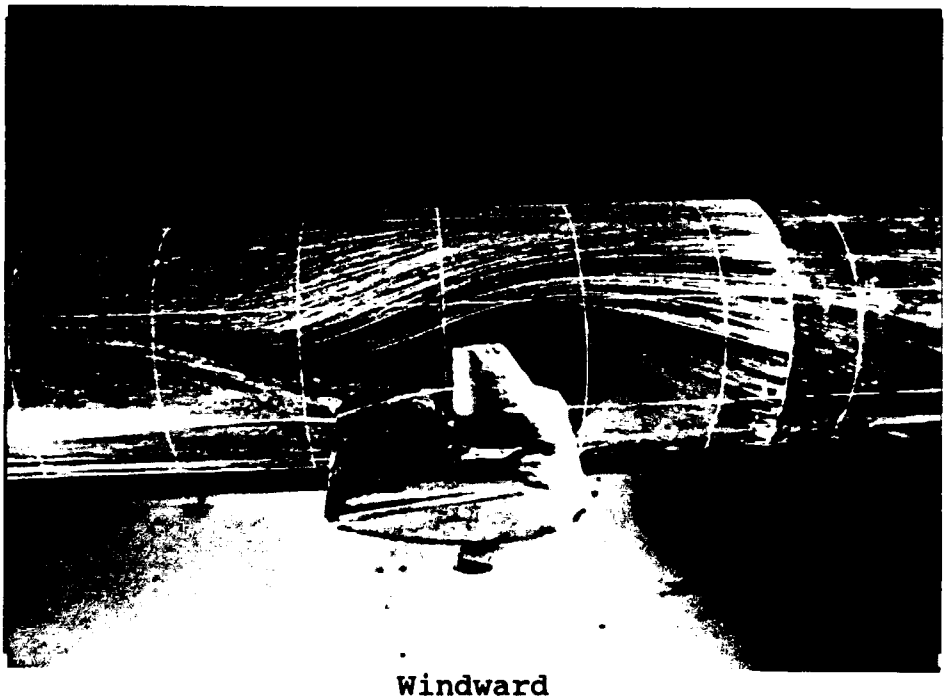

Windward

Figure 128. Oil flow 6, naked submarine, Re = 6.77×10^6, β = 10°.

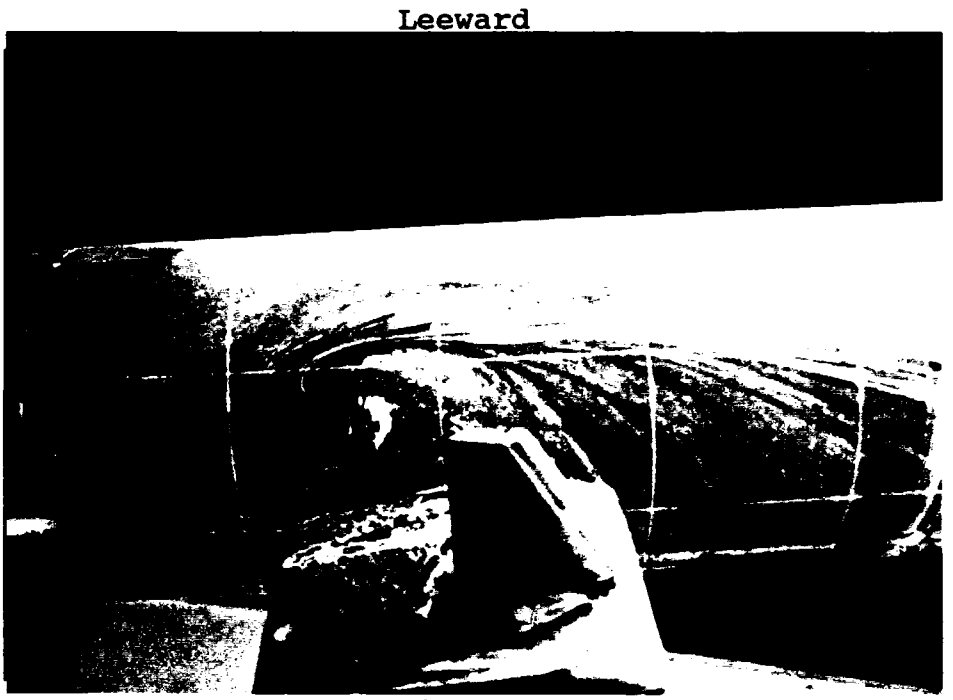

Figure 129. Oil flow 1, naked submarine, Re = 6.78×10^6, β = 15°.

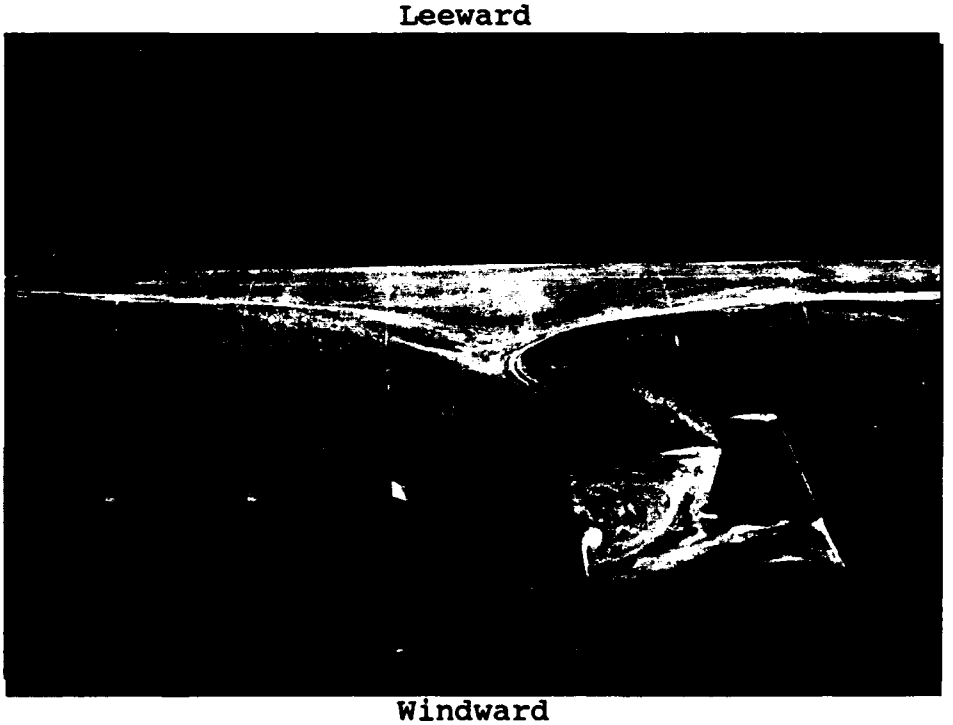

Figure 130. Oil flow 20, subarine with vortex generators, Re = 6.43×10^6, β = 15°.